IMPLEMENTATION OF HIGHLY REACTIVE POZZOLANS IN THE KEY ROYALE BRIDGE REPLACEMENT

By

EDWARD K. ROSKE

A THESIS PRESENTED TO THE GRADUATE SCHOOL
OF THE UNIVERSITY OF FLORIDA IN PARTIAL FULFILLMENT
OF THE REQUIREMENTS FOR THE DEGREE OF
MASTER OF ENGINEERING

UNIVERSITY OF FLORIDA

2007

To my loving family (my mother Joyce Roske, my sister Tiere Roske, and my brother Dustin Roske) as they have offered their unyielding love and support.

ACKNOWLEDGMENTS

I thank my supervisory committee members for their ideas and assistance. My supervisory committee chair (Dr. H. R. Hamilton) provided his valuable time and knowledge of the subject, as well as financial support, to make this research successful. I thank Dr. Robert E. Minchin, Jr. and Dr. Mang Tia for their guidance and knowledge.

I thank Mike Bergin and Charles Ishee and their staff at the Florida Department of Transportation for contributing knowledge, assistance, and funding. Special thanks go to Richard Delorenzo for his tremendous knowledge and assistance in the laboratory

I would like to acknowledge Sal Depolis and Wayne Allick Jr. for their assistance in laboratory testing. I also thank everyone in the Department of Civil and Coastal Engineering who contributed time and effort to my study. They include Mahir Dham, Christopher Ferraro, Samuel Smith, Tanya Reidhammer, Yu Chen, Beyoung Il Kim and Xiaoyan Zheng.

My deepest appreciation goes to Stephanie Lloyd for her continual support and encouragement throughout the research and writing of this thesis.

TABLE OF CONTENTS

LIST OF TABLES

LIST OF FIGURES

Abstract of Thesis Presented to the Graduate School
of the University of Florida in Partial Fulfillment of the
Requirements for the Degree of Master of Engineering

IMPLEMENTATION OF HIGHLY REACTIVE POZZOLANS IN THE KEY ROYALE BRIDGE REPLACEMENT

By

Edward K. Roske

May 2007

Chair: H. R. Hamilton III
Major: Civil Engineering

The objective of our study was to assess the use of alternative mineral admixtures to improve the service life of bridges constructed in severe marine environments. Our study evaluated the effects of highly reactive pozzolanic materials in conjunction with fly ash on the plastic, mechanical, and durability properties of portland cement concrete. Additionally, mixtures using these highly reactive pozzolans were designed for use in the precast, prestessed piling for the Key Royale bridge replacement project.

Thirteen different trial mixtures were prepared using varying proportions of several highly reactive mineral admixtures. Two of the thirteen were control mixtures; one contained only portland cement and the other contained 18% fly ash. The remaining eleven mixtures contained 18% fly ash with varying proportions of slag, metakaolin, ultrafine fly ash, and silica fume.

Plastic property tests were conducted on temperature, air content, slump, bleeding, and setting times. Mechanical test procedures included compressive strength, flexural

strength, splitting tensile strength, modulus of elasticity, and Poisson's ratio. Several durability tests were performed including surface resistivity, rapid migration test, volume of voids, absorption, water permeability, shrinkage, sulfate expansion, and corrosion of embedded steel reinforcement.

Using results from the laboratory testing, we created a decision matrix to select the relative mineral admixture proportions to be used to construct the piles. One mixture from each group of mineral admixtures was selected. The decision matrix included ratings for cost, mechanical properties, and durability. Although the costs of several mixtures were considerably higher than the controls, each mixture showed an overall improvement in mechanical and durability properties. Proportions determined to provide the most effective mixtures were 30% slag, 10% metakaolin, 12% ultrafine fly ash, and 9% silica fume.

Based on the decision matrix, each mixture showed consistent mechanical properties. The silica fume and metakaolin mixtures, however, performed the best overall in the durability tests. Silica fume mixtures showed improvement in durability over the cement only control ranging from 21 to 23%. Metakaolin also showed improvements of 17 to 20%.

CHAPTER 1
INTRODUCTION

The Florida Department of Transportation (FDOT) has set a goal to build bridges that will last at least 100 years. Currently, the acceptance criteria consist of measuring the plastic properties, water-to-cementitious ratio and compressive strength. None of these acceptance criteria can be used to predict the ultimate service life of the structure. By performing more durability-related tests on local materials, the Department can develop a better understanding of how long a structure can be expected to last.

Current design standards (2004 *Structures Design Guidelines for Load and Resistance Factor Design*) allow only corrosion inhibitors or silica fume for reducing permeability of the concrete. Silica fume is currently specified in Florida concretes under certain conditions; "when the environmental classification is Extremely Aggressive due to the presence of chloride in the water, specify microsilica in the splash zone of all piles, columns or walls. Microsilica may be specified for the entire pile, column or wall but shall not be specified for drilled shafts. The splash zone is the vertical distance from 4 feet below MLW to 12 feet above MHW." Under new specifications proposed by AASHTO, other materials could be allowed in place of silica fume for concrete placed under such conditions.

Mixtures containing highly-reactive pozzolans such as metakaolin and superfine fly ash will provide similar strength as silica fume, while avoiding the detrimental workability issues. Currently, the availability and cost of the highly reactive pozzolans designated in this study are both better than for silica fume. However, newer materials require investigation to determine which mixture design criteria should be implemented in order to provide the desired service life to FDOT structures.

The present research evaluated the durability and mechanical properties of concrete made with highly reactive pozzolans other than silica fume. Four of these concrete mixture designs were selected for use in fabricating piles for a bridge structure to be built in a severely aggressive environment. The field project was funded by the Federal Highway Administration through their Innovative Bridge Research & Construction (IBRC) program.

This investigation tested several alternative materials to provide the FDOT with the means to assess the applicability for utilization in the splash zone of a Florida concrete in a severely aggressive environment. These materials include slag, metakaolin, and ultrafine fly ash. Research was conducted on the effects of implementing these highly reactive pozzolanic materials in conjunction with fly ash to the plastic, mechanical, and durability properties of portland cement concrete. Additionally, this study provided the FDOT with a recommendation of the most effective mixtures containing various pozzolans for the utilization in the piling of the Key Royale bridge replacement project.

CHAPTER 2
LITERATURE REVIEW

Presently, the Florida Department of Transportation (FDOT) only allows the use of silica fume in the splash zone of concretes in a severely aggressive environment. There are, however, several other mineral admixtures that provide an improvement in the mechanical and durability characteristics of a concrete. Many researchers have presented data relating to the effects of mineral admixtures on the plastic, mechanical, and durability properties of a concrete. Therefore, this chapter presents a comprehensive review of the currently available literature.

Unhydrated Cement Chemistry

Portland cement is a hydraulic cement which is typically produced by initially heating limestone with clay in 2550 to 2900°F kiln to produce clinker (Mindess et al. 2003). The clinker is then ground to a specific fineness. Small amounts of gypsum is interground with the clinker to control the hydration rate of the finished cement product.

Shorthand notation used to represent the actual chemical formulas for oxides found in cements and mineral admixtures are shown in Table 2 - 1. Chemical compounds that are the major constituents in cement are formed from these oxides in the calcining process of cement manufacturing. The chemical name, chemical formula and shorthand notation for the five most abundant compounds are found in Table 2 - 2.

Table 2 - 1 Typical Oxides and Their Shorthand Notation

Common Name	Chemical Formula	Shorthand Notation
Lime	CaO	C
Silica	SiO_2	S
Alumina	Al_2O_3	A
Ferric Oxide	Fe_2O_3	F
Magnesia	MgO	M
Alkali	K2O	K
Alkali	Na_2O	N
Sulfur Trioxide	SO_3	$\hat{S}$
Carbon Dioxide	CO_2	$\hat{C}$
Water	H_2O	H

Table 2 - 2 Typical Chemical Compounds and Their Shorthand Notation

Chemical Name	Chemical Formula	Shorthand Notation
Tricalcium Silicate	$3CaO{\cdot}SiO_2$	C_3S
Dicalcium Silicate	$2CaO{\cdot}SiO_2$	C_2S
Tricalcium Aluminate	$2CaO{\cdot}Al_2O_3$	C_3A
Tetracalcium Aluminoferrite	$4CaO{\cdot}\ Al_2O_3{\cdot}Fe_2O_3$	C_4AF
Calcium Sulfate Dihydrate (gypsum)	$CaSO_4{\cdot}2H_2O$	$C\hat{S}H_2$

Estimations of the quantity of these compounds can be made through Bogue equations (Neville 1995). Bogue equations are used to predict the properties of cement, such as rate of strength development and heat liberation. Moreover, manipulation of the cement, based on results of these equations, can be made to modify certain properties to make it more appropriate to a particular application (Mindess et al. 2003). The formula is as follows.

Case A: $A/F \geq 0.64$

$C_3S = 4.071C - 7.600S - 6.718A - 1.430F - 2.852\hat{S}$
$C_2S = 2.867S - 0.7544\ C_3S$
$C_3A = 2.650A - 1.692F$
$C_4AF = 3.043F$

CaseB: $A/F < 0.64$

$C_3S = 4.071C - 7.600S - 4.479A - 2.859F - 2.852\hat{S}$
$C_2S = 2.867S - 0.7544\ C_3S$
$C_3A = 0$
$C_4AF = 2.100A + 1.702F$

Each cement and mineral admixture is composed of some or all of these compounds and oxides. A more detailed analysis of the typical compositions for each material is discussed in the succeeding section.

Hydration Chemistry

The chemical reactions of pozzolans and cement hydration have been widely studied in which a few commonly accepted equations have been established (Mindess et al. 2003). These equations are presented in the subsequent sections for cement hydration and pozzolanic reactions.

Cement Hydration

The hydration of the calcium silicates in portland cement produces calcium silicate hydrate and calcium hydroxide. The C_3S and C_2S reactions are very similar, with the only difference being the quantity of calcium hydroxide (CH) formed.

$$2C_3S + 11H \rightarrow C_3S_2H_8 + 3CH \quad (2\text{-}1)$$

$$2C_2S + 9H \rightarrow C_3S_2H_8 + CH \quad (2\text{-}2)$$

The composition of this calcium silicate hydrate product can vary widely—typically in water content. Presented here, the product is in its saturated state. In contrast, CH has a fixed composition.

Another hydration reaction occurs in the presence of sulfate ions supplied by the dissolution of gypsum. These ions react with C_3A to form a calcium sulfoaluminate hydrate.

$$C_3A + 3C\hat{S}H_2 + 26H \rightarrow C_6A\hat{S}_3H_{32} \quad (2\text{-}3)$$

The calcium sulfoaluminate hydrate is a stable hydration product commonly known as ettringite. However, if there is an insufficient supply of sulfate ions present, the C3A will not be completely hydrated. Ettringite will then be reacted with C3A to form another

calcium sulfoaluminate hydrate with less sulfate, commonly known as monosulfoaluminate.

$$2C_3A + C_6A\hat{S}_3H_{32} + 4H \rightarrow 3C_4A\hat{S}H_{12} \quad (2\text{-}4)$$

If a new source of sulfate ions comes in contact this monosulfoaluminate, ettringite is able to be reformed:

$$C_4A\hat{S}H_{12} + 2C\hat{S}H_2 + 16H \rightarrow C_6A\hat{S}_3H_{32} \quad (2\text{-}5)$$

Pozzolanic Reaction

Pozzolan are not cementitious, but rather amorphous silica which will react with CH and water to form a cementious product, C-S-H:

$$CH + S + H \rightarrow C\text{-}S\text{-}H \quad (2\text{-}6)$$

If the silica content in the pozzolan is very high, a secondary reaction will occur:

$$C_3S + 2S + 10.5H \rightarrow 3[CSH_{3.5}] \quad (2\text{-}7)$$

When the pozzolan has large quantity of reactive alumina, the CH will react with alumina to form a calcium aluminate hydrate (C-A-H):

$$CH + A + H \rightarrow C\text{-}A\text{-}H \quad (2\text{-}8)$$

Effect of Cement and Mineral Admixtures on Concrete Properties

Portland Cement

Portland cements are produced with a specific composition and fineness to ensure a satisfactory performance for a particular application, such as high early strength or low heat of hydration. ASTM created a cement classification to standardize cements so that a more consistent product can be manufactured. These standardized cements are designated ASTM Types I, II, III, IV, and V.

Before an explanation of how the standardized ASTM cements are produced, knowledge of the hydration characteristics of cement compounds needs to be understood.

It is useful to know how the chemical compounds listed in Table 2 - 2 affect strength development and rate of heat evolution. Calcium silicates provide most of the strength development in a concrete. (Mindess et al. 2003) C_3S react moderately to contribute early strength development. In later ages, C_3S will contribute to ultimate strength. The reaction of C_3S liberates a moderate amount of heat. However, because of its high proportion in cement, its contribution to the overall heat liberation is high. C_2S has a much slower reaction and a low heat generation. Therefore, at early ages, C_2S provides very little strength development. However, its contribution to ultimate strength is high. The hydration of C_3A is a fast and highly exothermic reaction. Therefore, its contribution to the overall heat liberation is very high. The hydration of C_4AF is moderate and is slowed by the presence of gypsum.

The ASTM Type I is the most commonly used cement, as it is general purpose. It has average strength gain and heat of hydration. However, if a more specialized application, such as sulfate resistance or high early strength development, is needed, a different type should be selected. Type V cements was developed to combat sulfate attack. Sulfate attack involves the hydration products formed from C_3A. Therefore, lowering the percentage of C_3A will serve to increase the sulfate resistance of a cement. Type III cement was developed to create a high early strength concrete. This was accomplished by increasing the proportions of C_3S or, more effectively, grinding the cement finer. However, much heat is generated during the hydration process because of the increase surface area of C_3S. Therefore, this cement cannot be used where high temperatures create adverse effects, such as in mass concrete, where thermal cracking can become a problem. It is for this reason that Type IV was created. Type IV cement was

developed to create a low heat of hydration product. The proportions of the highly exothermic compounds, C_3A and C_3S, were reduced. However, there are problems associated with this cement also. Because of the lower C_3S composition, this cement has a slow strength gain; therefore, a Type II cement was developed. The C3S proportion remains the same, while C_3A is slightly lowered. This cement has a better strength development, as well as being fairly sulfate resistant. Table 2 - 3 was recreated from Mindess (et al. 2003), detailing typical chemical compositions and properties of ASTM Types I to V cements.

Table 2 - 3 Typical Chemical Compositions and Properties of ASTM Type I to V cements

	I	II	III	IV	V
C_3S	55	55	55	42	55
C_2S	18	19	17	32	22
C_3A	10	6	10	4	4
C_4AF	8	11	8	15	12
$C\hat{S}H_2$	6	5	6	4	4
Fineness (m^2/kg)	365	375	550	340	380

Fly ash

Fly ash is precipitated from the exhaust gases of a coal burning power station. The majority of particles are spherical, glassy, and either hollow or solid in shape and have a high fineness. Typically, particles have a diameter range of 1 μm to 100 μm and a specific surface between 250 to 600 m^2/kg (Neville 1995). The main components in the composition of fly ash are oxides of silicon, aluminum, iron, and calcium. The varying calcium content in fly ash composition led to the creation of ASTM C 618. This standard created two classes of fly ash—Class C and Class F. ASTM C 618 requires a Class F fly ash to be composed of a minimum of 70% silicon oxide (SiO_2) plus aluminum oxide (Al_2O_3) plus iron oxide (Fe_2O_3), while a Class C has a minimum of 50%. Derived from

the burning of subbituminus coal or lignite, Class C fly ash has a high lime (CaO) content. Because of this, it is also slightly cementitious. Problems arise with high water demand, early stiffening, and rapid setting. Class F fly ash is derived from the burning of bituminous coal or anthracite. Its calcium content is lower than a Class C fly ash.

Because fly ash is a pozzolan, the silica and alumina will react with CH to form a cementitious compound, C-S-H and C-A-H, respectively. The reactions depend on the breakdown and dissolution of silica and alumina by the hydroxide ions and heat generated by the hydration of portland cement. The glass material in fly ash is only broken down when the pH value of the pore water is at least 13.2 (Neville 1995). In other words, the fly as will consume CH and form a hydration product as long as enough CH is present in the pore solution and there is sufficient void space present for the hydration product to fill.

Fly ash influences the properties of a fresh concrete in a variety of ways. Workability, bleeding, and time of setting are all affected by the addition of fly ash. For the most part, the changes due to the addition of fly ash are because of the shape and size of the particles and its chemical composition.

A reduction in water demand and an increase is workability is attributed to the spherical shape of the particles. The particle shape reduces the interparticle friction within the mixture, effectively increasing the workability. This also allows for a reduction in water to keep the same workability for a concrete mixture. Neville (1995) has found that another mechanism of fly ash may be dominant in decreasing the water demand. The finer fly ash particle may become electrically charged and cover the surface of the cement particles. He states that action deflocculates the cement particles,

thus reducing the water demand for a given workability. Another benefit of fly ash is the small particle size, which allows them to pack between the cement particles. This is known as particle packing; it reduces bleeding, lowers the mean size of the capillary pores, and can reduce water requirements (Mindess et al. 2003).

The composition of fly ash also extends setting times and decreases the overall heat liberated during hydration. Delayed setting times are ascribed to the slow pozzolanic reactions of fly ash. As mentioned above, the glassy fraction of fly ash will only breakdown when sufficient hydroxide ions are present in the pore solution. This process takes place only after a certain amount of hydration of portland cement has taken place (Neville 1995). A consequence of the delay in the cement hydration is the slow pattern of heat evolution. Much of the heat is generated during the early stages of hydration of the C_3S and C_3A within the paste. The delayed setting time allows the concrete to slowly liberate the heat generated. In addition, when fly ash is used a cement replacement, smaller quantities of the high heat generating compounds, C_3S and C_3A, are present. Therefore, the overall heat of hydration is reduced.

Fly ash influences the properties of a hardened concrete in a variety of ways. Compressive strength and rate of strength gain, modulus of elasticity, permeability, sulfate resistance, and drying shrinkage are all affected by the addition of fly ash. For the most part, the changes due to the addition of fly ash are because of the shape and size of the particles and its chemical composition.

The rate of strength gain is reduced by the addition of a Class F fly ash. As mentioned above, the pozzolanic reactions of fly ash depend on a high pH pores solution. Because this takes time to occur, the early hydration of mixtures containing fly ash is

slow. Consequently, the early age compressive strengths are low. However, over time, the Class F fly ash will react to produce a stronger concrete than that of the same mixture containing only portland cement (ACI 232.2R-03). Conversely, Class C fly ash concrete often exhibit higher rate of reaction at early ages, but lower strength gain at late ages when compared to a Class F fly ash concrete (ACI 232.2R-03).

ACI (232.2R-03) has found that the effects of fly ash on the modulus of elasticity are not as significant as the effects on compressive strength. Furthermore, they suggest that cement and aggregate characteristics will have a greater effect on modulus of elasticity that the use of fly ash. Similar to modulus of elasticity, creep strain is more affected by compressive strength than fly ash. Lower compressive strengths result in higher creep strains (ACI 232.2R-03).

The consequence of using the slow reacting fly ash is that the initial permeability is higher than that of the same concrete containing only portland cement (Neville 1995). However, over time the fly ash concrete will develop a very low permeability through pozzolanic reactions (ACI 232.2R-03). CH is susceptible to leaching, leaving voids in which deleterious solution can ingress. However, fly chemically combines with CH to form a cementitious product, C-S-H. This action reduces the risk of leaching, and further reduces permeability as the pore structure becomes occupied with C-S-H. Consequently, the durability of a concrete exposed to aggressive environments containing sulfates and chlorides is improved because of the reduction in permeability (Neville 1995). In addition, sulfate resistance is further improved through the removal of CH (Mindess et al. 2003).

Ultrafine fly ash

Ultrafine Fly ash, similar to ordinary fly ash, is precipitated from the exhaust gases of a coal burning power station. However, the larger particles are removed through filters or separators. The majority of particles are spherical, glassy, and either hollow or solid in shape and have a very high fineness. Boral (2003) states that the average particle diameter is 3 μm and the distribution of particle size is as follows:

- Minimum of 50% of particle sizes less then 3.25 microns
- Minimum of 90% of particle sizes less than 8.50 microns.

Little research has been conducted on the effects of ultrafine fly ash on the durability and mechanical properties of a concrete. However, estimations on the behavior can be made through relations with ordinary fly ash based upon chemical composition and particle size.

The addition of ultrafine fly ash will influence the properties of a fresh concrete similarly to ordinary fly ash. Differences in workability and bleeding from that of ordinary fly ash are attributed to the smaller average particle size.

The higher surface area of the ultrafine particles increases water demand. Therefore, the addition of ultrafine fly ash reduces workability when compared to ordinary fly ash. However, workability is increased when compared to a cement only mixture (Boral 2003). Bleeding is also affected by the particle size. The ultrafine fly ash particles will pack between cement grains and aggregate. Consequently, the mixture is more cohesive and a reduction in bleeding is achieved.

Jones (et al. 2003) conduced 72 hour heat of hydration experiments on 30% ultrafine fly ash and 30% ordinary fly ash mixtures. Because of the retardation of C3A

hydration, the rate of heat evolution was impeded by 2 hours and 5 hours for the ordinary fly ash and ultrafine fly ash mixtures, respectively. They have shown that both mixtures lower the total heat of hydration when compared to the control. The ultrafine fly ash mixture showed the lowest total heat until 18 hours. Beyond 18 hours, the ordinary fly ash mixture had the lowest total heat.

Because the mineral composition is the same, ultrafine fly ash will have similar chemical reactions to that of ordinary fly ash. However, because the average particle size of ultrafine fly ash is much smaller, the reactivity will increase. Consequently, the strength and durability on the concrete will be higher at early ages.

Boral (2003) has found that at 7 days there is an increase in strength activity index of 107% of the control, and 124% at 28 days. Furthermore, they have conducted compressive strength tests on 8% silica fume, 6% ultrafine fly ash, and 9% ultrafine fly ash mixtures with the following characteristics: w/cm of 0.26 – 0.28, cement = 823 lb/yd^3, and fly ash = 100 lb/yd^3. They have shown that a 6% replacement of ultrafine fly ash has nearly equal compressive strength at 7 and 28 days, and roughly a 5% increase at 91 days when compared to an 8% silica fume concrete. A 9% replacement showed increases over the 8% silica fume concrete of roughly 6%, 8%, and 11% at 7, 28, and 91 days, respectively. Jones (et al. 2006) researched the effects of 15% and 30% replacements of ordinary and ultrafine fly ash at a 0.50 w/cm on cube strength. They found that at 28 days, the control mixture had the highest strength (Table 2 - 4). At 90 and 180 days, both ultrafine fly ash mixtures showed higher strength than the control, while both ordinary fly ash mixtures were lower.

Table 2 - 4 Summary Table Comparing Cube Strength (Jones et al 2006)

	% of Control		
Mixture	28 day	90 day	180 day
Control	100	100	100
15% Ordinary Fly Ash	75	85	87
30% Ordinary Fly Ash	54	30	64
15% Ultrafine Fly Ash	96	116	110
30% Ultrafine Fly Ash	87	102	104

At each age, the ultrafine fly ash mixtures showed an improvement over the ordinary fly ash (Table 2 - 5). Therefore, it is evident that the decreased particle size of the ultrafine fly ash increases the strength development at early ages.

Table 2 - 5 Percent Improvement of Ultrafine Fly Ash vs. Ordinary Fly Ash

	% of Ordinary Fly ash		
Mixture	28 day	90 day	180 day
15% Ultrafine Fly Ash	27	36	39
30% Ultrafine Fly Ash	61	45	64

Research conducted by Boral (2003) has also shown that there is an improvement in a concrete against chloride penetration. They found chloride diffusion coefficients for 8% silica fume, 8% ultrafine fly ash, and 12% ultrafine fly ash mixtures (0.40 w/cm) at 40 days and 2 years. At both ages, the ultrafine fly ash mixtures showed lower coefficients when compared to the control. It appears that the 12% replacement showed slightly better results that the 8% mixture. However, neither ultrafine fly ash mixture had lower coefficients than the silica fume mixture.

Jones (et al. 2003) researched the effects of 30% replacement of ordinary fly ash and ultrafine fly ash on the total CH content within a mixture. They found that from age

of 3 days to 90 days, the ultrafine fly ash mixtures showed a lower CH content when compared to the ordinary fly ash mixtures. This indicates that ultrafine fly ash is more reactive and has consumed more CH through pozzolanic reactions

Slag

Blast furnace slag is the residue wastes formed from the production or refinement of iron. Slag is removed from the molten metal and rapidly cooled. The raw slag is then dried and ground to a specific fineness so that it can be used as a cement replacement. ASTM C 989 provides three grades for slag based upon its relative strength to a reference mortar made with pure cement (Table 2 - 6).

Table 2 - 6 Slag Activity Index (ASTM C 989)

Designation	7 day (%)	28 day (%)
Grade 80	---	75
Grade 100	75	95
Grade 120	95	115

Typically, silica, calcium, aluminum, magnesium and oxygen constitute over 95% of the chemical composition (ACI 233R-03). Because of the high lime content, slag is a hydraulic admixture, meaning it will react with water to form a cementitious compound.

The addition of slag in a fresh concrete increases the workability, but make it more cohesive. This is attributed to the better dispersion of cementitious particles and of the surface characteristics of the slag particles (Neville 1995). ACI (233R-03) has found that the smooth, dense surfaces of the slag particles absorb little water and act as slip planes in the paste.

Neville (1995) has suggested that slag leads to retardation of setting times at normal temperatures of typically 30 to 60 minutes. ACI (233R-03) has found that setting times of slag mixtures is significantly affected by portland cement setting characteristics

and the amount of portland cement within the mixture. They state that setting times are delay when more than 25% slag is used as a replacement.

Bleeding is reduced when slag is ground to a high fineness (Neville 1995). ACI (233R-03) supports this statement. They suggest that if slag is ground to a higher fineness than the cement particles and is replaced on an equal-mass basis, bleeding may be reduced; conversely, if the slag particles are larger, the rate and amount of bleeding may increase.

The addition of slag in a mixture increases the silica content and decreases the total lime content. Consequently, more C-S-H is produced resulting in a microstructure that is denser than that of a cement only mixture (Neville 1995). However, the rate of strength gain is initially very slow because of the presence of impervious coatings of amorphous silica and alumina on the slag particles (Mindess et al. 2003). These coatings are broken down in a slow process by hydroxyl ions that are released during the hydration of the portland cement (Neville 1995).

ACI (233R-03) has found that when compared with a portland cement only concrete, the use of Grade 120 slag typically reduces the strength at ages before 7 days; at 7 days and later, Grade 120 slag increases strength. Grade 100 slag reduces strength at ages less than 21 days, while producing equal or greater strength at later ages. Grade 80 slag shows lower strength at ages less than 28 days, and comparable strength at 28 days and later.

Modulus of rupture is generally increased with the addition of slag at ages beyond 7 days (ACI 233R-03). They suggest that the improvement in modulus of rupture is because of an increased density of the paste and improved bond at the aggregate-paste

interface. Neville (1995) has stated that the incorporation of slag does not significantly alter the usual relations between compressive strength and modulus of rupture.

ACI (233R-03) has suggested that water cured slag concretes have do not have an effect of modulus of elasticity at early ages; however, at later ages, modulus is increased. Conversely, air cured specimen exhibited reductions in modulus. This is attributed to inadequate curing. Mindess (et al. 2003) has found that modulus of elasticity is most dominantly affected by porosity. Therefore, prolonged moist curing is particularly important in a slag concrete in which the low early hydration results in a system of capillary pores which allow for the loss of water under dry conditions (Neville 1995). Consequently, hydration is halted, leaving a porous concrete. Consequently, modulus of elasticity is reduced.

This compound adds to the strength of the mix, while also increasing durability by decreasing the interconnectivity of the voids. In addition, the high silica and alumina content promote pozzolanic reactions. The CH produced from cement hydration will be consumed and transformed into more cementitious compounds. These compounds are in the forms of C-S-H or C-A-H, depending on whether the reactive compound was silica or alumina. These new hydration products are denser and more homogenous than that produced by cement hydration alone.

At early ages, the incorporation of slag in a mixture will increase shrinkage; however, at later ages shrinkage and creep are not adversely affected (Neville 1995). ACI (233R-03) supports the statement in which there is no significant affect on shrinkage or creep.

The heat of hydration has been found by ACI (233R-03) to be lower in a 75% slag replacement concrete than in a 30% fly ash concrete or cement only concrete. Slag reduced the early rate of heat generation and lowered the peak temperature.

One benefit of the addition of slag into a concrete arises from the denser microstructure of hydrated cement paste in which more of the pore space is filled with C-S-H than in a cement only paste (Neville 1995). As a result, the permeability is decreased. ACI (233R-03) has found that as the slag content increases, the permeability decreases. Consequently, the resistance to sulfate attack is increased. The resistance to sulfate attack is further increased through consumption of CH, the major component in sulfoaluminate corrosion (Mindess et al 2003). ACI (233R-03) found that 50% blends of slag with a Type I concrete had the same sulfate resistance as a Type V cement concrete. They have found that the use of slag in a well hydrated concrete reduces the penetrability of chloride ions and the depth of carbonation. However, Neville (1995) has a conflicting opinion in regards to improvements in depths of carbonation with the addition of slag. He states that the slag can have a detrimental effect at early ages when there is very little CH present in the concrete. Because of the decreased presence, CH cannot react with carbon dioxide to form calcium carbonate in the pores. Consequently, the depth of carbonation is significantly greater than in a concrete containing only cement. Conversely, the reduced permeability of slag concrete at later ages prevents continued increases in depth of carbonation.

Metakaolin

Metakaolin is manufacture by calcining clay at high temperatures. This results in a material that is largely composed of highly reactive amorphous aluminosilicates. Mindess (et al. 2003) has reported that, typically, the reactive silica and alumina content

in metakaolin ranges from about 55% and 35 to 45%, respectively. The particles are plate-like and have an average size of 1 to 2 μm, with a surface area of about 15 m^2/g. ACI (232.1R-00) has reported an average size of highly reactive metakaolin to range from 1 to 20 μm. Through pozzolanic reactions, CH will react with both silica and alumina to form a cementitious hydration product. These can be in the form of C-S-H or C-A-H, depending on whether the reactive compound is silica or alumina, which are denser and more homogenous than that produced by cement hydration alone. (Mindess et al. 2003).

Zongjin and Ding (2003) have found that a 10% blend of metakaolin reduces the fluidity of the mixture. They have shown that the water demand was increased by roughly 11%, which is attributed to the plate-like particle shape and its tendencies to absorb water. Setting times were also shown to decrease by 26% and 36% for initial and final setting times. ACI (232.1R-00) has reported lower adiabatic temperatures for 15 and 30% metakaolin replacements over a cement only concrete. Conversely, a 10% replacement showed higher temperatures when compared to the control.

ACI (232.1R-00) has shown improvements in compressive strength of 0.3 and 0.4 w/cm concretes with blends of 8 and 12% metakaolin. At ages up to 45 days, each metakaolin mixture showed higher compressive strengths; compressive strength increased as proportion increased and w/cm decreased. Badogiannis (et al 2005) researched the strength development of 0.4 w/cm concrete with metakaolin replacements rates of 10% and 20%. Compressive strength was tested at ages of 1 to 180 days. They have shown that, at these ages, a 10% replacement will increase the compressive strength. However, 20% replacement has shown that the compressive strength was not higher than

the control until ages of 7 days and later. In addition, the 20% replacement concrete showed lower compressive strength than the 10% blend at all ages.

Kim (et al. 2007) conducted research on metakaolin blends of 5, 10, 15, and 20%. They have shown that there is no significant effect on the flexural strength or splitting tensile strength for replacement levels of 5 to 15%. However, their appears to be slight decreases in strength in the 20% blends at ages less than 28 days.

ACI (232.1R-00) has reported improvements in chloride penetration resistance for both 0.3 and 0.4 w/cm concretes with an 8 and 12% blend of metakaolin. Furthermore, they state that the 12% replacement improved the chloride penetration resistance more than reducing the w/cm from 0.4 to 0.3 in a concrete containing no metakaolin. By reducing the w/cm from 0.4 to 0.36, chloride permeability values for a 10% metakaolin concrete were reduced. Research conduced by Kim (et al. 2007) supports the findings by ACI, in which increasing metakaolin contents (5 to 20%), reduce chloride ion penetrability at 28, 60, and 90 days. They have also reported on the effects of increasing metakaolin contents on the depth of carbonation. They have found that increasing metakaolin contents will increase the depth of carbonation at age of 7, 14, 28, and 56 days. This data suggests that decreased in CH present in the concrete because of the pozzolanic reaction with the additional metakaolin can have a detrimental effect. Because of the decreased presence, CH cannot react with carbon dioxide to form calcium carbonate in the pores (Neville 1995). Consequently, the depth of carbonation is significantly greater in the metakaolin concretes than in a concrete containing only cement. However, the reduced permeability of metakaolin concrete at later ages prevents continued increases in depth of carbonation.

Silica Fume

A by-product of producing silicon metals or ferrosilicone alloys, silica fume is highly reactive pozzolanic material that is commonly used as a cement replacement in concrete. Escaping gases condense to form a large quantity of highly amorphous silicon dioxide, typically 85 to 98% by weight (ACI 234R-06). Its particle size is very small, typically 0.1 to 0.3μm with a surface area of 15 to 25 m^2/g, and spherical in shape (Mindess et al 2003). Silica fume comes is four major forms: as produced, slurried, densified, and pelletized.

Because of the large surface area, silica fume has a higher water demand which must be offset in low w/cm mixtures with a superplasticizer (Neville 1995). However, he has found that the effectiveness of the superplasticizer is enhanced in a silica fume mixture. This is because of its spherical shape and small particle size which allow it to pack between cement particles and act as a lubricant (Mindess et al. 2003). Further benefit of the small silica fume particles packing between cement grains is the reduction in bleeding (Neville 1995). ACI (234R-06) has stated that bleeding is reduced as the content of silica fume is increased because there becomes very little free water available to bleed.

Typically, air entraining admixture in a silica fume concrete must be increased by 125 to 150% than in a similar concrete with cement only (ACI 234R-06). This has been attributed to the high surface area of the particle (Neville 1995).

ACI (234R-06) has found that there is no significant delay in setting time. However, they have shown that there is an increase in heat of hydration. Peak temperatures increase with higher contents of silica fume because of its interactions with C_3S. Silica fume tends to accelerate the exothermic hydration of C3S; consequently,

more CH is produced. In-turn this action starts the pozzolanic reaction with the silica fume, which further increases the concrete temperature. However, they have also suggested that the total heat is somewhat decreased as the increase in silica fume dosage.

The effect of silica fume on the hardened properties is directly a function of the pore structure, cement paste-aggregate transition zone, and chemical composition (ACI 234R-06). As hydration continues, the pore structure becomes more homogenous and capillary pores sizes are reduced and become disconnected (Neville 1995). However, ACI (234R-06) has found that total porosity is largely unaffected by silica fume at all w/cm.

Mindess (et al.2003) has found that the cement paste-aggregate zone, or interfacial transition zone (ITZ), is composed of less C-S-H, has a higher localized w/cm and permeability, and contains large crystals of CH and ettringite. They have stated that silica fume greatly improves the ITZ by eliminating large pores and making the structure more homogeneous, eliminating the growth of CH or transforming the already present CH to C-S-H by pozzolanic reaction, and altering the rheological properties of a fresh concrete by reducing internal bleed because the small size of the silica fume particles allow it to pack between cement particles and aggregate.

ACI (234R-06) has found that concretes made with silica fume exhibit higher compressive strengths at earlier ages, up to 28 days. They have also found that there is minimal contribution to compressive strength after 28 days. Neville (1995) has found that the behavior of silica fume beyond the age of 3 months depends on the moisture conditions. In wet cured conditions, he supports ACI in which the silica fume concrete showed only a small increase in compressive strength for up to 3.5 years of age.

Conversely, under dry conditions a retrogression of strength, typically 12% below the peak at 3 months, was observed. These findings indicate the tendencies of a silica fume concrete to self-desiccate. Therefore, adequate curing is essential for a full development of strength.

The trends of the development of compressive strength to flexural and splitting tensile strength of a concrete made with silica fume is similar to that of a cement only concrete (ACI 234R-06). In other words, as compressive strength increases, the tensile strength also increases, but a decreasing ratio. They have found that a 20% silica fume had a compressive to flexural strength ratio that ranged from 0.13 to 0.15. They have also found splitting tensile strength at various ages to range from 5.8 to 8.2% of the compressive strength.

As mentioned before, the use of silica fume results in a refinement of the pore structure. Consequently, silica fume reduces the permeability of not only the paste, but also the ITZ (Neville 1995). He found that a 5% replacement of silica fume resulted in a reduction of the coefficient of permeability by 3 orders of magnitude. Conversely, ACI (234R-06) has found that a 5 to 12% silica fume replacement resulted in only a 1 order of magnitude reduction in permeability, in which no statement of w/cm was reported. However, they have also found that for a 0.20 w/cm concretes containing 10 and 20% silica fume, showed coefficient of permeability of $3*10^{-13}$ and $0.3*10^{-13}$, respectively. The control showed a higher permeability at $12*10^{-13}$.

A consequence of reduced permeability is the greater resistance to chloride penetration (Neville 1995). ACI (234R-06) has found that an 8% substitution in a 0.40 w/cm concrete resulted in a reduction in diffusion coefficient by a factor of seven.

Furthermore, addition rates above 8% resulted in little additional improvement to resistance of chloride penetration. Reduced permeability is the primary mechanism in which silica fume increases the resistance to sulfate attack by sodium sulfate (ACI 234R-06). However, an additional increase in sulfate resistance occurs from the pozzolanic reactions with silica fume as there is a large consumption of CH, the major component in sulfoaluminate corrosion (Mindess et al 2003).

CHAPTER 3
MIX DESIGN

This chapter discusses the materials and proportions used in the concrete mixtures that were evaluated in this investigation. Preparation of the concrete mixtures, specimen fabrication, and curing conditions are also described.

Materials

The materials used in the concrete mixtures are described in the following sections. These constituents can be divided into three categories: Basic Ingredients, Mineral Admixtures, and Chemical Admixtures.

Basic Ingredients

There exist a few materials that can be found within all of the concrete mixtures in this investigation. These ingredients are water, fine aggregate, coarse aggregate and cement.

Water

The water used in the concrete mixtures was obtained from the local city water supply.

Fine Aggregate

Silica sand from pit number 11-067 was used as fine aggregate in all concrete mixtures. The sand from this pit was tested and passed the gradation requirements of Section 902 of the 2004 Florida Department of Transportation Standard Specification for Road and Bridge Construction (FDOT Spec.). Additional testing of the sand determined a fineness modulus of 2.39 and a bulk specific gravity of 2.65, which were used in the mixture design to calculate yield. Specific test results on the fine aggregate are provided in Appendix A.

This sand was placed into cloth bags and dried in the oven until all moisture was removed. Prior to integration in the concrete mixtures, the sand was allowed to cool to the ambient temperature.

Coarse Aggregate

Crushed limestone from pit number MX-411was used as the coarse aggregate in all concrete mixtures. The aggregate from this pit was tested and passed the gradation requirement of Section 901 in the FDOT Spec. for a ¾-in. maximum diameter aggregate. Additional testing of the limestone determined a bulk specific gravity of 3.61, which were used in the mixture design to calculate yield and adjust for moisture content. Specific test results on the fine aggregate are provided in Appendix A.

The coarse aggregate was used in its approximate saturated surface dry (SSD) condition. This SSD condition was obtained by filling woven polypropylene bags with coarse aggregate. The bags were then submerged in water for a minimum of 48 hours to fully saturate the aggregate. One day prior to mixing, the coarse aggregate bags were removed from the water and allowed to drain for approximately one hour.

Cement

Type II portland cement manufactured by Holcim in the Theodore plant was used in each mixture. This cement complied with Section 921 of the 2004 FDOT Spec. Tests showed that the cement had an initial set time of 140 minutes, and a final set time of 215 minutes. This information is useful when determining the effects of the mineral admixtures and set retarding chemical admixture on a mixture. Additional test results are provided in Appendix A.

Mineral Admixtures

Evaluating highly reactive mineral admixtures was an integral part of this research. The following sections describe the individual admixtures used along with its source and role in the modification of fresh and hardened concrete properties. General information was obtained from Mindess (et al. 2003).

Fly ash

Fly ash is the waste product from the burning of pulverized coal in boiler furnaces used to generate electricity at power stations. It is commonly used as a cement replacement in concrete. In addition to the obvious environmental advantages, use of concrete containing fly ash is advantageous because of the cost, particle size and shape and mineral composition. The cost of fly ash is typically slightly less than half that of portland cement. The spherical shape of fly ash particles increases workability, which allows a lower water to cementious material (w/cm) ratio to be used. In addition, the small particle size increases the packing density of the cementitious system. Thus, the permeability through interconnected voids is reduced, further improving durability. The mineral composition is also advantageous because of the high volume of reactive silica. This silica allows for a pozzolanic reaction to consume calcium hydroxide (CH) and creates more calcium aluminate silicate hydrates (C-S-H), which forms a denser paste structure.

A class F fly ash meeting the requirements of ASTM C 618, AASHTO M-321, and AASHTO M-295 was used in this investigation and was obtained from the Big Bend Power Station in Tampa, Florida. The fly ash also complied with Section 929-2 of the 2004 FDOT Spec. This class F fly ash satisfies the requirements of ASTM C-618 and AASHTO M-295. Specific tests results are provided in Appendix A.

Slag

Blast furnace slag is the residue wastes formed from the production or refinement of iron. Slag is removed from the molten metal and rapidly cooled. The raw slag is then dried and ground to a specific fineness so that it can be used as a cement replacement. Slag is advantageous for its chemical composition; it is rich in lime, silica, and alumina. Because of the high lime content, slag is a hydraulic admixture, meaning it will react with water to form a cementitious compound. This compound adds to the strength of the mix, while also increasing durability by decreasing the interconnectivity of the voids. In addition, the high silica and alumina content promote pozzolanic reactions. The CH produced from cement hydration will be consumed and transformed into more cementitious compounds. These compounds are in the forms of C-S-H or C-A-H, depending on whether the reactive compound was silica or alumina. These new hydration products are denser and more homogenous than that produced by cement hydration alone.

CAMCEM, produced by Civil and Marine (Holdings) Ltd., is a Grade 100 ground granulated blast furnace slag used in this study. The slag complied with Section 929-5 of the 2004 FDOT Spec by meeting the requirements of ASTM C 989. Specific tests results are presented in Appendix A.

Ultra-fine fly ash

Ultra-fine fly ash is the same material as regular fly ash. However, it has been sieved to greatly reduce the average particle size. The advantage of using an ultrafine fly ash over a standard fly ash is because the particle size is typically four times smaller; the small particles increase reactivity by increasing surface area, resulting in higher early strengths and lower permeability than a standard fly ash mixture of the same proportions.

In addition, smaller particles have the ability to pack between the cement grains and aggregate creating a less permeable paste structure by reducing the interconnectivity of the voids.

The ultra-fine fly ash used in this investigation was Micron^3, a product of Boral Material Technologies. The typical mean diameter of Boral's Micron^3, is 3.0 μm. As certified by Boral Material Technologies Inc., the distribution of particle size measured by a laser particle size analyzer is as follows:

- Minimum of 50% of particle sizes less then 3.25 microns
- Minimum of 90% of particle sizes less than 8.50 microns.

This class F fly ash satisfies the requirements of AASHTO M-321, ASTM C-618, and AASHTO M-295. The ultra-fine fly ash complied with Section 929-2 of the 2004 FDOT Spec. Specific test data are presented in Appendix A.

Metakaolin

Metakaolin is manufacture by calcining clay at high temperatures. This results in a material that is largely composed of highly reactive amorphous aluminosilicates. Therefore, metakaolin is advantageous for use as a cement replacement because of this chemical composition. Typically, the reactive silica and alumina content in metakaolin is over 85%. Through pozzolanic reactions, CH will react with both silica and alumina to form a cementitious hydration product. These can be in the form of C-S-H or C-A-H, depending on whether the reactive compound is silica or alumina. These new hydration products are denser and more homogenous than that produced by cement hydration alone. In addition to the composition, the small particle size of metakaolin is advantageous.

With a typical particle size of 1.4 μm, particle packing will occur to create a less permeable paste structure by decreasing the interconnectivity of the voids.

The metakaolin used for this study was OPTIPOZZ, manufactured by Burgess. The requirements of ASTM C 618 Class N were met with a few modifications proposed by the FDOT Spec.:

- The sum of silica, iron, and alumina oxides was 87.9%.
- The loss on ignition was 0.8%.
- The percentage of available alkalis was negligible.
- The strength index at 7 days was 96%.
- Tests on the concrete containing metakaolin included ASTM C 39, ASTM C 157, ASTM C 1012, ASTM G 109, and FM 5-516.

Therefore, the metakaolin complied with Section 929-4 of the 2004 FDOT Spec. Specific test results are presented in Appendix A.

Silica fume

Silica fume is the byproduct of producing silicon metals or ferrosilicon alloys. It is commonly used as a cement replacement in concrete because of its size, shape, and chemical composition. The spherical shape of silica fume decreases interparticle friction. This increases workability, thus allowing a lower w/cm while maintaining the same slump. The small size, typically 0.1 to 0.3μm, allows the silica fume particles to pack between cement grains. These particles will pack between cement grains, and decrease segregation and bleeding while reducing permeability by reducing the interconnectivity of the voids. In addition to the benefits related the shape and size of the particles, the chemical composition of silica fume is also advantageous. The extremely high reactive

silica content, typically 85-98%, will allow for large volumes of CH to be converted into C-S-H. Also, because the silica content is so high, a secondary pozzolanic reaction will occur that converts tricalcium silicate (C3S) to a C-S-H product. These reactions will create a stronger, more homogenous paste matrix.

Force 10,000 D, produced by W. R. Grace & Co., was used as the silica fume in this investigation. It is a dry, densified microsilica powder made from silica fume. The silica fume is densified by air floatation in silos. The tumbling action induces progressive entanglement of particle to form dense clusters. These clusters allow for much easier transporting and handling, in contrast to the original form. Force 10,000 D complied with Section 929-3 of the 2004 FDOT Spec by meeting the requirements of ASTM C 1240. Specific test data is presented in Appendix A.

Chemical Admixtures

Air entrainer

Air entraining admixtures are composed of an aqueous solution of neutralized resin acids and rosin acids in which the molecules have ends that are hydrophilic and hydrophobic. In other words, one end of the molecule is attracted to water, while the other end is repelled by water. This behavior causes the molecules to attach to air bubbles within a fresh concrete mixture forming a tiny, stable bubble that is disconnected from other bubbles. The advantages of having a disconnected air void structure is because it will increase the resistance of a concrete to freezing and thawing cycles, improve the workability and cohesiveness of a fresh concrete mixture, and reduce segregation and bleeding (Mindess et al. 2003). Because Florida concretes are not exposed to freezing and thawing cycles, the addition of air entraining admixture in this investigation was to increase workability and decrease segregation.

The air entrainer used in this study was Daravair 1000, produced by W. R. Grace & Co. This admixture complied with Section 924 of the 2004 FDOT Spec by meeting the requirements of AASHTO M 154.

Water reducer/retarder

Set retarding admixtures are typically composed of a polymer based aqueous solution of lignosulfonate, amine, and compound carbohydrates. These carbohydrates extend the setting time of fresh concrete mixture by slowing down the rate of early hydration of C_3S and C_3A. A set retarding admixture was used in this investigation because of the large number of test specimen fabricated from each mixture. By increasing the setting time, all specimens were able to be properly consolidated before mixture began to harden.

WRDA 60, produced by W. R. Grace & Co., was the set retarding admixture used in this investigation. WRDA 60 complied with Section 924 of the 2004 FDOT Spec by meeting the requirements of AASHTO M 194.

Superplasticizer

Surface charges on particles within a fresh concrete will cause flocculation. A considerable amount of water is usually tied up in these agglomerations, leaving little available to reduce the viscosity of the paste. The addition of a superplasticizing admixture, which is typically composed of an aqueous solution of carboxylated polyether, will serve to break up the bonds found between particles. This releases the available water within the mixture, thereby increasing workability. This increase in workability then allows for a decrease in water to cementitious material ratio. Consequently, the strength and durability of a mixture is improved.

The superplasticizer used in this study was ADVA 140, a product of W. R. Grace & Co. It complied with Section 924 of the 2004 FDOT Spec. by meeting the requirements of AASHTO M 194.

Proportions

Selection of the mix proportions and other mix design parameter for bridges in Florida is based on the local environment. The Structures Design Guidelines (July 2005) defines three exposure conditions:

- Slightly Aggressive
- Moderately Aggressive
- Extremely Aggressive.

For substructure elements, such as piling, the environment classification is a function of the chloride content or pH level of the surrounding soil or water. Higher chloride content, lower pH, or both will result in a more aggressive environment and a more restrictive rating.

If prestressed concrete piles are used in an extremely aggressive environment that is due to elevated chlorides in a marine environment, then silica fume must be used in the concrete mixture. The object of this research was to evaluate the use of other highly reactive mineral admixtures on the fresh and hardened properties of concrete. These admixtures included slag, ultrafine fly ash, metakaolin, and fly ash.

Prestressed concrete piling must use Class V (Special) or Class VI concrete for any environment. Class V (Special) is the mix design typically specified and has the following characteristics:

- Maximum water to cement ratio of 0.35

- Minimum total cementitious material content of a 752 lb/yd^3
- Air content range of 1 to 5%
- Target slump of 3 inches, which may be increased to 7 inches when a water reducing admixture is used.

When the piles are in a moderately or extremely aggressive environment, the use of fly ash, slag, or both is required. Fly ash cement replacement rate is 18% to 22%, while slag is 25% to 70% for moderately aggressive and 50% to 70% for extremely aggressive environments.

Larsen and Armaghani (1987) found that the most effective addition rate of fly ash was between 18% and 22%. They found the rate in excess of this range caused the additional mineral admixture to stop reacting and essentially become fillers. Furthermore, rates below this range caused no significant improvement in durability. Consequently, the FDOT Spec. adopted this range and now requires the use of fly ash in moderately aggressive environments.

The dosage rates in the current FDOT Spec for slag and metakaolin are based on the manufacturers recommendations. The suggested addition rate for slag is 25% to 70% by weight for moderately aggressive environments, while metakaolin is 8 to 12% (Personal Communication with Mike Bergin 2005). At addition rates below the minimum, there were not significant improvements to mechanical properties and durability. Addition rates above the maximum will not react and become expensive fillers.

The effect of Silica fume replacement rates on modulus of rupture and permeability were investigated by Tia (et al. 1990). They found that the most effective replacement

rate was in the range of 7% to 9% by weight. Replacement rates below the minimum did not significantly improve the permeability and had little affect on the modulus of rupture, while rates above the maximum did not show any improvement in test data. Consequently, the FDOT Spec. has adopted this range for silica fume replacement levels.

Although the ultrafine fly ash addition rates are not provided in the current FDOT Spec., the manufacturer has suggested that the range should be from 10% to 14% (Personal Communication with Charles Ishee 2005).

Two control mixtures were designed. The first control mixture contained only Portland cement as the binder; no mineral admixtures or other cementious materials were used. A second control mixture was designed to contain Portland cement and fly ash at an addition rate of 18% by weight. Therefore, the proportion of fly ash used in every mixture was selected to be 18%. The FDOT Spec. minimum was selected because fly ash would be used in conjunction with other mineral admixtures.

To thoroughly investigate the effects of the mineral admixtures, three mixtures containing different proportions of each admixture were designed. For example, three mixtures containing metakaolin at proportions of 8%, 10%, and 12% were designed. These percentages were selected based on the metakaolin guidelines in the FDOT Spec. The minimum and maximum proportions were selected. In addition, a percentage that was midway between the maximum and minimum was selected to provide a broad distribution of data. The ultrafine fly ash mixtures were also designed in this manner; proportions of 10%, 12%, and 14% were selected. Because the range of silica fume replacement rates in the FDOT Spec was narrow (7 to 9%), only mixtures containing the minimum and maximum proportions were designed. The range of replacement rates for

slag in an extremely aggressive environment is 25 to 70% by weight. Because slag was being used in conjunction with fly ash, the maximum slag replacement rate would be too high to create a durable concrete because the proportion of cement would be too low. Neville (1995) found that for the highest medium term strength, the cement to cementitious material should be about 1:1. Therefore, smaller proportions of slag replacement in combination with 18% fly ash were selected to be investigated; slag proportions of 25%, 30%, and 35% were used. The cementitious material proportions for all mixtures are presented in Table 3 - 1 and Table 3 - 2

Table 3 - 1 Proportions of Cementitious Materials a)

	CTRL1	CTRL2	SLAG1	SLAG2	SLAG3
Cement	100%	82%	57%	52%	47%
Fly Ash (FA)	---	18%	18%	18%	18%
Slag	---	---	25%	30%	35%
Metakaolin	---	---	---	---	---
Ultrafine (FA)	---	---	---	---	---
Silica Fume	---	---	---	---	---

Table 3 - 2 Proportions of Cementitious Materials b)

	META1	META2	META3	UFA1	UFA2	UFA3	SF1	SF2
Cement	74%	72%	70%	72%	70%	68%	75%	73%
Fly Ash (FA)	18%	18%	18%	18%	18%	18%	18%	18%
Slag	---	---	---	---	---	---	---	---
Metakaolin	8%	10%	12%	---	---	---	---	---
Ultrafine (FA)	---	---	---	10%	12%	14%	---	---
Silica Fume	---	---	---	---	---	---	7%	9%

The volume occupied by the cementious materials, water, and air was subtracted from the total concrete volume to determine the required aggregate volume. Proportions of coarse aggregate were selected from Table 6.3.6 (Volume of Coarse Aggregate per Unit Volume of Concrete) in ACI 211.1-91. The fine aggregate content was determined by subtracting this coarse aggregate volume from the total aggregate volume. These

proportions of fine and coarse aggregate were determined to be 35% and 65%, respectively. The resulting mixture designs are shown in Table 3 - 3 and Table 3 - 4.

Table 3 - 3 Mix Designs a) (lb/yd^3)

Material	CTRL1	CTRL2	SLAG1	SLAG2	SLAG3
Cement	752	617	429	391	354
Fly Ash	0	135	135	135	135
Slag	0	0	188	226	263
Micron^3	0	0	0	0	0
Metakaolin	0	0	0	0	0
Silica Fume	0	0	0	0	0
Water	263	263	263	263	263
Fine Agg.	1055	1042	1035	1034	1032
Coarse Agg.	1078	1743	1736	1734	1734
Air Entrainer	3 oz.	3 oz.	3 oz.	3 oz.	4 oz
Water Reducer	23 oz.	23 oz.	23 oz.	23 oz.	23 oz.
Superplasticizer	68 oz.	68 oz.	68 oz.	68 oz.	68 oz.
Additional	0 oz.	0 oz.	0 oz.	0 oz.	7 oz.
Total	68 oz.	68 oz.	68 oz.	68 oz.	75 oz.

Table 3 - 4 Mix Designs b) (lb/yd^3)

Material	META1	META2	META3	UFA1	UFA2	UFA3	SF1	SF2
Cement	557	542	527	542	527	512	564	549
Fly Ash	135	135	135	135	135	135	135	135
Slag	0	0	0	0	0	0	0	0
Micron^3	0	0	0	75	90	105	0	0
Metakaolin	60	75	90	0	0	0	0	0
Silica Fume	0	0	0	0	0	0	53	68
Water	263	263	263	263	263	263	263	263
Fine Agg.	1030	1027	1024	1037	1037	1035	1032	1029
Coarse Agg.	1731	1728	1726	1739	1737	1737	1734	1731
Air Entrainer	5 oz	6 oz	6 oz	6 oz	7 oz	8 oz	8 oz	8 oz
Water Reducer	23 oz.	23 oz.	23 oz.	23 oz.	23 oz.	23 oz.	23 oz.	23 oz.
Superplasticizer	68 oz.	68 oz.	68 oz.	68 oz.	68 oz.	68 oz.	68 oz.	68 oz.
Additional	20 oz.	30 oz.	41 oz.	0 oz.	0 oz.	0 oz.	0 oz.	0 oz.
Total	88 oz.	98 oz.	109 oz.	68 oz.	68 oz.	68 oz.	68 oz.	68 oz.

Several chemical admixtures were used to control the fresh properties of the concrete, including air entraining, set retarding, and high-range water reducer.

Recommended addition rates for air entraining admixtures are not typically provided by the manufacturer because many factors affect the process of air entraining a concrete mixture. These factors included cement and mineral admixture, coarse and fine aggregate, mixer type, mixing time, and vibration. Therefore, laboratory experience was used to determine the addition rate, which was 0.4 oz. per 100 lb of cementitious materials.

The set retarder, WRDA 60, had a recommended dosage rate of 2.5 to 6 oz. per 100 lb of cementitious materials. In this investigation, 2.5 oz. was used for each mixture. The lower end of the range was used because only a short delay in setting time was needed to ensure that all specimens could be fabricated before the mixture stiffened.

To ensure consistency among the various mixes, the water content was held constant. It was deemed important, however, that the slump also remain consistent to ensure that the specimens were consolidated similarly. Consequently, slump was adjusted with a high-range water reducer, rather than with additional mixing water. The manufacturers recommended dosage rate for the superplasticizer, ADVA 140, is 6 to 20 oz. per 100 lb of cementitious materials. Because each mineral admixture affects the mixture differently, the quantity of superplasticizer needed to get the desired slump was different for each mixture. An initial estimation of 9 oz per 100 lb of cementitious materials was used for each mixture. Slump readings were taken immediately after mixing was completed. If the slump was below the target range, additional superplasticizer was added at the lab manager's discretion. Addition rates that were too large would cause segregation resulting in loss of strength and durability. This would be evident by large percentages of bleeding. However, the small variations in quantity of

superplasticizer in each mixture of this investigation do not affect the durability or strength, but rather ensure consistent consolidation among specimens.

Preparation of Concrete Mixtures

In preparation for mixing, the coarse aggregate was placed in woven polypropylene bags which were submerged in water for a minimum of 48 hours to fully saturate the aggregate. One day prior to mixing, the coarse aggregate bags were removed from the water and allowed to drain for approximately one hour. The coarse aggregate was then batched and sealed for casting on the following day. This was done to keep the coarse aggregate in a saturated surface dry condition so that it would not affect the water requirements of a mixture by absorbing or releasing water during mixing. Moisture content was measured on representative samples taken from the batched material. Variations from saturated surface dry were adjusted for during mixing.

The fine aggregate was placed in cotton sand bags. The bags were then dried in an oven to remove any in-situ moisture. One day prior to casting, batch quantities were weighed and sealed in plastic 5-gallon buckets.

All mineral admixtures and cement were collected from their receptacle one day prior to casting. The materials were then weighed and sealed in plastic 5-gallon buckets.

All thirteen concrete mixtures were produced in the two cubic feet rotary drum mixer shown in Figure 3 - 1. A butter mixture, which is a small scale replica of a concrete mixture that contains no coarse aggregate, was used prior to mixing. This butter mixture was used to completely cover the interior surface of the concrete mixer. This limits changes in paste content due to adherence to the interior mixing surfaces; butter mixtures improve the consistency of concrete mixtures.

Figure 3 - 1 Rotary Drum Mixer

The procedure for mixing complied with ASTM C 192. Initially, the coarse and fine aggregates were placed in the mixer with approximately half of the water and air entraining admixture. These constituents were then mixed for two minutes. Next, the cement, mineral admixtures, set retarding and superplasticizer admixtures, and remaining water were added to the mixer and mixed for three minutes. The mixture was then allowed to rest for three minutes. A slump test was then conducted to evaluate the mixture. If the slump was not within the desired range, additional superplasticizing chemical admixture was integrated into the fresh concrete and mixed for an additional three minutes.

Specimen Fabrication

The desired testing scheme, discussed in chapter 4, required the fabrication of various concrete specimens. These included cylinders, beams, prisms, and ASTM G 109 specimens. Each specimen was fabricated in accordance to the requirements of ASTM C 192. The 6-in. diameter x 12-in. long cylinders were constructed in 3 lifts. Other specimens were placed in two lifts. Specimens were consolidated by means of external vibration. Vibration continued until the surface of the concrete became smooth and large air bubbles ceased to break the surface. Specimen molds were then sealed to prevent evaporation. Twenty-four hours after fabrication, all specimens were removed from their molds and placed in the curing environment called for by the applicable test methods.

Curing Conditions

The curing condition of each specimen was dictated by their respective test method. These conditions included full submersion in aqueous solutions containing aggressive agents, dry cure in a controlled environment, wet cure in a controlled environment, and a wet cure in an elevated temperature water bath.

With the exception of the specimens tested according to ASTM G 109, ASTM C 157, ASTM C 512, ASTM C 1556, and ASTM C 1012, curing procedures of ASTM C 511 were followed. This standard calls for demolding after 24 hours and placement into a curing environment that is controlled at 73.4 ± 3.0°F and 100% humidity, so that free water is maintained on the surfaces at all times.

Specimens used for ASTM G 109 were cured for 28 days in accordance to ASTM C 511. Upon removal from moist room, specimens were dry cured for two weeks in an environment controlled at a temperature of 73 ± 3°F and a relative humidity of 50 ± 4%.

The epoxy barrier was then applied. Each specimen was then returned to the controlled dry curing environment for an additional two weeks. Next, the specimens were placed in their exposure conditions. ASTM C 157 calls for specimens to be place in a curing environment that is maintained at 73 ± 3°F and a relative humidity of 50 ± 4% immediately after demolding. ASTM C 512 also required that specimen be moved into a controlled dry cure after a 7-day initial cure in 100% humidity room. For ASTM C 1556, a portion of the specimens followed an accelerated curing regime to simulate an older age. This was accomplished by placing the appropriate specimens in a water bath maintained at 105 ± 5°F for 28 days. All specimens were then placed into their exposure solutions. Specimens used for ASTM C 1012 had no curing period prior to testing. These specimens were demolded at 24 hours and immediately placed into an exposure solution.

Additional Mixtures

When analyzing the data gathered from the testing regime, it became evident that there were errors and inconsistencies between specimens. This variability in test data prompted the recreation of specimens for several test methods. The data gathered from these new specimens were used to supplement the existing data. Specimens were fabricated, cured, and tested identically to the initial mixtures.

New specimens were created for the modulus of elasticity, Poisson's ratio, splitting tensile strength, and flexural strength tests. Errors in the testing apparatus for modulus of elasticity and Poisson's ratio led to the full replacement of the existing data. The variability in the data gathered from splitting tension also prompted the full replacement of the existing data. Although the data from the flexural strength tests were consistent

and showed low variability, the results were inconclusive. Additional test specimens were needed to be created to test at later ages than was originally designed to determine the long range effects on the flexural strength of the mineral admixtures.

CHAPTER 4
LABORATORY TESTING

Evaluating the durability of concrete made with highly reactive pozzolans involved not only durability tests, but also plastic properties and mechanical properties. This chapter describes the test methods used to evaluate these important properties. To the extent possible, standard test methods were used. However, in some cases it was necessary to deviate from standard procedures or specimen configurations.

Plastic Properties Tests

The plastic properties tests were conducted to check the consistencies between mixtures and evaluate the affects of the mineral admixtures to the properties of the fresh concrete. The following plastic properties were measured: density, slump, air content, bleed water, time of set, and temperature.

Density (ASTM C 138)

The unit weight plastic property test is often conducted because of its simplicity. Typically, unit weight is measured as part of the air content procedure. From these results, yield estimation can be calculated. The use of different mineral admixtures have little affect on density as it is more greatly affected by aggregate type and entrained air (Mouli and Khelafi 2006).

Slump (ASTM C 143)

The slump test is a relatively simple field test that gives an estimate of concrete workability. This test is typically used to ensure a consistent workability and is sometimes used to determine if sufficient superplasticizer has been added to a mixture. The target slump of the design mixtures for the present research was 7 inches. Slump readings were taken immediately after the concrete was mixed. If the slump was less

than the target, high range water reducing admixture was added and slump was retested until the target slump was achieved. Because the recommended manufacture's dosages were not exceeded, it is expected that the physical characteristics of the hardened concrete remained unaffected.

Because of the spherical shape of the particles, fly ash reduces interparticle friction and increase slump (Neville 1995). Silica fume and ultrafine fly ash particles, however, because of their small size, have high surface areas and tend to increase the cohesiveness of the mixture (Mindess 2003). This results in a decrease in slump and a need for greater high range water reducer dosages to maintain the target slump. Slag and metakaolin also decrease the slump because of their angular and plate like particles (Bai et al 2003).

Air Content (ASTM C 173)

This test measures, by the volumetric method, the air contained in the mortar fraction of the concrete, without being affected by air contained within aggregate pores. This test method is unable to distinguish between entrapped and entrained air, as it only measures total air content. However, it does provide the means of evaluating the effects of an air entraining admixture when a mixture is properly consolidated to remove all entrapped air.

The addition of mineral admixtures will alter the effect of air entraining admixtures. High carbon content of some mineral admixtures will adsorb the entrained air, rendering the chemical admixture less effective. However, the carbon levels of the mineral admixture used in this investigation are low enough so that air entrainment will be unaffected. The high surface areas also alter the effectiveness of the air entraining admixture by requiring a larger dosage of air entrainer to reach the same air content

(Neville 1995). Therefore, if the same dosage of air entrainer was used for mixtures containing mineral admixtures as was with the control, the air content will be lower.

Air entraining admixture was implemented to decrease the bleeding, as well as increase the workability and cohesiveness of the concrete mixtures. The measurements of air content were used to establish a correlation between bleeding and air content.

Bleeding of Concrete (ASTM C 232)

This test measures the percentage of bleeding of a fresh concrete mixture. A metal beaker is filled with concrete and then consolidated. After troweling the surface level, the bleed water is collected and measured.

Bleeding is a form of segregation in which there is an upward movement of water after the concrete has been consolidated. This causes the upper layer of the concrete to have a high water-to-cement ratio resulting in increased porosity and lower durability in the cover concrete. Strength will also be reduced when large water pockets, caused by the upward movement of water during excessive bleeding, form under aggregate or reinforcing bars. Yet another adverse affect of bleeding is laitance. This occurs when a film of fine particles are carried to the surface by the bleed water. If the concrete is poured in lifts, this surface film will create a poor bond to the next lift. (Mindess et al., 2003)

Bleeding is reduced by using an air entraining admixture. The entrained air increases the cohesiveness of the particles, thus reducing bleeding segregation. Bleeding is also reduced by the use of mineral admixtures. Silica fume, ultrafine fly ash, and metakaolin have small particles that allow it to pack between cement grains, thus reducing the porosity; consequently, bleeding is reduced (Neville 1995). Research has shown, however, that slag may increase bleeding (Wainwright and Rey 2000).

Time of Setting (ASTM C 403)

The initial and final setting times of a freshly mixed concrete were determined by measuring the stress needed to penetrate the surface of a concrete. A stress of 500 lb/in^2 and 4000 lb/in^2 determined the initial and final setting, respectively.

Excessively long or short set times indicate possible problems with cement manufacturing, adverse chemical admixture reactions, or excess gypsum. Specific setting time patterns can indicate which problem may be the cause. Time of setting is also an important measurement to predict maximum mixing and transit times and to gauge the effectiveness of set-controlling admixtures.

The use of mineral admixtures affect the setting times of concrete mixture. Research has shown that all mineral admixtures used in this investigation lengthen the setting time (Brooks et al. 2000). Fly ash retards the early hydration of C_3S (ACI 232.2R-03). Mixtures containing over 25% slag will see delays in setting time (ACI 233R-03). Conversely, metakaolin mixtures have shown increases in setting (Zongjin and Ding 2003). ACI (234R-06) have suggested that silica fume does not affect the setting times.

Temperature (ASTM C 1064)

Temperature measurements were taken immediately from fresh concrete, and completed within 5 minutes after obtaining the sample. The temperature of fresh concrete mixes becomes a critical factor when placing in hot or cold environments. In hot weather concreting, problems can occur when concrete temperatures become too high. High temperatures can cause plastic shrinkage cracking, loss of workability and decreased setting times. In cold weather concreting, problems can arise if the fresh concrete temperatures becomes low enough to freeze early in its life. Therefore, a

measurement of fresh concrete temperature can provide an estimate on how it will perform in extreme temperature environments.

Generally, low reactivity mineral admixtures as small cement replacements will result in lower mixture temperatures. Conversely, high reactivity admixtures will increase the fresh concrete temperature. Research has shown that the incorporation of the low reactivity slag mineral admixture will result in a lower heat of hydration (Sioulas and Sanjayan 2000). On the other hand, Metakaolin additions have been shown to increase the fresh concrete temperature (Frias et al 2000). Research has shown that, separately, fly and silica fume will also reduce the temperature of a fresh concrete mixture (Langan et al 2002). However, this research has also shown that the combination of fly ash and silica fume retarded the initial hydration, resulting in lower temperatures.

Mechanical Tests

Standard test methods were conducted to determine the mechanical characteristics of the concrete. These characteristics are frequently used in structural design to estimate a variety of other concrete properties. Physical behavior also can be predicted based on the results of these mechanical tests, such as deflection and prestressing losses.

Compressive Strength (ASTM C 39)

The addition of mineral admixtures has a significant affect on the compressive strength of concrete. The early strength will be reduced if a low reactivity admixture, such as fly ash and slag, are used in a mixture (ACI 232.2R-03 and ACI 233R-03). The increased fineness of ultrafine fly ash makes it more reactive than ordinary fly ash. However, research by Jones (et al 2006) has shown that there is still a reduction in early strength development of ultrafine fly ash mixtures when compared to the control. Conversely, early age strengths are typically higher than the control for high reactivity

pozzolans such as metakaolin and silica fume (Qian 2001 and ACI 234R-06). Late age strengths of concretes containing these mineral admixtures will be higher than the control. This is attributed to the stronger, more homogenous paste matrix created by the pozzolanic reactions.

The compressive strength of three 6 inch diameter x 12 inch long cylinder were tested at ages of 3, 7, 28, 91, and 365 days. In lieu of capping, the ends of each cylinder were ground smooth using a DIAM-end Grinder manufactured by M&L Testing Equipment as shown in Figure 4 - 1.

Figure 4 - 1 DIAM-end Grinder

All cylinders were cured in a moist condition at a temperature of 73.4 ± 3.0°F, so that free water was maintained on the surface at all times. Each test was completed within an hour of removal from the curing room on a Test Mark load frame as shown in Figure 4 - 2. Cylinders were loaded continuously and without shock at 20 to 50 pounds per square inch per second.

Figure 4 - 2 Test Mark Load Frame

Because cracking is initiated in the tensile region of the beam, the behavior of a concrete beam during a beam tests is governed by the tensile strength. Since the tensile strength of a concrete is largely a function of the aggregate to paste bond, flexural strength is sensitive to the strength and size of the interfacial transition zone (ITZ). Mineral admixtures consume Calcium Hydroxide (CH) and reduce ettringite formation,

creating a stronger concrete ITZ. Therefore, the use of mineral admixtures will typically improve the flexural strength of a concrete over time. Early strength development is reduced in the admixture with low reactivity, such as fly ash and slag (ACI 232.2R-03 and ACI 233R-03). Conversely, the higher reactivity mineral admixtures, silica fume and metakaolin, will have higher modulus of rupture when compared to the control (ACI 334R-06 and Kim et al 2007). Research related to the effect of ultrafine fly ash on flexural strength seems to be unavailable. However, it is expected that because the surface area is increased, the ultrafine fly ash mixtures will show a larger flexural strength at early ages when compared to the ordinary fly ash mixtures. At later ages, the mineral admixtures will provide an increase in flexural strength when compared to the control mixtures because of the improvement in the ITZ.

Specimens were cast into 4 inch wide x 4 inch high x 14 inch long beams and tested at two ages—7 day and 28 day. All beams were cured in a moist condition at a temperature of $73.4 \pm 3.0^{o}F$, so that free water was maintained on the surface at all times. Each test was completed within an hour of removal from the curing room. Beams were loaded continuously and without shock at a rate of 125 to 175 pounds per square inch per minute on an Instron load frame as shown in Figure 4 - 3 and Figure 4 - 4.

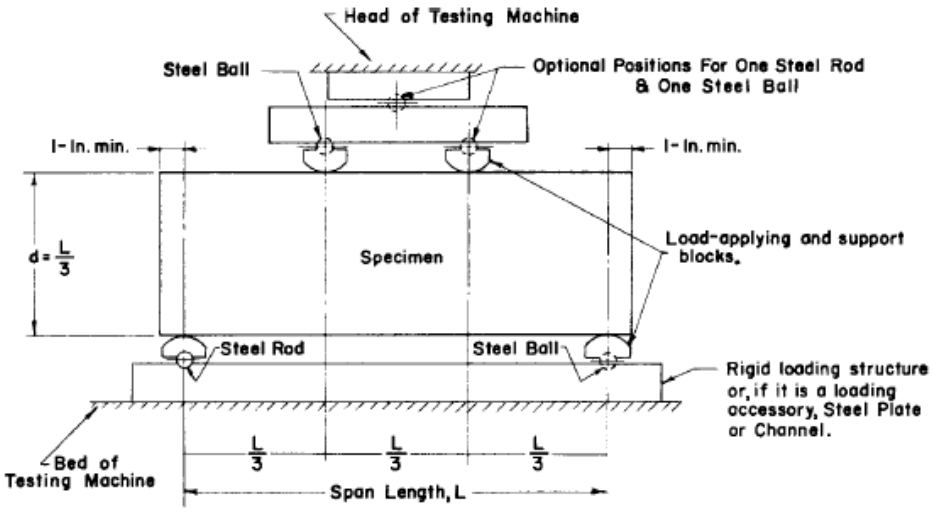

Figure 4 - 3 Diagram of the Third-Point Loading Flexure Testing Apparatus

Figure 4 - 4 Instron Load Frame Testing Flexural Strength

Static Modulus of Elasticity and Poisson's Ratio (ASTM C 469)

Research has shown (Nassif et al. 2004) that the addition of mineral admixtures will increase the modulus of elasticity of the concrete at late ages. However, for high volume replacement of low reactive mineral admixtures such as fly ash and slag, early age modulus of elasticity may be reduced. The amount of decrease will depend on the type and quantity of admixture implemented.

Very little research has been conducted to find the relationship of various mineral admixtures to Poisson's ratio. The research that had been conducted shows no discernable change in Poisson's ratio with the addition of mineral admixtures. (Mirza et al 2002) However, this data is not sufficient to make a definitive prediction of the affects of mineral admixtures.

The procedure was performed in slight variation to ASTM C 469. The Standard calls for the specimen to be loaded to 40% of its ultimate strength. However, slight damage may be induced at this level. Bond cracks will exist in concrete at zero load due to differences in the elastic moduli between the hardened cement paste and the aggregates, different coefficients of thermal expansion, as well as different responses to moisture content. For stress levels up to 30% of the ultimate, little additional cracking will be observed. Bond microcracking begins to increase at stresses above 30 to 40% of the compressive strength. (Mindess et al., 2003) Therefore each specimen was only load to 25% of its ultimate strength. The rest of the procedure was conducted in accordance to the Standard. Figure 4 - 5 shows the instrumentation and testing apparatus used to measure the Modulus of Elasticity and Poisson's Ratio.

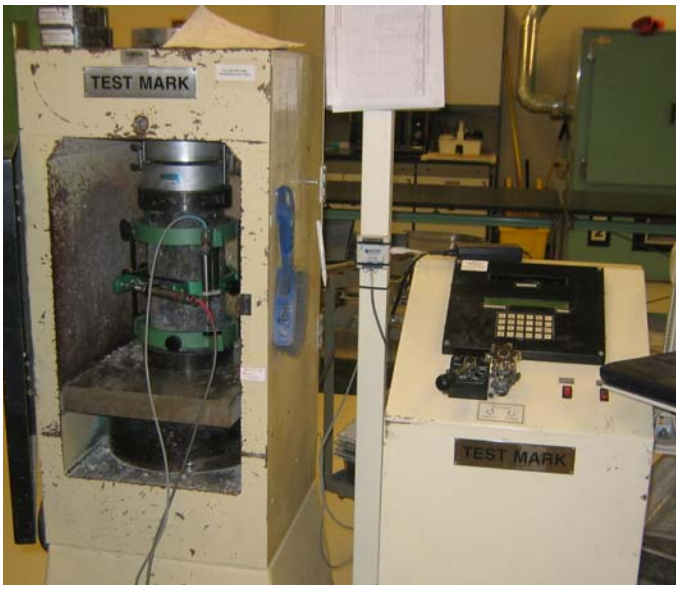

Figure 4 - 5 Modulus of Elasticity and Poisson's Ratio Test Setup on the TEST MARK system

Because of the low stress levels used to test for Modulus of Elasticity (MOE), the same 6 inch diameter x 12 inch long cylinders that were used for MOE could be used for compressive strength tests. An initial test of compressive strength was conducted on the first cylinder from each set of three. Each of the two remaining cylinders were loaded three times to measure the MOE. The initial load, which was primarily for seating the gages, was ignored. The two subsequent loadings were then used to calculate an average modulus of elasticity for that cylinder. An average was then taken of the results from the two cylinders. Testing was conducted at 3, 7, 28, 91, and 365 day ages.

Poisson's Ratio was also obtained when testing for MOE. The results from the second and third loading were averaged for each cylinder. The data from both cylinders were used to calculate an average Poisson's ratio for each mix. Testing was conducted at 3, 7, 28, 91, and 365 day ages.

Splitting Tensile Strength (ASTM C 496)

ASTM has yet to adopt a standard test method to provide a direct measurement of tensile strength. This is because the problems with secondary stresses from gripping make it is very difficult to get consistent and reproducible results. However, a standard test, ASTM C 496, has been created to estimate tensile strength through indirect tension.

Because the failure of concrete in tension is governed by microcracking, the ITZ will control the tensile strength of a concrete. (Mindess et al., 2003) The use of mineral admixtures will result in consumption of CH and reduction of ettringite formation, creating a stronger ITZ. As with flexural strength tests, the use of mineral admixtures in concrete used for splitting tensile strength tests will improve the tensile strength of a concrete as the pozzolanic reactions take place.

Specimens cast into 4 inch diameter x 8 inch long cylinders were tested at 3, 7, 28, 91, and 365 days of age. All cylinders were cured in a moist condition at a temperature of 73.4 ± 3.0^{o}F, so that free water was maintained on the surface at all times. Each test was completed within an hour of removal from the curing room on a Forney Load frame as shown in Figure 4 - 6.

Figure 4 - 6 Splitting Tensile Strength Test on Forney Load Frame

Durability Tests

The deterioration of concrete is the result of poor performance of the three major components: reinforcement, paste, and aggregate. This can be the result of either chemical or physical causes. The durability tests performed in this investigation involve the assessment of each concrete mix's physical characteristics and response to chemical attack. The use of mineral admixtures will alter the concrete paste and paste structure by creating a stronger, more homogenous paste matrix, less permeable void space, and refined capillary pore structure—all of which result in an improvement to durability.

Linear Shrinkage (ASTM C 157)

The linear shrinkage test assesses volumetric expansion or contraction of concrete due. Moisture loss through the concrete pore structure is the dominant factor in shrinkage (Mindess et al. 2003). Because of the typical reduction in capillary porosity, the use of mineral admixtures will reduce linear shrinkage by decreasing the porosity in a concrete. Research has shown that metakaolin mixtures exhibit a reduction in total linear shrinkage (Brooks and Megat Johari 2001). ACI has suggested that slag will reduce linear shrinkage (ACI 363R-03). Research conducted by Akkaya (et al. 2007) has shown that fly ash and ultrafine fly ash show little decrease in total shrinkage compared to the control. ACI (364R-06) states that silica fume also has little effect on total shrinkage.

ACI also states that silica fume and fly ash has no significant affect on linear shrinkage at small replacements levels (ACI 364R-06 and ACI 323.2R-03). Research on the effects of ultrafine fly ash on linear shrinkage seems to be unavailable.

Linear shrinkage specimens were cast into 3 inch wide x 3 inch high x 11.25 inch long prism molds. Immediately after removal from the molds, the specimens were dry

cured by placing them an environment controlled at a constant temperature of 73 ± 3 °F and a constant relative humidity of 50 ± 4%. Due to mechanical problems with the environmental control system, temperature and relative humidity were slightly varied from that specified in ASTM C 157. The actual temperature and relative humidity readings are presented in Appendix A. Comparator readings were taken on all specimens at an age of 4, 7, 14, and 28 days, and after 8, 16, 32, and 64 weeks.

Volume of Voids (ASTM C 642)

This method was used to measure the percentage of voids within a hardened concrete. If exposed to a corrosive environment, these voids are susceptible to becoming filled with deleterious chemicals. A reduction in void volume is therefore beneficial to a concrete. Mineral admixtures will reduce the volume of voids through an increase denser hydration products produced from the pozzolanic reactions.

Samples were cut from 2 inches below the finished surface of a molded 4 inch diameter x 8 inch long concrete sample. Tests were conducted on each mixture at 28 days of age.

Sulfate Expansion (ASTM C 1012)

Length change measurements permit the relative assessment of the sulfate resistance of concrete or mortar subjected to total immersion in a sulfate solution. The sulfate ions in the solution combine with gypsum and CH to create an expansive reaction. This reaction, however, can be limited by the use of mineral admixtures. There are two means that mineral admixtures inhibit sulfate expansion: a refinement of the capillary porosity and a reduction in CH. ACI (232.2R-03; 233R-03; 234R-06) suggests that fly ash, slag, and silica fume increase a concrete's resistance to sulfate attack. Research has shown that metakaolin also improves the resistance to sulfate attack (Khatib and Wild

1998). Little research has been conducted on the relations of ultrafine fly ash with sulfate attack. It is expected, however, that ultrafine fly ash will perform better than fly ash concretes, because the smaller particle size will further reduce permeability.

Specimens for the present research were cast into 3 inch wide x 3 inch high x 11.25 inch long and 1 inch wide x 1 inch high x 11.25 inch long molds for concrete and mortar, respectively. Mortar was sampled from the fresh concrete mix; fresh concrete was passed through a 3/8 inch sieve to remove the coarse aggregate. All specimens were immersed into a 5% SO_4 solution at 24 hours after casting, immediately after their removal from the molds. The water temperature of the sealed tanks containing the sulfate solution was maintained at $73.5 \pm 3.5^{o}F$. Readings were taken at 1, 2, 3, 4, 8, 13, and 15 weeks of exposure.

Absorption (ASTM C 642)

There are four transport mechanisms that allow the penetration of deleterious chemicals into concrete. These mechanisms are permeability, diffusivity, evaporative transport, and absorptivity. In an unsaturated concrete, absorption will play a significant role in chemical transport. Absorption is controlled, in large part, by the connectivity of the capillary pore system. Solution is drawn by capillary suction allowing harmful chemicals, such as chlorides and sulfates, to enter the concrete. This test method gives a means of assessing the capillary pores structure by measuring the absorptivity of an unsaturated concrete. The use of mineral admixtures will refine the capillary pore structure through pozzolanic reaction. Consequently, the absorptivity of a concrete will be reduced.

Specimens for the present research were prepared using a 4 inch diameter x 8 inch long cylinder molds. Each cylinder was cured in a moist condition at a temperature of 73.4 ± 3.0°F, so that free water was maintained on the surface at all times. From each of these cylinders a 2 inch thick slice was cut from 6 inches below the finished surface. This test was conducted on each mixture at 28 days of age.

Corrosion of Embedded Steel Reinforcement (ASTM G 109)

Corrosion is a particularly problematic phenomenon in reinforced concrete structures subjected to chloride ions. Because it is an expansive reaction, corrosion of steel reinforcement leads to the cracking and spalling of the adjacent concrete. This will then lead to a direct, unobstructed path for additional elements to corrode the underlying steel reinforcement. This method provides the means of assessing a concrete's ability to inhibit the corrosion of embedded steel reinforcement. The use of mineral admixture will delay or even prevent the corrosion of the embedded steel reinforcement by improving the surrounding concrete. The mineral admixtures refine capillary porosity, reduce permeability, and improve the ITZ. Each of these effects will reduce the ingress of chloride ions.

Each specimen was fabricated using a mold containing three #4 deformed steel reinforcing bars and a titanium reference electrode as shown in Figure 4 - 7. At an age of 24 hours, each specimen was demolded and allowed to cured in a moist condition at a temperature of 73.4 ± 3.0°F, so that free water was maintained on the surface at all times until they were 28-days of age. At this time, each specimen was placed in an environmental chamber maintained at 50% relative humidity for a period of two weeks. Following this conditioning, a 6 inches long x 3 inches wide x 3 inches high plastic dam

was installed on the top of each specimen. All sides were then sealed, with the exception of the bottom and the inside of the damned area, using Sikadur 32 High Mod epoxy. Figure 4 - 8 shows the ASTM G109 specimen after the dam and epoxy seal was constructed.

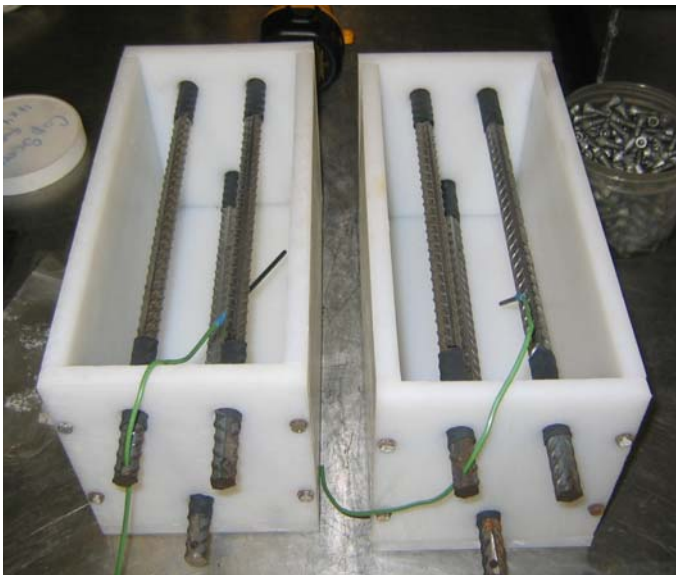

Figure 4 - 7 ASTM G109 Specimen Molds containing the Reinforcing Bars and Reference Electrode

Figure 4 - 8 ASTM G109 Specimen After The Epoxy Has Been Applied

Samples were then placed back into the environmental chamber until they were of 56 days of age. At this time, a non-standard testing procedure was followed. ASTM G

109 states that samples should be ponded with a 3% NaCl, and stored at 73 ± 5.0°F and a relative humidity of 50 ± 5%. To accelerate corrosion, a 15% NaCl solution was used with the specimens exposed to 90 ± 5°F. The specimens were connected to automated monitored device that measured current and potential once daily at the FDOT SMO. A photograph of this setup can be seen in Figure 4 - 9. Each specimen was subjected to a cycled regime of the 15% NaCl solution; the cycles were maintained at two weeks of sealed continuous ponding, followed by two weeks of drying. An electrical diagram of the test setup is presented in Figure 4 - 10.

Figure 4 - 9 Environmental Room Containing the Automated Monitoring Device and Corrosion Specimens

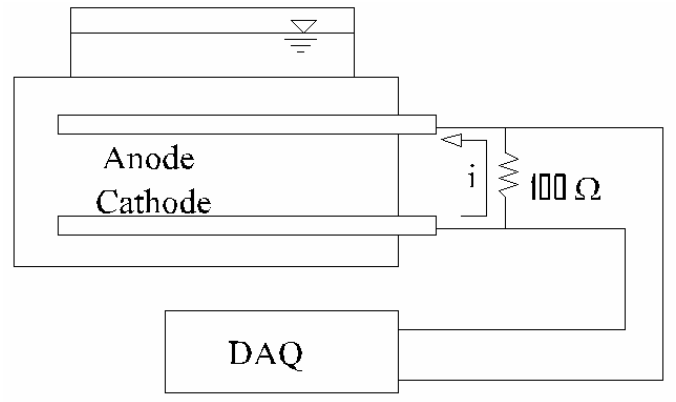

Figure 4 - 10 Electrical Diagram of Corrosion Specimens

Background Chloride Level (FM 5-516)

This method is used to determine the background levels of chloride in a concrete mixture. The results were used in calculations to determine the absolute level of chloride intrusion for ASTM C 1556. The use of mineral admixtures has no affect on this test, as their compositions do not contain chlorides.

A concrete and paste sample was taken from the fresh concrete and allowed to hydrate for 3 days. Next, the hydrated concrete and paste was pulverized so that samples could be taken for chloride analysis. A chemical titration was performed to find the initial chloride content of each mix.

Surface Resistivity (FM 5-578)

This non-destructive test measures the electrical resistivity across the face of a concrete specimen to provide an indication of its permeability. As the surface resistance increase, the correlated permeability decreases. The use of mineral admixture will increase the surface resistivity by lowering the permeability of the concrete.

All specimens were water-saturated 4 inch diameter x 8 inch long molded cylinders. These samples were cured in a moist room containing no saturated lime water, as this decreases the resistivity of the concrete. A Surface Resistivity meter with a Wenner linear four-probe array was implemented as shown in Figure 4 - 11. Surface resistivity was found in accordance with FM 5-578 for concrete cylinders at 3, 7, 28, 91, and 365 days of age.

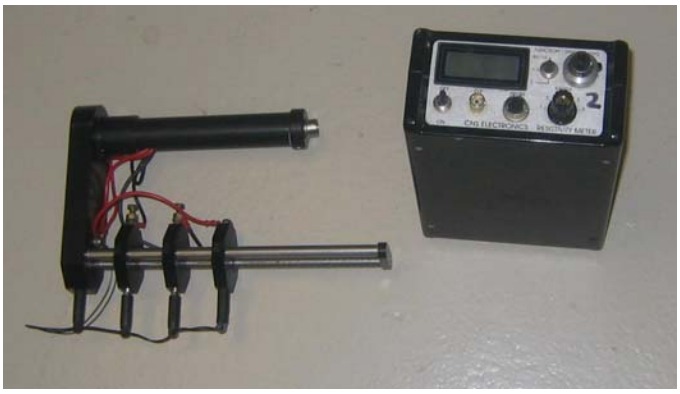

Figure 4 - 11 Wenner Linear Four-Probe Array and Display

Rapid Migration Test (NTBuild 492)

This procedure was used to determine the chloride migration coefficient in concrete from non-steady-state migration experiments. A low migration coefficient effectively indicates that the porosity is low enough to limit the migration of chloride ion into a concrete. The implementation of mineral admixtures will create a denser, less permeable concrete. The paste structure will be composed of a more homogenous C-S-H matrix, smaller ITZ, and less interconnectivity of pores. Therefore, the use of mineral admixtures will reduce chloride ion penetration.

Samples for this research were cut from 4 inches below the finished surface of molded 4 inch diameter x 8 inch long concrete cylinders. Cylinders were cured in a moist condition at a temperature of 73.4 ± 3.0^{o}F, so that free water was maintained on the surface at all times. Tests were conducted at 28, 56, and 91 days of age. At the appropriate test date, specimens were remove from the curing room and preconditioned by desiccating for three hours. Next, while maintaining vacuum, the desiccation chamber was filled with a saturated $Ca(OH)_2$ and vacuumed for an additional hour. The specimens were kept in the solution for 18 ± 2hours. Each specimen was then placed in the test setup as shown in Figure 4 - 12. A 30V potential was applied to the sample to

measure the initial current. From that reading the voltage was adjusted to the standardized value for each specimen. Table 4 - 1 details the test voltage and duration corrections given in NTBuild 492. The test was then conducted for 18 hours.

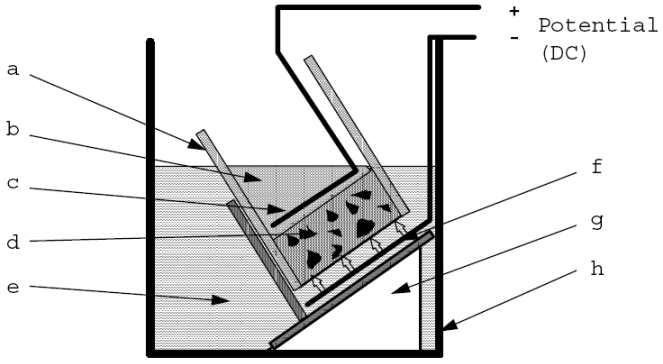

a. Rubber sleeve
b. Anolyte
c. Anode
d. Specimen
e. Catholyte
f. Cathode
g. Plastic support
h. Plastic box

Figure 4 - 12 RMT Test Setup

Table 4 - 1 Test Voltage and Duration for NTBuild 492

Initial Current @ 30V [mA]	**Applied Voltage [Volts]**	**Test Duration [hr]**	**Expected Penetration [mm]**	**V*t [V-hr]**
< 5	60	96	< 23	5,760
5-10	60	48	12-20	2,880
10-15	60	24	10-15	1,440
15-20	50	24	12-16	1,200
20-30	40	24	12-18	960
30-40	35	24	15-21	840
40-60	30	24	18-27	720
60-90	25	24	22-33	600

90-120	20	24	26-35	480
120-240	15	24	26-54	360
240-400	10	24	36-77	240
400-600	10	24	36-77	240
> 600	10	6	> 19	60

Immediately following the test, each specimen was removed and split longitudinally. A silver nitrate solution was then sprayed on exposed surface to highlight the chloride penetration. Measurements to the nearest 0.1 mm were then made using a digital caliper. From these measurements the migration coefficient was calculated from the following equation:

$$D_{nssm} = \frac{0.0239(273 + T)\cdot L}{(U - 2)\cdot t}\cdot\left[x_d - 0.0238\sqrt{\frac{(273 + T)\cdot L\cdot x_d}{U - 2}}\right] \quad (4\text{-}1)$$

where D_{nssm} is the migration coefficient, x 10^{-12} m^2/s; U is the absolute value of the applied voltage, V; T is the average value of the initial and final temperature in the anolyte solution, °C; L is the thickness of the specimen, mm; x_d is the average value of the penetration depths, mm; t is the test duration, hr.

Water Permeability (UF Method)

A concrete structure can be severely compromised through direct intrusion of deleterious chemicals, such as chloride and sulfate. Therefore the concrete's ability to resist sulfate or chloride ion penetration is an essential factor in the performance of a durable concrete. It is for this reason that permeability becomes an important

characteristic of a concrete. The implementation of mineral admixtures will create a less permeable concrete. The concrete rheology and hardened structure will be altered by the pozzolans. Better consolidation and less bleeding can be achieved. This creates a concrete with less capillaries and interconnected pores. The mature concrete is also affected; through pozzolanic reaction, a denser and less permeable C-S-H product is produced.

In previous research (Soongswang et al., 1989) a testing method was developed to directly measure the water permeability of a concrete sample. Permeability specimens were created for this method from molded 4 inch diameter x 8 inch long molded concrete cylinders. All cylinders were cured in a moist condition at a temperature of $73.4 \pm 3.0^{o}F$, so that free water was maintained on the surface at all times. From each of these cylinders a 2 inch thick slice was cut from 3 inches below the finished surface. Around each slice, a 2 inch wide impermeable epoxy (Sikadur 32 High-Mod) ring was cast and allowed to cure for 24 hours. This epoxy ring serves to bond with the sides of the concrete so that a one-dimensional flow will be achieved during the permeability test. Sikadur 32 High-Mod epoxy was utilized because it has a higher strength and a similar coefficient of thermal expansion as the concrete used in this investigation. The permeability testing specimens was then installed into the Plexiglas fixture as shown in Figure 4 - 13.

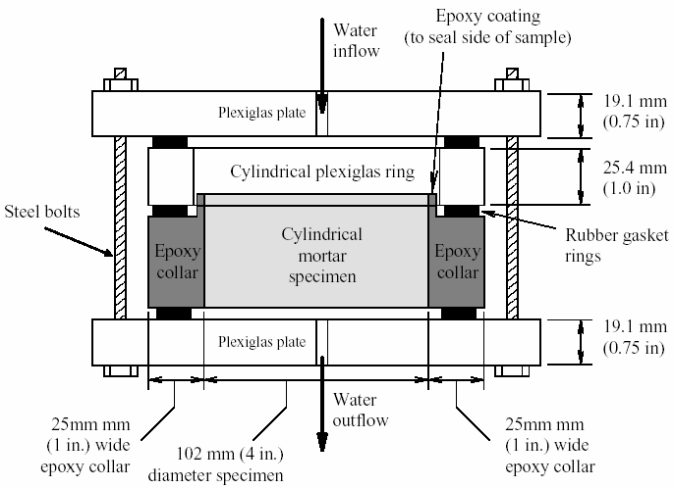

Figure 4 - 13 Cross-Section of Water Permeability Specimen Fixture

The specimen and fixture was then attached to the permeability testing apparatus as shown in Figure 4 - 14. A constant 80 pound per square inch water pressure was applied to each specimen. After steady state had been achieved, the specimen was then removed from the apparatus.

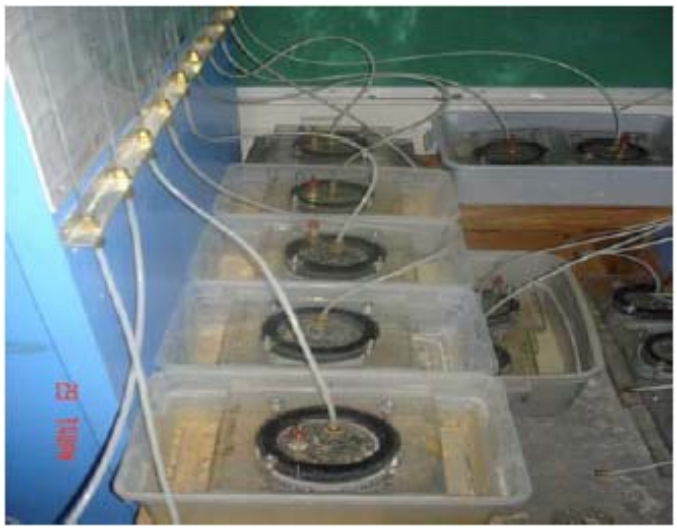

Figure 4 - 14 Water Permeability Test Setup

CHAPTER 5
RESULTS AND DISCUSSION

This chapter describes and discusses the results obtained through experimental analysis. Inconsistencies in test data prompted the re-creation of test specimens for MOE, Poisson's ratio, and flexural strength tests. These changes are presented in the mechanical test section below.

Plastic Properties Tests

The results from the plastic properties tests are presented in Table 5 - 1. Each value represents either a single test result or an average of individual tests, depending on the test method. Unit weight, for example, was taken during mixing and represents a single test. The values differed by no more than 2% from the extreme measured values. All plastic properties tests were performed at the Florida Department of Transportation's State Materials Office (FDOT SMO).

Table 5 - 1 Plastic Properties

Mix	Density (lb/ft^3)	Slump (in)	Air (%)	Bleed (%)	Initial Set (min)	Final Set (min)	Mix Temp. (^oF)	Air Temp. (^oF)
CTRL1	145	5.75	2.0	0.00	300	395	81	75
CTRL2	145	6.00	1.5	0.10	330	400	84	75
SLAG1	144	6.50	1.1	0.19	340	430	81	75
SLAG2	144	6.00	1.0	0.17	355	460	81	75
SLAG3	146	6.50	0.6	0.27	300	445	80	75
META1	144	6.25	1.4	0.00	375	435	84	75
META2	144	7.25	1.5	0.00	390	470	80	75
META3	144	6.00	1.4	0.00	N/A	N/A	80	75
UFA1	146	5.75	0.6	0.55	375	465	78	75
UFA2	145	6.75	1.8	0.00	385	485	78	75
UFA3	144	8.00	1.6	0.00	400	480	78	75
SF1	143	6.25	2.3	0.00	370	445	76	75
SF2	143	6.00	2.3	0.00	385	465	76	75

Density was measured and found to vary by 2% for all mixtures. This indicates that there are no large variations in entrapped air or aggregate volume among mixtures.

Slump measurements were between 5.75 to 8 inches, indicating reasonably consistent results. Due to natural variability of concrete workability, a consistent concrete slump from mix to mix is difficult to obtain. For most mixtures, however, the slump values were within ± 1 inch of the 7-in. target value. This allowed for consistent consolidation among mixtures, thus minimizing variation in test results due to inconsistent specimen fabrication.

Air content was found to range from 0.6% to 2.3%, which was below the target air content of 3%. The measured values, however, were within the acceptable range of 1 to 5% except for SLAG3 and UFA1, which had an air content of 0.6%. These lower air contents appeared to result in an increase in bleeding when comparing the results for SLAG3 and UFA1 of 0.27% and 0.55%, respectively. CTRL2, SLAG1, and SLAG2, however, also showed some bleeding, but without an extremely low air content.

Setting times conducted on the cement paste found that initial set was at 140 minutes and final set at 215 minutes. The concrete mixtures in this investigation had initial setting times that ranged from 300 to 400 minutes; final setting times ranged from 395 to 485 minutes. These setting times are greater than that of the paste by 114% to 185% and 84% to 126% for initial and final setting times, respectively. For CTRL1, the setting time increased by 114% for initial set and 84% for final set over the cement tests. This indicates that the addition of the retarder was successful in delaying the setting times. CTRL2 (18% fly ash) also shows extended setting times when compared to CTRL1 (cement only), revealing that the replacement of cement with fly ash retards the setting times. In addition, all other mixtures show an increase in setting times over CTRL2, indicating that the larger quantity of mineral admixtures further delays the setting times. The literature has suggested that metakaolin shortens the setting times, while silica fume has no affect (Zongjin and Ding 2003; ACI 234R-06). However, when looking at the mixtures with the same proportions of mineral admixtures, such as META1 (18% fly ash and 8% metakaolin) and SF1 (18% fly ash and 7% silica fume), little difference in setting times are noticed. This suggests that setting time is more greatly affected by the decreases in proportions of cement, rather than the addition of a particular admixture.

Fresh concrete temperatures ranged from 76 to 84°F, while the air temperature remained constant at 75°F. This temperature range is small; therefore, with this level of replacement, there was little affect on the fresh concrete temperature from the addition of the mineral admixtures.

Mechanical Tests

The mechanical test results for compressive strength, flexural strength, MOE, Poisson's ratio, and splitting tensile strength are presented below. Trends and relationships have been noted in the results of each test. However, errors and inconsistencies have been found in the results from the MOE and Poisson's ratio tests. This prompted the re-creation of duplicate test specimens. These specimens were created for testing at 7, 28, and 365 day ages and tested under the same conditions.

Compressive Strength (ASTM C 39)

Figure 5 - 1 shows the strength gain curve for all the mixtures. Early compressive strength of concrete made with slower reacting mineral admixtures, such as slag and fly ash, was less than that of the concretes made with portland cement alone, as seen in the lower values of early strength in the plot. In contrast, mixtures made with silica fume and metakaolin exhibited a higher strength than with portland cement alone. At later ages, however, the low reactivity mineral admixtures continued to react and by 365 days, the compressive strength had converged to values of just about 10.5 ksi. The lower compressive strength of SLAG3 was likely the result of errors in mixing that will be discussed subsequently.

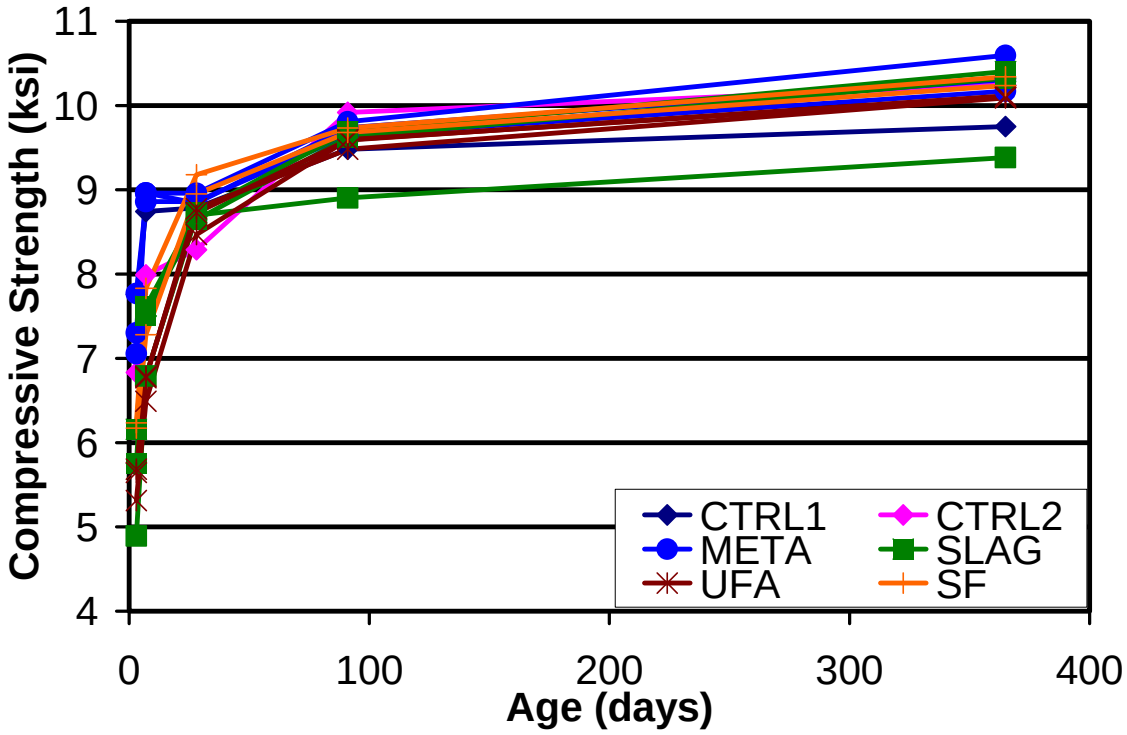

Figure 5 - 1 Compressive Strength of All Mixtures

Although the strength gain curve is not linear, it is also useful to examine the rate of strength gain by considering the slopes of the lines between the 91 and 365 day strengths. These slopes presented in Table 5 - 2 show the average 365 day compressive strength for each mixture. The compressive strengths are also normalized to the CTRL1 strength to show the improvement and relative value. Disregarding SLAG3, the compressive strengths vary from CTRL2 by no more than 3%, indicating vary consistent values at late ages. The slopes of CTRL1 and CTRL2, however, are nearly parallel, indicating that their rates of hydration are comparable even though CTRL2 contains fly ash.

Table 5 - 2 Average Compressive Strength at 365 days, Normalized 365 day Compressive Strength to CTRL2, and 91 to 365 day Slope

	365 day Compressive Strength (ksi)	Normalized Compressive Strength	91 to 365 day Slope (ksi*10^5/day)
CRTL1	9.75	0.95	9.8
CTRL2	10.25	1.00	11.9
SLAG1	10.40	1.02	26.0
SLAG2	10.33	1.01	25.8
SLAG3	9.38	0.92	17.5
META1	10.17	0.99	19.1
META2	10.31	1.01	20.7
META3	10.59	1.03	28.8
UFA1	10.09	0.99	18.3
UFA2	10.09	0.98	22.3
UFA3	10.11	0.99	19.2
SF1	10.24	1.00	20.4
SF2	10.34	1.01	22.1

Furthermore, the slopes of the slag mixtures are parallel and are steeper than that of the control mixtures, indicating a higher rate of hydration. Similarly, the metakaolin, ultrafine fly ash, and silica fume mixtures show steeper slopes than the control mixtures. Therefore, it is likely that these mixtures will produce higher compressive strength than the controls at later ages. However, because the strength gain curves are non-linear, accurate predictions of later compressive strengths cannot be made.

At various ages, the compressive strength of a concrete plays at key role in the selection of a mixture. For example, in the prestressing industry, early compressive strength is needed to allow for the release of prestressed concrete member from the prestressing bed. Conversely, higher compressive strength at later ages is needed for piling to prevent damage during driving. Therefore, a more refined analysis of the early and late compressive strengths of each mixture is discussed.

Figure 5 - 2 shows the early age strength development of the concrete mixtures containing ground granulated blast furnace slag compared to the two control mixtures.

Figure 5 - 3 presents the late age strength development. The control mixture, CTRL1 (cement only), had a higher early strength than CTRL2 (18% fly ash), which is typical of low early strength developing mixtures containing low reactive mineral admixtures. Generally, a mixture with a slower initial hydration rate will produce a denser calcium silicate hydrate (C-S-H) matrix at a later age. It is this C-S-H matrix that will have the largest contribution to a concrete's compressive strength, producing a higher strength later when compared to a high early strength mixture.

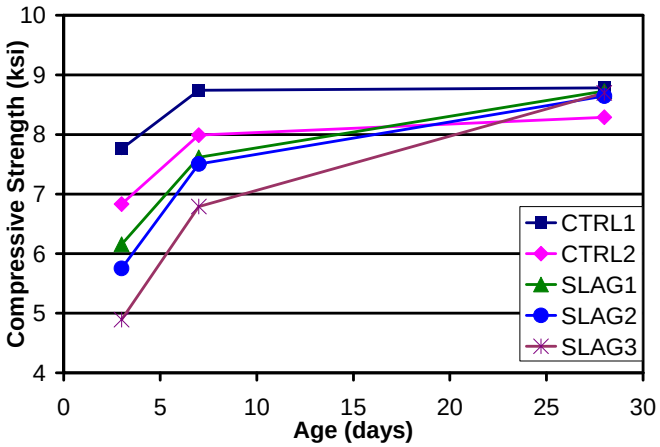

Figure 5 - 2 Average Early Strength of Slag Mixtures

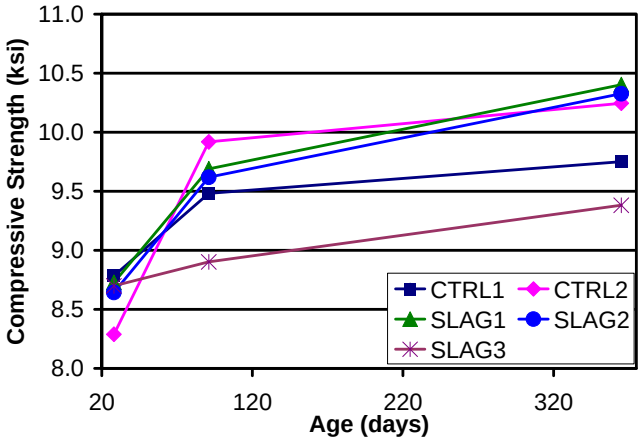

Figure 5 - 3 Average Late Strength of Slag Mixtures

The data show that the average compressive strength of each slag mixture at 3 days and 7 days age is below that of the two control mixtures, which is a result of the further

delay caused by the replacement of portland cement with slag. Generally, slag has low reactivity at early ages and therefore will not contribute to early strength development. Indeed, it is not until around an age of 91 days when the slag mixtures begin to have a higher compressive strength than CTRL1. At 365 days, the compressive strength of both SLAG1 and SLAG2 show a strength well above that of CTRL1, and slightly higher than CTRL2.

The data from Figure 5 - 2 and Figure 5 - 3 show that SLAG3 exhibits lower strength than SLAG1 and SLAG2. As mentioned before, the higher mineral admixture content in SLAG3 was expected to develop higher compressive strengths than SLAG1 and SLAG2. However, this did not happen. From Table 5 - 1, it is clear that SLAG3 shows a high bleed percentage when compared to other mixtures. This would suggest that there were problems with mixing. If the mixed proportions were incorrect, this may lead to a worse performing concrete than would be expected. Indeed, this trend of poor performance of SLAG3 is noted throughout subsequent test procedures.

Figure 5 - 2 also shows that at early ages, the average compressive strength decreases as mineral admixture content is increased. In contrast, this trend seems to be reversed as the age of specimens increases. The data show that at 91 days of age, all slag mixtures are very close to having the same compressive strength. As mentioned before, ground granulated blast furnace slag generally has low reactivity at early ages and will begin to develop a dense C-S-H matrix as hydration continues. Therefore, the mixtures containing higher proportions of slag will exhibit a low early strength. At later ages, however, the slag will begin to react and eventually develop a higher strength concrete in the mixtures containing higher volumes of slag.

Figure 5 - 4 shows the early age strength development of the mixtures containing metakaolin compared to the two control mixtures. Figure 5 - 5 presents the late age strength development. Because of its high reactivity, the metakaolin mixtures show a high early strength when compared to the control mixtures. As expected, all metakaolin mixtures have an average compressive strength above that of CTRL2 for 3 day, 7 day and 28 day ages. The strength of the metakaolin mixtures then begin to overtake that of CTRL1 at an age of apparently 7 days. At an age of 91 days, however, CTRL2 has developed a higher strength than CTRL1 and all mixtures containing metakaolin. This is explained by the denser C-S-H matrix developed in slower hydration of the fly ash itself in CTRL2. By 365 days, however, the compressive strength of META1 and META2 are nearly equal to that of CTRL2. META3 shows that highest strength.

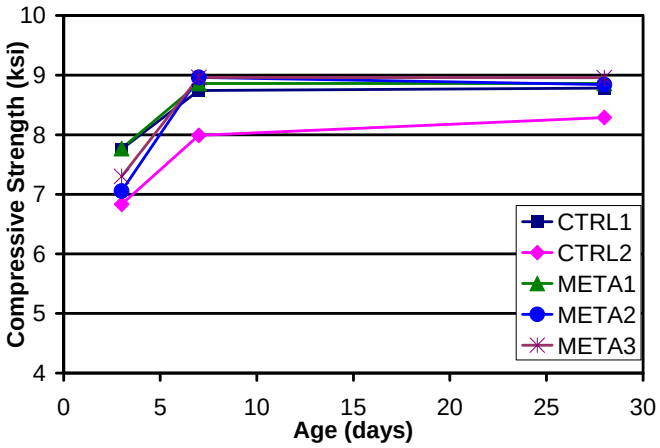

Figure 5 - 4 Average Early Strength of Metakaolin Mixtures

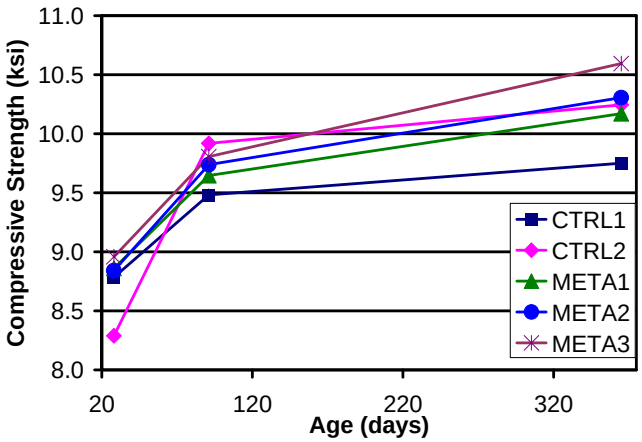

Figure 5 - 5 Average Late Strength of Metakaolin Mixtures

As the proportion of metakaolin increases, the data show a higher average compressive strength at later ages. The higher content of mineral admixture results in a larger amount of available silicate oxide (S) to react with calcium hydroxide (CH) to produce a denser matrix of C-S-H compounds.

Figure 5 - 6 shows the early age strength development of the mixtures containing ultrafine fly ash compared to the two control mixtures. Figure 5 - 7presents the late age strength development. The mixtures containing ultrafine fly ash have a similar strength development as the mixtures containing slag. Because both slag and ultrafine fly ash have low reactivity, their early age strength gain will be slow. At 3 day and 7 day ages, all mixtures containing ultrafine fly ash have a lower average compressive strength than both CTRL1 and CTRL2. At 28 day age, all three ultrafine fly ash mixtures have a higher strength than CTRL2, while CTRL1 remains at nearly the same strength. As the strength begins to develop, CTRL2 compressive strength becomes the highest. This again is due to the dense C-S-H matrix formed by the slow hydration rate of fly ash. At 91 days, CTRL2 continues to develop strength, while the ultrafine fly ash mixtures and CTRL1 have nearly the same compressive strength. However, by 365 days, the

compressive strength of the ultrafine fly ash mixtures are only slightly lower than CTRL2. The strength of CTRL1 is still considerably lower than the other mixtures.

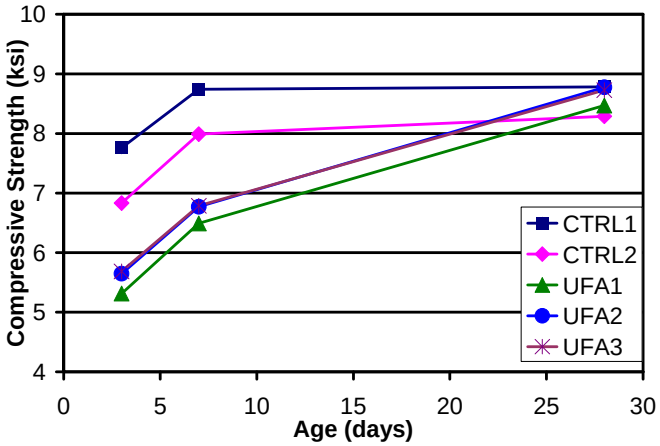

Figure 5 - 6 Average Early Compressive Strength of Ultrafine Fly Ash Mixtures

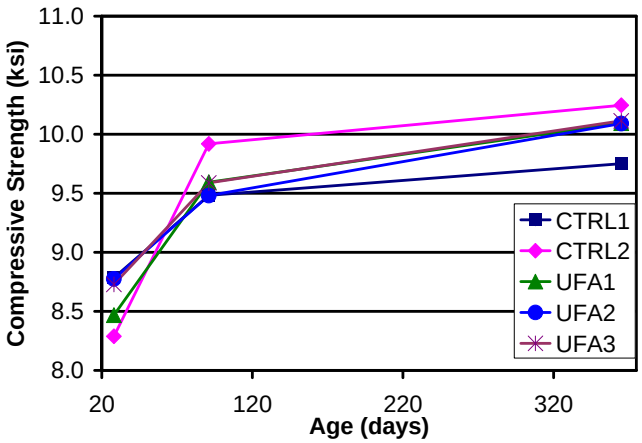

Figure 5 - 7 Average Late Compressive Strength of Ultrafine Fly Ash Mixtures

It is apparent that the compressive strength increases as the dosage of ultrafine fly ash is increased. Due to the increase in S as mineral admixture is increased, a large quantity of CH is consumed. Thus, a denser matrix of C-S-H will form as proportions of ultrafine fly ash are increased.

Figure 5 - 8 shows the early age strength development of the mixtures containing silica fume compared to the two control mixtures. Figure 5 - 9 presents the late age strength development. Because of its high reactivity, the silica fume mixtures show a

comparable early strength to the control mixtures. At 3 day and 7 day tests, the strength of the silica fume is nearly the same as CTRL2 and only slightly less than CTRL1. At 28 days of age, the silica fume mixtures have gained strength and surpassed the average compressive strength of both CTRL1 and CTRL2. At 91 days, the silica fume mixtures have continued to gain strength and remain higher than CTRL1. The compressive strength of CTRL2, however, has increased considerably and now is the highest. By 365 days, both silica fume mixtures show a large increase in strength, and are now nearly equal to that of CTRL2.

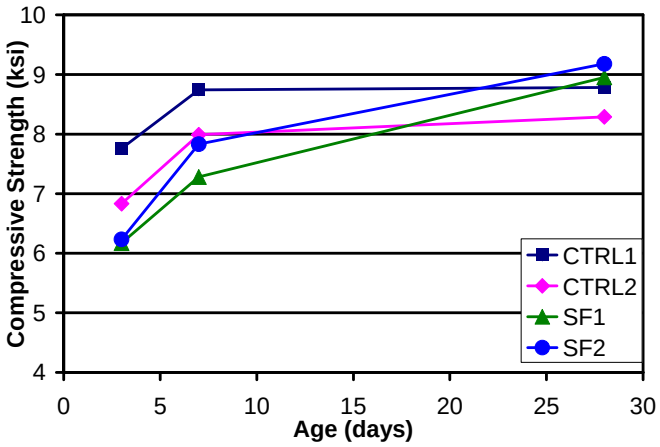

Figure 5 - 8 Compressive Strength of Silica Fume Mixtures

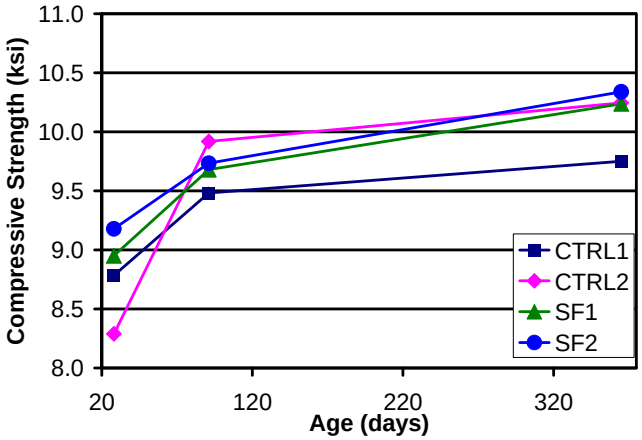

Figure 5 - 9 Compressive Strength of Silica Fume Mixtures

From Figure 5 - 8, it is apparent that the mixture with the higher proportion of silica fume, SF2, has a higher strength at all ages when compared to SF1. This is explained by the larger quantity of reactive silica, S, gained by increasing the proportion of the mineral admixture. Again, a stronger, denser C-S-H matrix is formed, thus increasing the compressive strength.

Manufacturing of prestressed concrete piles depends primarily on the early strength development of the concrete mixture. Prestress cannot be tranfered until a minimum compressive strength is achieved. Consequently, production is slowed and profits are reduced while the member remains in the forms. Consequently, it is likely that the manufactures would prefer a high early strength mixture. Typically, prestressed forces are transferred when the concrete has a compressive strength in the range of 3,500 to 4,500 psi. At 3 days, all mixtures in this investigation exceeded this range. Therefore, in relation to early removal from prestressing forms, the mineral admixtures did not improve the mixture over the controls.

The compressive strength also becomes important during pile driving because the forces associated with driving damage may damage the piles. At levels above 30% of the compressive strength, microcracking begins to develop; at about 70%, the cracks begin to propagate through the paste (Mindess et al. 2003). Cracking that develops will reduced the durability by providing a direct path for deleterious chemicals to enter the concrete. Therefore, a higher compressive strength will reduce the amount of damage caused by the pile driving process. Typically at around 28 days, the piles are removed from storage and driven. At this age, CTRL2 showed the lowest compressive strength. The slag, metakaolin, and ultrafine fly ash mixtures had nearly the same compressive strength as

CTRL1. The silica fume mixtures, however, did show a slight improvement in compressive strength over CTRL1. Therefore, it appears that the silica fume mixtures provide the best resistance to damage caused by driving at this age.

Flexural Strength (ASTM C 78)

The number of flexural strength specimens cast in the first mix allowed testing at 7 and 28 day ages. A second mix was done so that test could be conducted at 7, 28, and 365 days. The data presented in this section are the results from both the first and second set of mixtures.

The early modulus of rupture (MOR) of concrete made with low reactivity mineral admixtures is usually less than that of portland cement alone. The slower reaction time results in a delay of strength gain, which varies with the type of mineral admixture. From Figure 5 - 10, the ultrafine fly ash and slag mixtures showed the lowest strength at early age. In contrast, concrete made with a highly reactive mineral admixture will gain strength faster, as seen with the metakaolin and silica fume mixtures. At 365 days, the silica fume and slag mixtures showed the highest MOR.

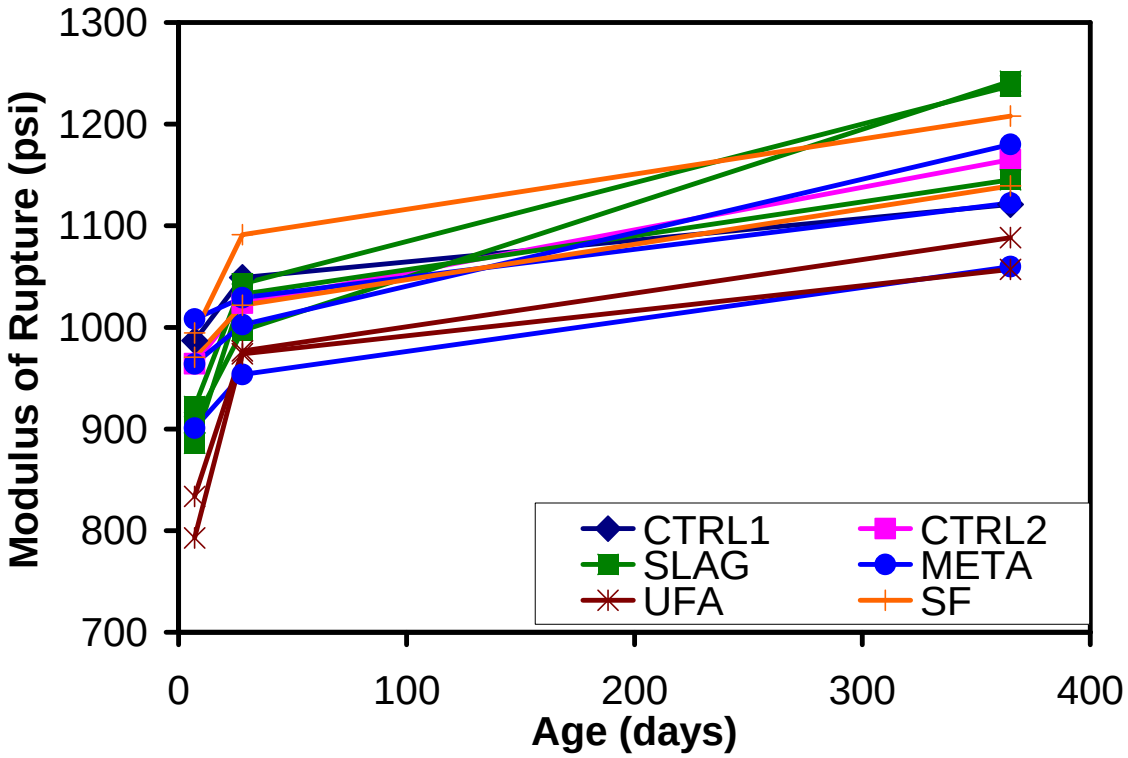

Figure 5 - 10 Modulus of Rupture of All Mixtures

Figure 5 - 11 shows the average MOR for the slag mixtures at 7, 28, and 365 days. The control mixture containing only cement, CTRL1, shows a higher MOR when compared with the control mixture containing cement and fly ash, CTRL2, for both 7 and 28 day ages. The low reactivity of fly ash affects the tensile strength similar to early age compressive strength. By 365 days, however, the fly ash in CTRL2 has reacted to produce a higher MOR than that of CTRL1.

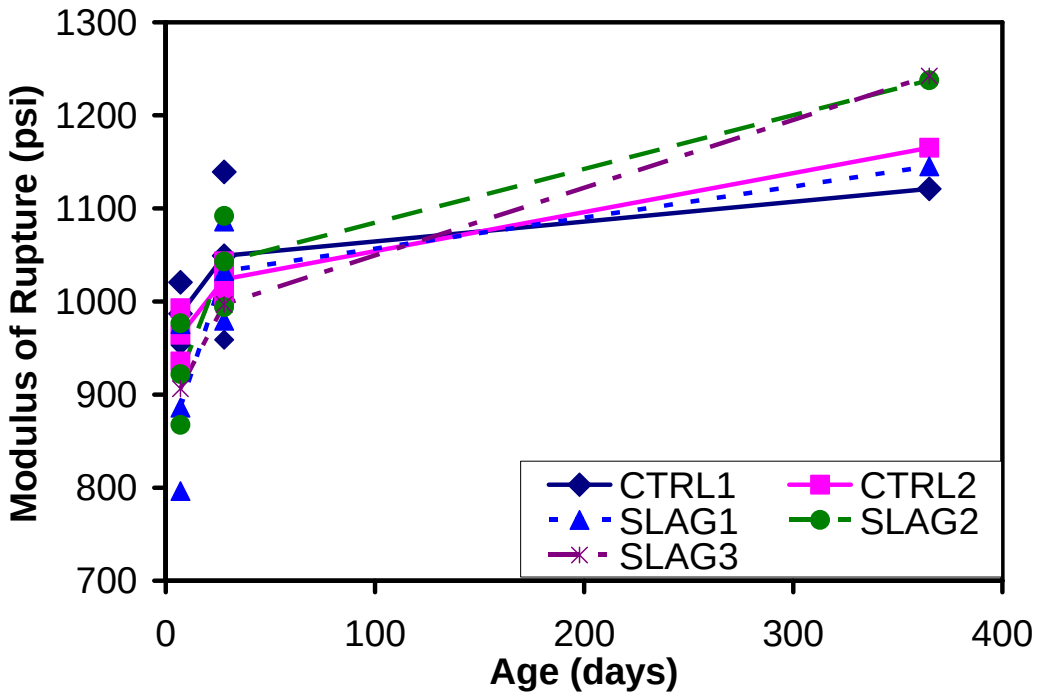

Figure 5 - 11 Average Modulus of Rupture of Slag Mixtures

The 7 day MOR for all slag mixtures was lower than both the control mixtures. Because the reactivity of slag is also low, the combination of the two mineral admixtures, slag and fly ash, produces an even slower strength developing concrete than CTRL2 in the 7 day MOR tests. By 28 days, however, the MOR for all slag mixtures are nearly equal to both the control mixtures. This indicates that the fly ash and slag has started reacting prior to 28 days to produce a concrete with equal MOR to the CTRL1. At 365 day age, SLAG1's MOR was slightly higher than CTRL1, while those of SLAG2 and SLAG3 were both well above both control mixtures. The hydration products of the slag and fly ash, have improved the tensile strength of the paste at 365 days similar to compressive strength.

Figure 5 - 12 shows the MOR development of the metakaolin mixtures. At 7 days, the metakaolin mixtures show high early strength. Each mixture has nearly the same MOR as the controls, with the exception of META1. The 28 day MOR for META1 was

also lower than the other metakaolin and control mixtures. Every other mixture at this age was nearly equal. At 365 days, META1 still has a lower MOR than the controls. META2 is equal to CTRL1, while META3 is nearly equal to CTRL2.

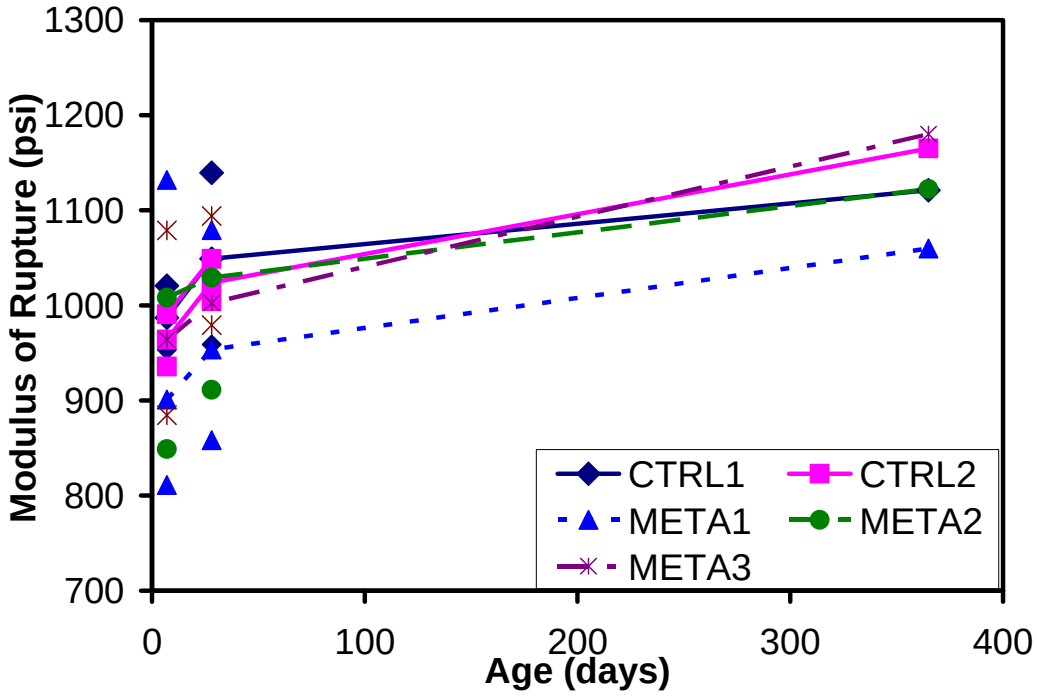

Figure 5 - 12 Average Modulus of Rupture of Metakaolin Mixtures

Because of the calcining, metakaolin is mainly composed of amorphous aluminosilicates. These aluminosilicates are highly reactive, and will rapidly convert CH to a hydration product. Thus, the high early strength of the metakaolin mixtures is because of its highly reactive composition. The MOR data show that an increase in proportion of metakaolin results in a higher MOR, as seen at all ages in Figure 5 - 12.

The average MOR for the ultrafine fly ash mixtures is presented in Figure 5 - 13. At 7 days, the MOR for all ultrafine fly ash mixtures were considerably lower than the control mixtures. By 28 days, there is a gain in MOR for the ultrafine fly ash mixtures; however, the MOR were below the control mixtures. The strength of the mixtures

continues to increase at 365 days. UFA3 now has a modulus that is nearly equal to that of CTRL1, while UFA1 and UFA2 are slightly lower.

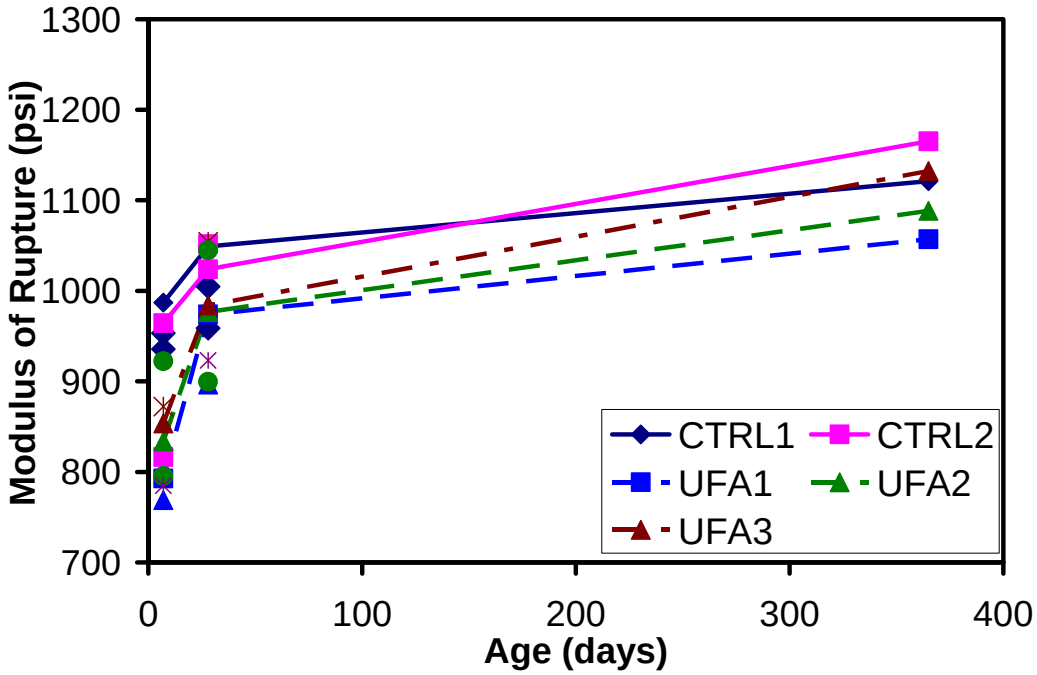

Figure 5 - 13 Average Modulus of Rupture of Ultrafine Fly Ash Mixtures

These mixtures have the lowest average 7-day MOR of all mixtures in this investigation. This is likely due to the higher total proportions of fly ash relative to the mixtures with other more reactive mineral admixtures. Although the ultrafine fly ash has a higher surface area when compared to regular fly ash, making it more reactive, the reaction equations are still the same. The fly ash needs a high alkalinity in the pore water to continue the pozzolanic reaction. At 7 days of age, the high volumes of total fly ash in the ultrafine fly ash mixtures (28 to 32%) slow the hydration considerably. By 28 days, however, the fly ash has begun to react, as shown in the significant MOR gain relative to the controls. At 365 days, the data shows a general increase in MOR as the proportion of mineral admixture is increased. By this age, the alkalinity in the pore solution has stabilized to allow for reactions of the full quantity of fly ash. Consequently, the larger

proportions of mineral admixtures increase the amount of available reactive silicate. From pozzolanic reactions, the CH is converted to C-S-H, creating a stronger paste.

Figure 5 - 14 shows the MOR development for the silica fume mixtures. At 7 days, the MOE of SF1 is practically equal to CTRL2; SF2 is nearly equal to CTRL1. However, by 28 days, the MOR in SF2 has increased more than all other mixtures, while SF1 remains close to CTRL2. By 365 days, the MOR for SF2 has surpassed CTRL1. SF2 and CTRL2 had a substantial increase in MOR.

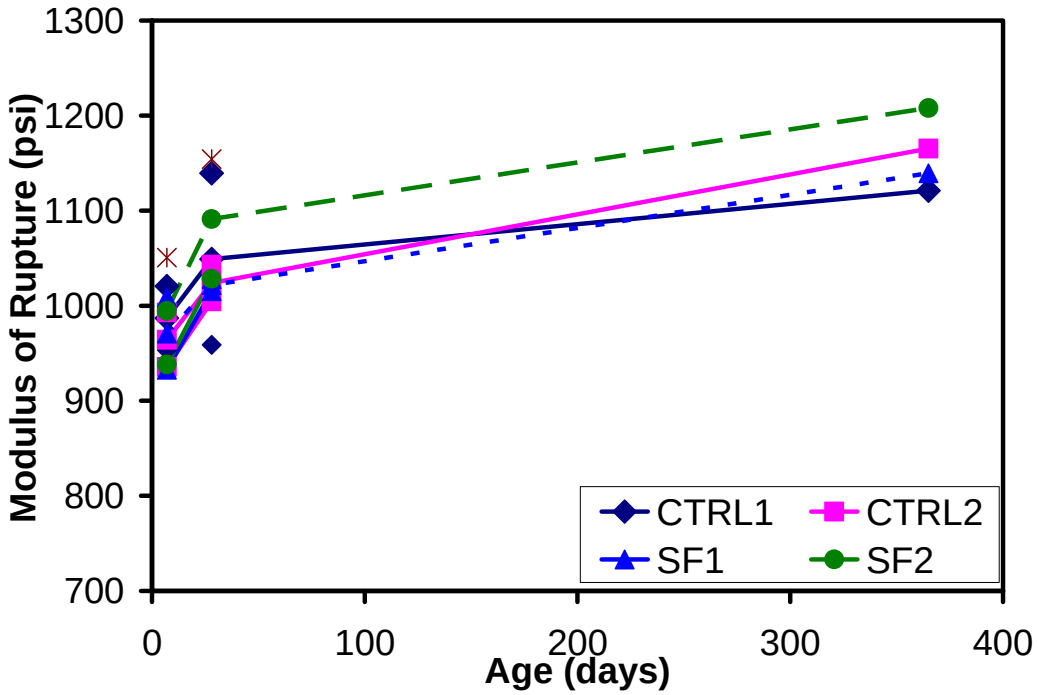

Figure 5 - 14 Average Modulus of Rupture of Silica Fume Mixtures

At 7 days, the MOR in SF1 is nearly the same as CTRL2. At the same age, however, SF2 showed an improvement in MOR over CTRL2. This illustrates that the larger replacement with silica fume has contributed to the tensile strength of the paste. Generally, as the proportions of silica fume are increased, the MOR will increase, because there is a larger quantity of reactive silica available to convert CH to a stronger C-S-H product. By 28 days, the additional silica content of SF2 increased the MOR over

all other mixtures. By 365 days, the MOR in CTRL2 has increased over CTRL1 indicating that fly ash has begun to react. SF2 had continued to hydrate and shows the largest MOR.

The MOR is an important parameter used to calculate the cracking strength of reinforced and prestressed concrete members. ACI (363R-92) has found that for both lightweight and normal weight high-strength concrete, the MOR falls in the range of $7.5*\sqrt{(f`_c)}$ to $12*\sqrt{(f`_c)}$ in psi. The following formula is recommended as a prediction of the tensile strength of concrete as measured by the MOR from the compressive strength:

$$Modulus\ of\ Rupture = 11.7 \times \sqrt{f`_c}\ \text{(psi)} \qquad (5\text{-}1)$$

where $f`_c$ is the compressive strength (psi). Table 5 - 3 shows the MOR and compressive strength data for all mixtures, along with a calculated coefficient based on the $\sqrt{(f`_c)}$. The average coefficient was calculated for each of the three test ages of 7, 28, and 365 days.

Table 5 - 3 Modulus of Rupture, Compressive Strength, and Coefficient

Mix	7 days			28 days			365 days		
	f_r (psi)	f'_c (psi)	$f_r/\sqrt{(f'_c)}$	f_r (psi)	f'_c (psi)	$f_r/\sqrt{(f'_c)}$	f_r (psi)	f'_c (psi)	$f_r/\sqrt{(f'_c)}$
CTRL1	987	8,741	10.6	1049	8,784	11.2	1,121	9,750	11.4
CTRL2	964	7,990	10.8	1024	8,289	11.2	1,165	10,246	11.5
SLAG1	886	7,616	10.2	1033	8,728	11.1	1,145	10,403	11.2
SLAG2	922	7,506	10.6	1043	8,644	11.2	1,238	10,326	12.2
SLAG3	906	6,791	11.0	997	8,699	10.7	1,242	9,382	12.8
META1	901	8,860	9.6	954	8,860	10.1	1,060	10,171	10.5
META2	1,008	8,962	10.7	1029	8,841	10.9	1,122	10,306	11.1
META3	964	8,962	10.2	1003	8,959	10.6	1,180	10,594	11.5
UFA1	793	6,490	9.8	974	8,469	10.6	1,057	10,094	10.5
UFA2	834	6,770	10.1	977	8,775	10.4	1,088	10,090	10.8
UFA3	853	6,787	10.4	984	8,729	10.5	1,132	10,114	11.3
SF1	971	7,281	11.4	1022	8,951	10.8	1,139	10,024	11.4
SF2	994	7,831	11.2	1091	9,178	11.4	1,208	10,272	11.9
Average			10.5			10.8			11.4

The coefficients range from 9.6 to 12.8, with an average of 10.5, 10.8, and 11.4 for 7, 28, and 365 days, respectively. The actual coefficients are slightly lower than what is predicted in the ACI equation. Therefore, ACI has overestimated the tensile strength of the concrete for all mixtures at 7 and 28 days, and nearly all mixtures at 365 days.

The data show that coefficients increase with both age and higher volumes of mineral admixtures. In other words, the tensile strength increased by a larger margin than the compressive strength as age and proportion of mineral admixture increased. The data also show that the silica fume mixtures had the highest coefficient at 7 days of age, while slag shows the highest at 365 days of age; at 28 days, all mixtures had nearly the same coefficient.

MOR is used to calculate the cracking strength of reinforced and prestressed concrete members. In this investigation, the cracking strength becomes important during transportation and driving of the piles.

Flexural stresses may develop at early ages during the handling and transportation of the piles from the prestress yard to the construction site. At 7 days, the slag and ultrafine fly ash mixtures showed lower MOR when compared to the control mixtures, while the metakaolin and silica fume mixtures were nearly equal. Therefore, the slag and ultrafine fly ash reduce the ability of a concrete to resist flexural stresses at this age, while silica fume and metakaolin have no affect.

In addition to flexural stresses from handling, tensile stresses are created in the pile during driving as stress waves propagate through the concrete and reflect back. Because driving typically takes place at around 28 days, the MOR becomes important at this age. The ultrafine fly ash mixtures show lower MOR than the controls, while the slag mixtures and metakaolin, with the exception of META1, were nearly equal. SF1 also had nearly equal MOR to the control mixtures at 28 days. SF2 showed an improvement in MOR over the controls. Therefore, the use of ultrafine fly ash reduces the ability of the concrete to resist tensile stresses from driving at 28 days of age, while silica fume at a 9% replacement level show an improvement. All other mineral admixtures had no significant affect to the MOR.

Modulus of Elasticity and Poisson's Ratio (ASTM C 469)

Due to testing errors it was necessary to prepare a second set of mixtures from which modulus of elasticity (MOE) specimens were fabricated. Detailed results from tests on both set of mixtures are included in Appendix A.

The MOE at early ages for concretes made with low reactivity mineral admixtures will usually be less than that of portland cement alone; the slower reactions results in a delay of MOE gain. Conversely, concrete containing highly reactive mineral admixtures will show higher MOE at early ages. This is apparent at 7 days, in which the metakaolin

mixtures showed a higher MOE than the controls (Figure 5 - 15). Subsequent ages showed nearly equal MOE to controls. Although silica fume is also a highly reactive pozzolan, its interactions with fly ash decrease MOE at 7 and 28 days. By 365 days, however, the silica fume mixtures showed the highest MOE of all mixtures. Generally, each other mixture showed lower MOE than the controls because of their low reactivity.

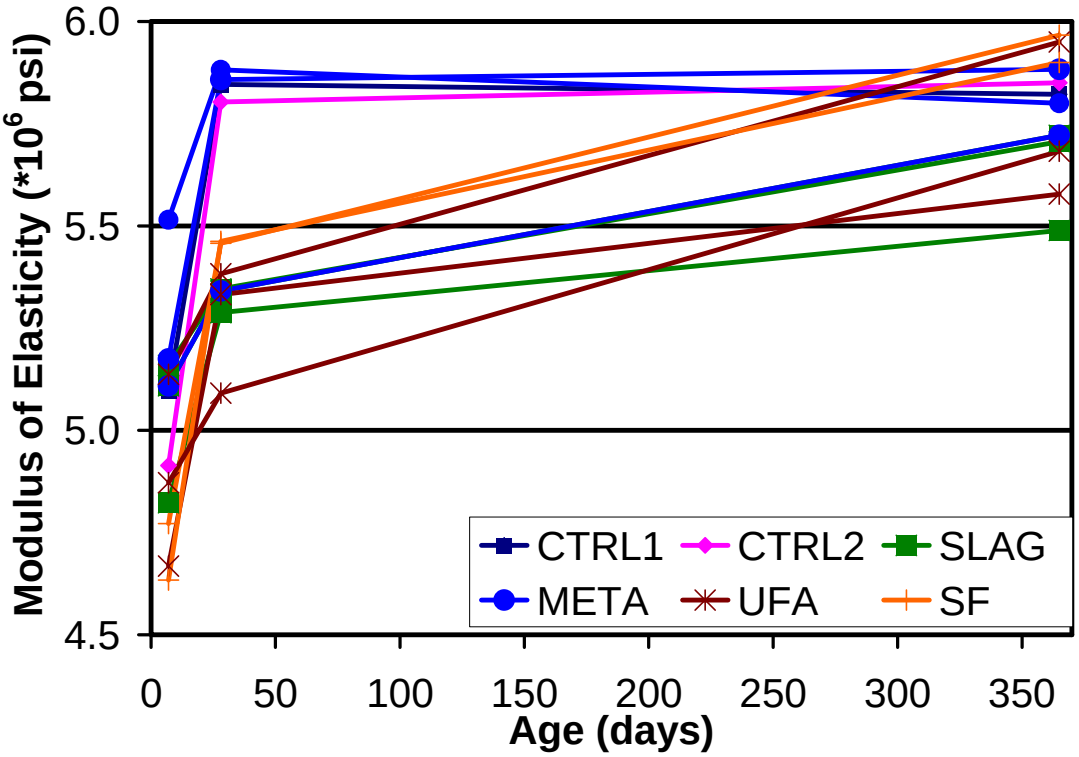

Figure 5 - 15 Average Modulus of Elasticity of All Mixtures

Figure 5 - 16 shows the change in MOE in the slag mixtures. At 7 days of age, SLAG1 and CTRL2 have a lower modulus than CTRL1; SLAG2 and SLAG3 are nearly the same as CTRL1. At 28 days, both control mixtures have shown a large increase in modulus to place them well above each slag mixture. Each slag mixture has shown small gains. Both CTRL2 and CTRL1 have shown almost no increase between 28 and 365 days of age, while the modulus in each slag mixture increased over this period.

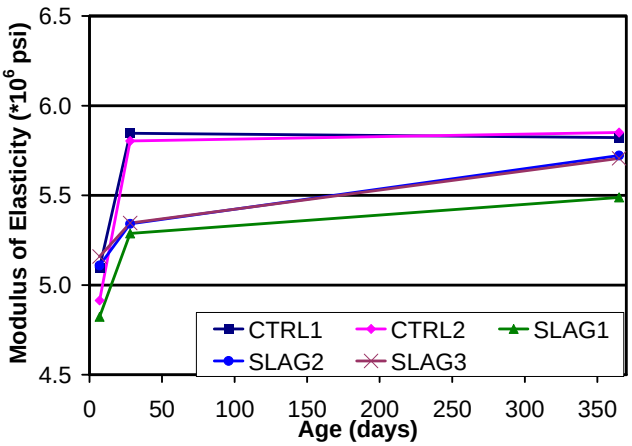

Figure 5 - 16 Average Modulus of Elasticity of Slag Mixtures

The slow gain in MOE for the slag mixtures is attributed to the low reactivity of slag. At early ages, the breakdown of the silica with in the slag is minimal. As cement hydrates, the release of hydroxyl ions increases, allowing the slag to be activated. As these mixtures hydrate, the porosity of the paste decreases. This effect is seen in Figure 5 - 16 by the slow increase in the MOE over time. In addition to the low reactivity of slag, the mixtures are somewhat retarded at early ages from the interactions of fly ash with the decreased presence of alkalis. The hydration of the fly ash requires a high alkalinity in the pore solution. However, slag hydration reduces the alkalinity. Therefore, the hydration of slag within mixtures reduces the reactivity of the fly ash. This is also seen from the dramatic increase in modulus in CTRL2 over the slag mixtures—which contain the same percentage of fly ash.

The MOE for metakaolin mixtures is presented in Figure 5 - 17. At 7 day, each mixture containing metakaolin has a higher MOE compared to the control mixtures. The higher early modulus of the metakaolin mixtures is attributed to the high reactivity of the mineral admixture. At early ages, the metakaolin mixtures have high strength development and low porosity. Therefore, when comparing the moduli to the controls,

the metakaolin mixtures perform well at 7 days. The modulus at 28 days for all mixtures is nearly the equal. There is almost no change in any mixture at 365 day age.

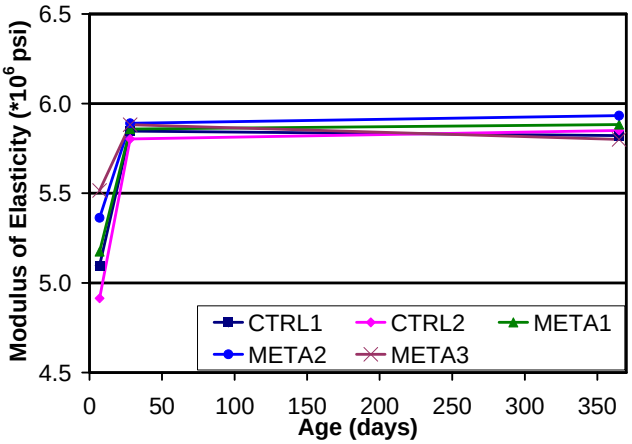

Figure 5 - 17 Average Modulus of Elasticity of Metakaolin Mixtures

Figure 5 - 18 shows the MOE of ultrafine fly ash mixtures. The 7 day MOE of the ultrafine fly ash mixtures and CTRL2 are below that of CTRL1, with the exception of UFA1. At 28 days, there has been only little improvement in the moduli of the ultrafine fly ash mixtures. However, both control mixtures have had a considerable gain in modulus and are nearly the equal. The results at 365 days show that there has been almost no increase for the control mixtures, while each ultrafine fly ash mix has shown a large improvement in MOE.

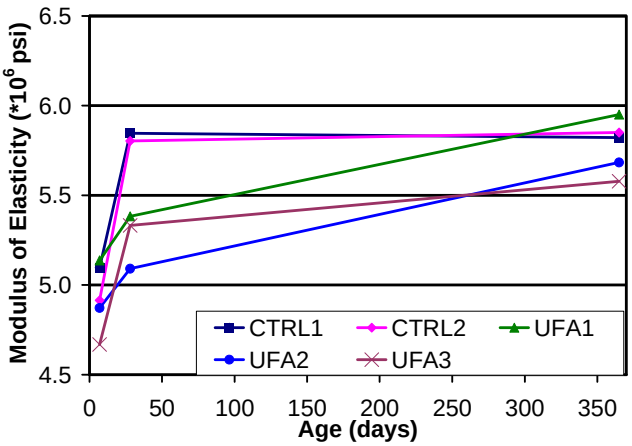

Figure 5 - 18 Average Modulus of Elasticity of Ultrafine Fly Ash Mixtures

Although the ultrafine fly ash has a higher surface area when compared to regular fly ash, making it more reactive, the reactions are still the same. The fly ash needs a high alkalinity in the pore water to continue the pozzolanic reaction. At 7 days of age, the high volumes of total fly ash of UFA2 and UFA3, 30% and 32% respectively, slow the hydration. The slow hydration, at this age, leaves a more porous concrete. Thus, MOE is lower for these mixtures. The data from UFA1 seems a little high, and may be bad data. The results from 28 days further illustrate the previous statement; the higher proportions of total fly ash have reduced the hydration compared to the control mixtures. However, by 365 days, the ultrafine fly ash mixtures have continued to hydrate to form a denser, less permeable concrete when compared to the control mixtures. This is seen in the large increase of the ultrafine fly ash mixtures in MOE between the ages 28 and 365 days, while the control mixtures have shown almost no increase.

The MOE for silica fume mixtures is presented in Figure 5 - 19. The modulus results at 7 days for the silica fume mixtures are below that on the control mixtures. By 28 days, the silica fume and control mixtures have all had nearly the same increase in MOE. The results at 365 days show that the control mixtures have not had any increase

in modulus. The silica fume mixtures have continued to increase; however, they are still below that of the control mixtures.

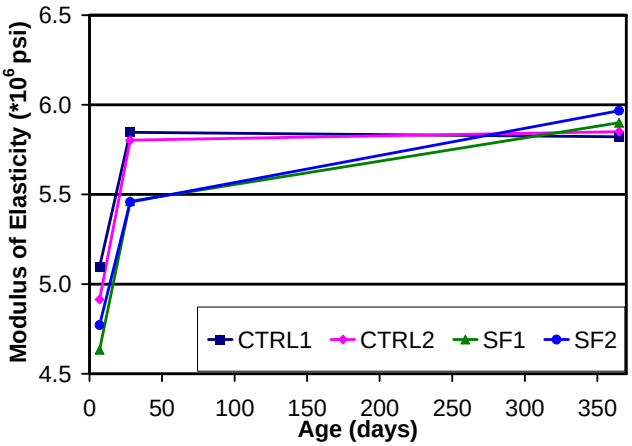

Figure 5 - 19 Average Modulus of Elasticity of Silica Fume Mixtures

It appears that the addition of silica fume in combination with fly ash lowers the MOE at 7 and 28 day ages. The reduction in modulus is attributed to the decreased reactivity of fly ash with silica fume. The alkalinity of the pore water is reduced with the pozzolanic reaction of silica fume, which causes the fly ash to remain inactive until the alkalinity is high enough to cause activation. This effect is seen at 7 and 28 day ages. By 365 days, the MOE of the silica fume mixtures has surpassed the control mixtures. This shows that the silica fume and fly ash has had enough time to continue hydration.

ACI (318R-02) has defined the concrete MOE for densities between 90 and 155 lb/ft^3 as:

$$E_c = 33 \times w_c^{1.5} \times \sqrt{f`_c} \quad (lb/in.^2) \qquad (5\text{-}2)$$

where E_c is the secant modulus, w_c is the density of the concrete in lb/ft^3, and $f`_c$ is the compressive strength in lb/in^2. Consequently, factors that affect strength also influence MOE. The most dominant factor is porosity as modulus will decrease markedly with the increase in porosity (Mindess et al. 2003). Therefore, the mixtures containing mineral

admixtures will have higher moduli of elasticity because of associated decreases in porosity through pozzolanic reaction.

The results from Poisson's ratio seem to be inconclusive. At all ages, the ratio appears to be about 0.25 (Table 5 - 4). Therefore, there is no discernable conclusion that could be drawn of the affects of different mineral admixtures on Poisson's ratio.

Table 5 - 4 Poisson's Ratio

Mix	7—day	28—day	365—day
CTRL1	0.26	0.28	0.27
CTRL2	0.18	0.28	0.18
SLAG1	0.26	0.26	0.20
SLAG2	0.28	0.26	0.31
SLAG3	0.25	0.26	0.30
META1	0.27	0.29	0.23
META2	0.26	0.26	0.21
META3	0.25	0.26	0.21
UFA1	0.24	0.24	0.26
UFA2	0.24	0.26	0.37
UFA3	0.24	0.25	0.22
SF1	0.23	0.26	0.28
SF2	0.25	0.26	0.22
Average	0.25	0.26	0.25

Splitting Tensile Strength of Cylindrical Concrete (ASTM C 496)

The data show high variability for all testing ages (Appendix B). Although care was taken to limit errors from affecting the results, the fact remains that the level of variability within the sample set is large enough to influence the trend. These errors are largely attributed to the specimen shape; many were not perfectly cylindrical through its entire length. Due to deformations in cylinder molds, the finished surface was oval shaped in many cylinders. This would allow a non-uniform load to be applied during the test, thus affecting the apparent tensile strength of the specimen. It is because of this high variability that no conclusions were able to be drawn from this set of data.

Durability Tests

The results obtained from tests of linear shrinkage, volume of voids, change in length due to sulfate exposure, absorption, surface resistivity, rapid migration tests, and water permeability are discussed below. Trends and relationships in the results have been noted in the discussion for each test.

Linear Shrinkage (ASTM C 157)

The average percent length change for a concrete age of 32 weeks is presented in Table 5 - 5. The two control mixtures, CTRL1 and CTRL2, have the highest levels of length change when compare to all other mixtures. This shrinkage is attributed mostly to the interconnectivity of the specimen porosity. CTRL 1 experiences the largest shrinkage because it contains no mineral admixture. Its paste most likely contains a higher volume C-S-H porosity and larger capillary pores. CTRL2 shows a less shrinkage when compared to CTRL 1 due to the addition of fly ash. The fly ash has reacted with CH to form a denser C-S-H matrix as well as decreased the amount and size of capillary pores (Neville 1995).

Table 5 - 5 Average Percent Length Change, COV, and Normalized (to CTRL1) Shrinkage Values at 32 Weeks of Age

Mix	Shrinkage (%)	COV	Normalized Shrinkage
CTRL1	0.0360	12.1	1.00
CTRL2	0.0330	6.1	0.92
SLAG1	0.0307	13.2	0.85
SLAG2	0.0247	27.0	0.69
SLAG3	0.0270	6.4	0.75
META1	0.0243	8.6	0.68
META2	0.0210	20.2	0.58
META3	0.0227	3.1	0.63
UFA1	0.0330	4.6	0.92
UFA2	0.0207	43.4	0.57
UFA3	0.0193	36.7	0.54
SF1	0.0287	17.6	0.80
SF2	0.0253	6.0	0.70

Generally, as the proportion of mineral admixture is increased, the average shrinkage is decreased. The increased mineral admixture provides a larger quantity of reactive silica that allows more CH to react, and thus forming a denser C-S-H matrix. The increased proportion of mineral admixture also reduces the quantity and size of capillary pores.

The ultrafine fly ash mixtures performed the best. However, UFA1 shows a high level of shrinkage; in fact, this mixture shows the same change in length as CTRL2. The most likely cause is from a high volume of large capillary pores; this mixture exhibited the highest level of bleeding, as shown in Table 5 - 1. The metakaolin mixtures also performed well, followed by the silica fume and slag mixtures.

The importance of shrinkage in structures is related to cracking. The cracking tendency of a concrete is function of not only shrinkage but also the tensile strength and restraint from shrinkage deformation. If the stress created from the shrinkage in a restrained concrete exceeds the tensile strength of the concrete, cracking will occur. The

limiting tensile strain ranges between 100 x 10^{-6} and 200 x 10^{-6} (Neville 1995). The linear shrinkage of all the mixtures ranged from 0.019% to 0.036%, suggesting that each mixture will begin to develop shrinkage cracking in a restrained system. However, the extent of shrinkage cracking will differ between mixtures. CTRL1 showed the highest level of linear shrinkage, while UFA3 showed the lowest, followed by UFA2 and META2. With each group of mineral admixtures, shrinkage decreased as the proportion increased. As a whole, the ultrafine fly ash mixtures showed the best performance.

Volume of Voids and Absorption (ASTM C 642)

The volume of permeable pore space, voids, range from 13.1 to 15.5%, while the average percent absorption ranges from 5.92 to 7.14% (Table 5 - 6). META3 has the maximum absorption and void content, while SLAG2 exhibits the lowest. However, the data are nearly equal for all mixtures. Therefore, neither voids nor absorption appears to be affected by the use of mineral admixtures. This is not supported by research by Parande (et al. 2006) and Gonen and Yazicioglu (2006) in which they have shown that use of metakaolin, fly ash, and silica fume each has resulted in a decrease in voids and absorption. However, this research was conducted on mixtures with water to cementitious material ratios (w/cm) of 0.45 and 0.50, which were higher that what was used in this investigation. The higher w/cm produces a larger quantity and size of capillary pores (Mindess et al. 2003). Neville (1995) has found that at a w/cm below 0.38, capillary pores will no longer be present and voids will be small and disconnected within the hydrated cement paste. In this investigation, a w/cm of 0.35 was used. Therefore, there were no capillary pores available for the hydration products to fill, which is the reason why the use of mineral admixtures had no affect on the volume of voids and absorption characteristics of the concrete.

Table 5 - 6 Average Percent Void and Absorption, COV, and Normalized (to CTRL1) Void and Absorption Values at 32 Weeks of Age

Mix	Voids			Absorption		
	(%)	COV	Normalized	(%)	COV	Normalized
CTRL1	13.9	4.1	1.00	6.31	4.9	1.00
CTRL2	13.8	2.6	0.99	6.30	2.5	1.00
SLAG1	13.6	2.4	0.98	6.20	1.3	0.98
SLAG2	13.1	2.3	0.94	5.92	1.7	0.94
SLAG3	14.5	1.7	1.05	6.66	1.9	1.05
META1	15.0	2.4	1.08	6.92	1.8	1.10
META2	15.0	3.7	1.08	6.89	1.9	1.09
META3	15.5	4.1	1.12	7.14	2.0	1.13
UFA1	14.2	2.3	1.03	6.52	2.0	1.03
UFA2	13.9	2.6	1.00	6.34	1.4	1.00
UFA3	14.3	1.4	1.03	6.56	1.9	1.04
SF1	13.6	2.1	0.98	6.31	1.8	1.00
SF2	13.3	2.9	0.96	6.18	2.8	0.98

Sulfate Expansion (ASTM C 1012)

Figure 5 - 20 depicts a plot of normalized values of average sulfate expansion for the concrete specimens. Each mixture was normalized to CTRL1 to provide a means of assessing the effects of the mineral admixtures of the sulfate resistance of the concrete. Generally, as the proportion of mineral admixture is increased, the average expansion is decreased. This is attributed to an increase in reactive silica, S, as the mineral admixtures are increased. As a result, more CH is consumed and thus lowering the gypsum corrosion.

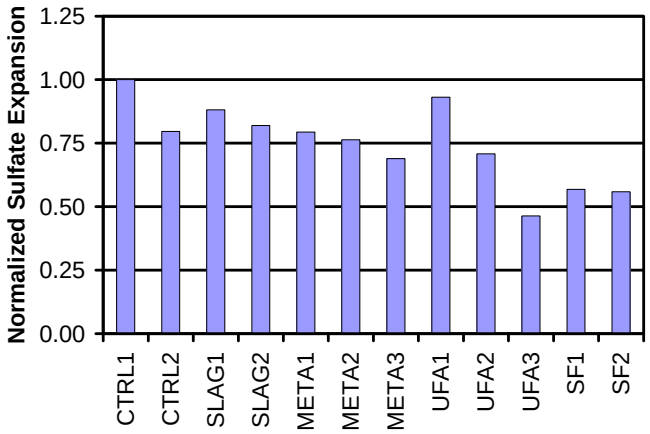

Figure 5 - 20 Normalized Values of Sulfate Expansion: Concrete Specimens

SLAG3 was excluded from Figure 5 - 20 because its high expansive behavior that is most likely attributed to its higher permeability. The bleed water measurements presented in Table 5 - 1 for this mixture, show a high value when compared to other mixtures. This would indicate that SLAG3 had slight problems with segregation. This in turn increases the size and quantity of capillary pores, thus increasing the permeability. Therefore the more permeable concretes will allow a large ingress of sulfate, and eventually a higher average expansion.

Figure 5 - 21 presents the normalized values of the average sulfate expansion each mixture for mortar specimens that were sieved after mixing to remove the coarse aggregate. The data for each mortar specimen was also normalized to CTRL1 so that a relative comparison can be made for each mixture. The first and most important indication is that mineral admixtures reduce sulfate expansion of the paste. As the proportion of mineral admixture is increased, the sulfate expansion is decreased. The increased proportions of mineral admixture increase the total available reactive silica within the mixture. This in turns allows for more CH to be consumed, thus lowering the gypsum corrosion.

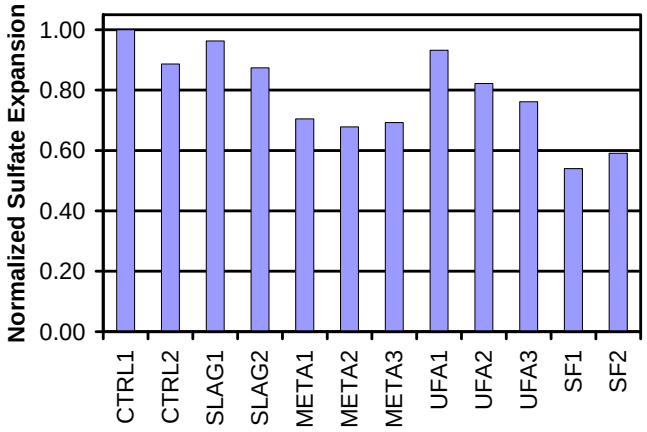

Figure 5 - 21 Normalized Values of Sulfate Expansion: Mortar Specimens

External sulfate attack is typified by expansion of concrete, leading to cracking and spalling. Skalany (et al. 2002) has found research that suggests several expansion limits as a failure criterion for mortar and concrete samples exposed to an external sulfate attack. A 0.1% expansion was proposed as the maximum acceptable criterion for failure for a moderate sulfate resistant concrete, while a 0.05% expansion was the limit for a high sulfate resistant concrete when tests were performed according to ASTM C 1012. According to these limits, each mixture could be classified has highly sulfate resistant as their expansion was well below the 0.05% limit (Table 5 - 7).

Table 5 - 7 Total Concrete and Mortar Expansion

Mixture	Concrete Expansion	Mortar Expansion
CTRL1	20.9	12.0
CTRL2	18.1	11.7
SLAG1	15.9	10.7
SLAG2	24.3	6.3
SLAG3	10.6	18.3
META1	18.2	6.7
META2	30.8	20.7
META3	15.7	4.7
UFA1	27.0	4.1
UFA2	49.8	13.0
UFA3	35.6	10.8
SF1	16.9	8.9
SF2	29.4	17.7

The percent expansions in the concrete prisms are about half as much as the mortar prisms (Figure 5 - 22). This is because the coarse aggregate is not susceptible to sulfate attack and therefore is not expansive. In both the concrete and mortar prisms, CTRL1 showed the highest levels of sulfate expansion. As a whole, the silica fume and metakaolin mixtures performed the best. However, these improvements may not significantly extend the life of the concrete as each concrete is well below the 0.5% expansion limit proposed by Skalny (et al. 2002). Extended sulfate attack tests are needed to determine the attributes of each mixture at later ages.

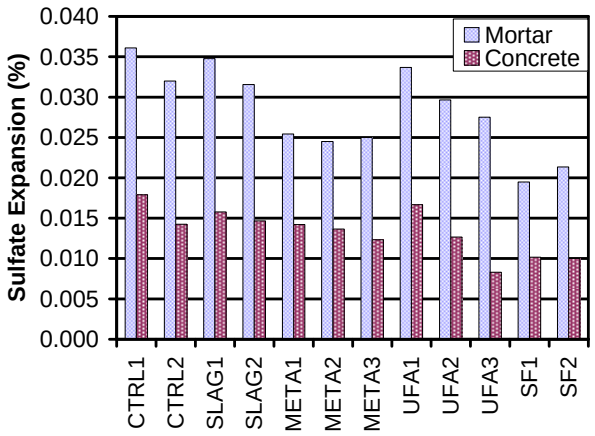

Figure 5 - 22 Comparison of Mortar and Concrete Sulfate Expansion Specimens

Corrosion of Embedded Steel Reinforcement (ASTM G 109)

A plot of current vs. ages for UFA3 is shown in Figure 5 - 23. It is apparent that there in no change in current throughout the test duration. This is typical of all mixtures in this investigation. Therefore, at the present time, corrosion has yet to initiate in the specimens for the corrosion of embedded steel reinforcement tests. Plots of all mixtures are shown in Appendix A.

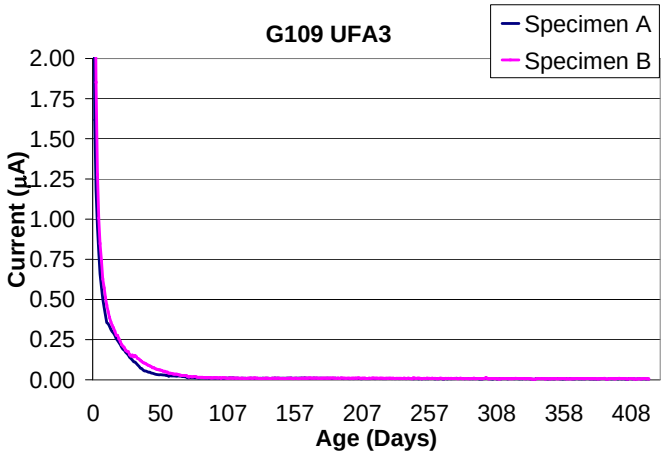

Figure 5 - 23 Corrosion of Embedded Steel Reinforcement

Surface Resistivity (FM5-578)

Whiting and Mohammed (2003) have found that the conductivity of a concrete is related to its permeability and diffusivity of ions through the concrete. Consequently, the

electrical resistance can be used as an estimation of chloride ion penetrability (Hooton et al. 2001). Research conducted by Chini (et al. 2003) relating the surface resistivity measurements to Rapid Chloride Penetration tests produced a reference table to aid the interpretation of the surface resistivity results, which was later adopted by FM 5-578. The table categorizes the chloride ion penetrability of a concrete from surface resistivity measurements.

Figure 5 - 24 compares the surface resistivity (SR) of the control and slag mixtures. At the early ages of the control and slag mixtures of 3 and 7 days, there was not much of a difference in the SR values of all slag mixtures from the control mixtures. However, beyond these early ages, there were noticeable increases in the slag mixture's resistivity. At the 28 day age, the slag mixtures had increased by roughly 150%, while the controls had only increased by about 50% (Table 5 - 8). At the 91 day age, all slag mixtures had continued to increase, but at a slower rate. CTRL2 had shown a large increased (128%) to about double the surface resistivity in CTRL1. The SR reading of CTRL1 had only increase by 20%. At 365 day age, the SR of all slag mixtures had continued to increase. The resistivity of CTRL2 has also continued to increase but at a faster rate than the slag mixtures. By this age, the surface resistance of CTRL2 is nearly equal to that of the slag mixtures. CTRL1 has shown only a minimal increase (8%) in surface resistance.

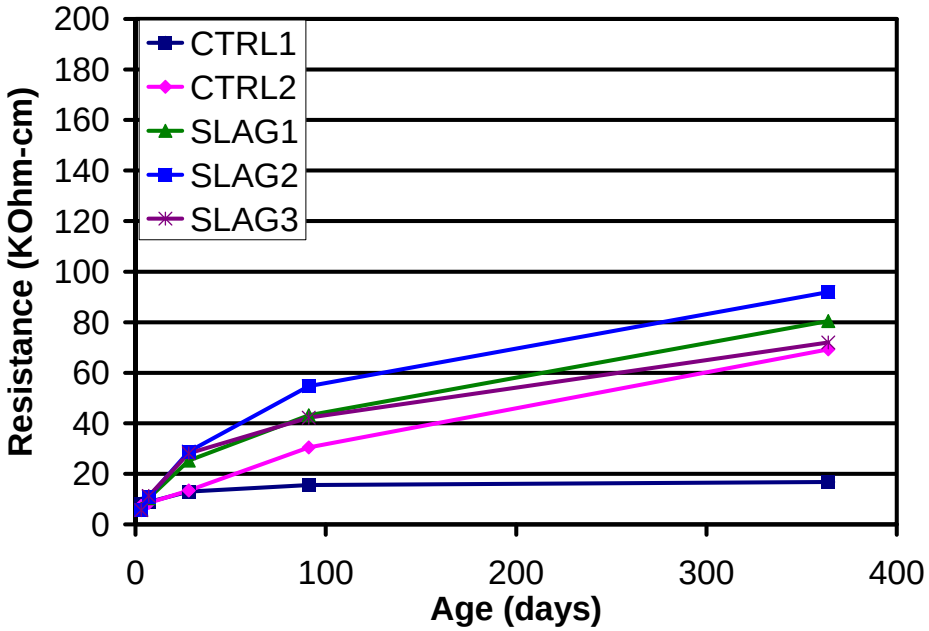

Figure 5 - 24 Average Surface Resistance of Slag Concrete Mixtures

Table 5 - 8 Increase in Surface Resistivity Between Test Ages (%)

Mix	Age (days)			
	3 to 7	7 to 28	28 to 91	91 to 365
CRTL1	8	46	20	8
CRTL2	15	58	128	127
SLAG1	70	142	71	86
SLAG2	91	164	90	68
SLAG3	101	150	50	70
META1	247	100	31	82
META2	309	80	54	89
META3	261	163	27	78
UFA1	34	250	200	126
UFA2	24	271	200	133
UFA3	27	332	200	109
SF1	107	461	79	43
SF2	154	501	89	14

As the proportion of mineral admixture is increased, larger volumes of reactive silica are available to chemically combine with CH to form more C-S-H. Consequently, a denser, less permeable concrete is produced. However, SLAG3 had the largest volume of mineral admixture, but was the worst performing slag mixture. This was most likely attributed to mixing problems. The bleed water measurements presented in Table 5 - 1

for this mixture, show a high value when compared to all others. This would indicate that SLAG3 had slight problems with segregation. This in turn increases the size and quantity of capillary pores, thus increasing the permeability. However, SLAG3 still performed better than both control mixtures at all ages.

From Table 5 - 1, it is clear that CTRL2 (18% fly ash) showed the increases in surface SR at 91 and 365 days; the earlier dates showed only small gains. This shows the low reactivity of the fly ash mineral admixture. It isn't until beyond 28 day that the fly ash will begin to react and improve the SR properties of the mixture. The slag mixture, on the other hand, showed larger increases in the earlier ages than fly ash; the largest gains were seen between 7 and 28 days, with a steady increase in SR throughout the testing regime. This indicates that the slag is more reactive and will contribute more to the early properties of the concrete than fly ash.

Figure 5 - 25 shows a plot of the average surface resistance of the metakaolin concrete mixtures compared with the control mixtures. At 3 days of age, there was not a noticeable difference between the metakaolin mixtures and the control mixtures. However, because of the high reactivity of metakaolin, the 7 day measurements showed a large increase (241% to 309%) in SR. At 28 days of age, the SR of the metakaolin mixtures had increased by 80% to 163% and now is about 3 to 4 times that of the control mixtures. By 91 day of age, the metakaolin mixtures had continued to show an increase in SR. At 365 days of age, the SR of all metakaolin mixtures had increased by about 80% and have a SR much higher than CTRL1 and about 2 or 3 times that of CTRL2.

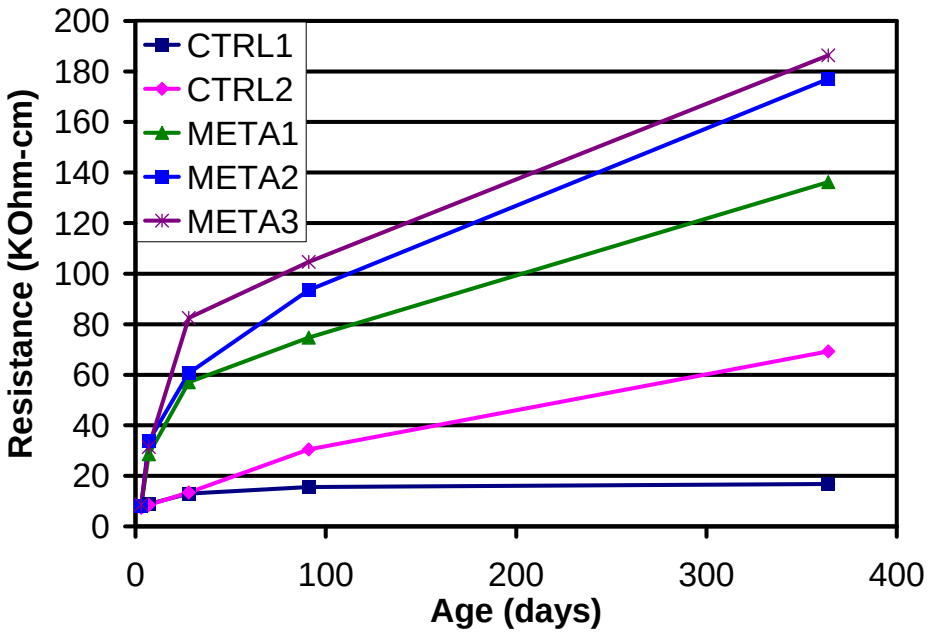

Figure 5 - 25 Average Surface Resistance of Metakaolin Concrete Mixtures

The largest gains in SR in the metakaolin mixtures were seen in the early ages. Each metakaolin mixtures showed an increase of roughly 275% and a 125% increase at 3 days and 7 days, respectively. This illustrates the very high reactivity of metakaolin. Indeed, the metakaolin showed the largest gain in SR between 3 and 7 days of all the mixtures in this investigation.

The SR of ultrafine fly ash concrete mixtures are compared with the control mixtures in Figure 5 - 26. At early ages, 3 day and 7 day, the ultrafine fly ash mixtures show nearly equal resistance when compared to the control mixtures. However, by 28 days, the ultrafine fly ash mixtures showed large increases in SR ranging from 250% to 332%. At 91 days of age, the ultrafine fly ash mixtures continued to have substantially increases (200%) in SR; they were nearly 4 times that of the control mixtures. At 365 days of age, the resistance of the ultrafine fly ash mixtures had increased by roughly 125%. The SR in the ultrafine fly ash mixtures were nearly 10 times greater than

CTRL1. The SR in the UFA2 and UFA3 may have been even larger because they had exceeded the measuring capabilities of the resistivity meter.

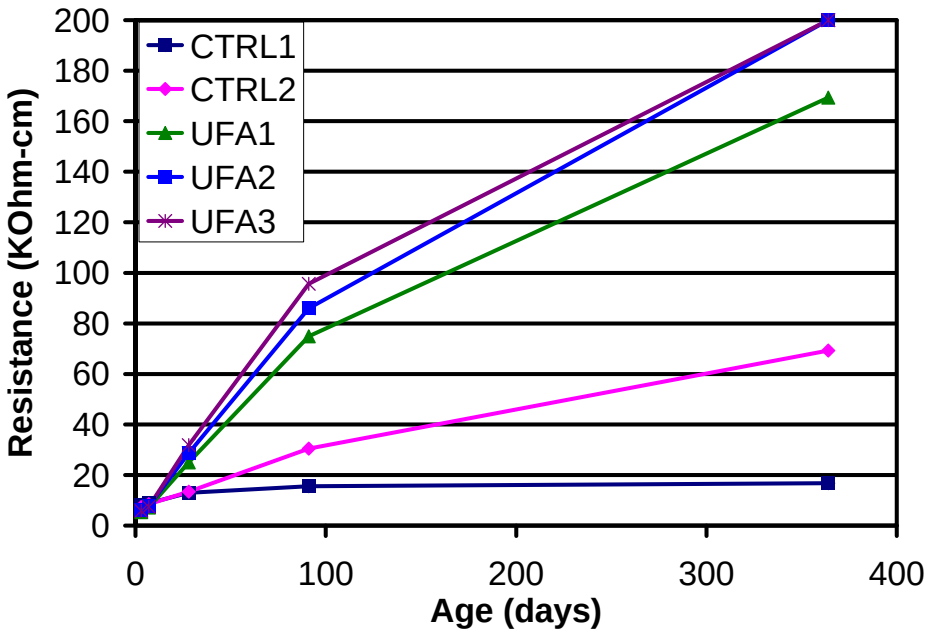

Figure 5 - 26 Average Surface Resistance of Ultrafine Fly Ash Concrete Mixtures

The ultrafine fly ash mixtures showed the larges increases in SR beyond 7 days. The largest gains were seen between 7 and 28 days. The subsequent testing dates also showed significant gains of 200% and roughly 125% at 91days and 365 days, respectively. The later age SR gains show the low reactivity of the fly ash. However, when comparing the data from CTRL2 to the ultrafine fly ash mixtures, it can be seen that the SR increase at an earlier age than CTRL2. This is attributed to the increased fineness of the ultrafine fly ash.

The SR of silica fume mixtures are compared with the control mixtures in Figure 5 - 27. At 3 day ages, silica fume mixtures and control mixtures have nearly equal SR. At 7 days of age, the silica fume mixtures begin to show an increase in SR (107% and 154%), while the control mixtures showed only a small increase (8 and 15%). At 28 day of age, the mixtures containing silica fume show a dramatic increase in SR (461% and

501%). The silica fume mixtures have a SR of nearly 5 or 6 times greater than the control mixtures. At 91 days of age, all silica fume mixtures showed an increase in SR of about 85%. At 365 days of age, the silica fume mixtures have surpassed the measuring capabilities of the resistivity meter.

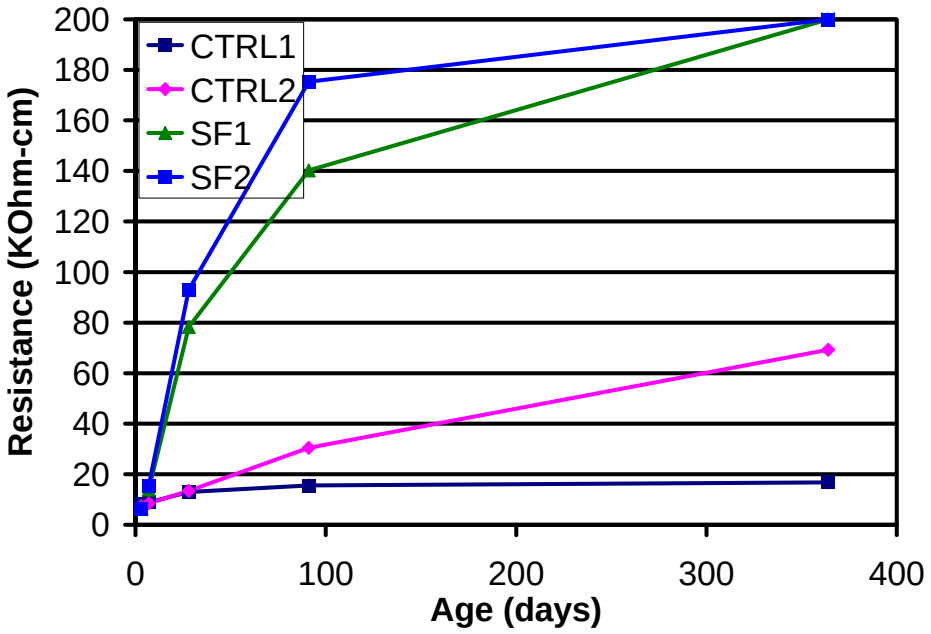

Figure 5 - 27 Average Surface Resistance of Silica Fume Concrete Mixtures

The silica fume mixtures showed the largest increases in SR at the early ages. The largest increases in SR was between 7 and 28 days. In fact, these mixtures showed the largest gains at this age of all mixtures in this investigation. This illustrates the high reactivity of the silica fume. When comparing the metakaolin mixtures with the silica fume, each show high early reactivity. However, the metakaolin seems to improve the SR at a slightly earlier age than the silica fume. This suggests that the metakaolin is slightly more reactive than silica fume. However, later, the silica fume increase the SR much higher than the metakaolin mixtures, which is likely attributed to the higher reactive silica content in the silica fume.

The research by Chini (et al. 2003) produced a reference table that was developed from their test data to aid the interpretation of the SR result. The table correlated SR with categories of chloride ion penetrability, which was established by Whiting (1981) based on the amount of coulombs passed from the rapid chloride penetration (RCP) test results. The categories of high, moderate, low, very low, and negligible penetrability were related to the depth of chloride penetration after a 90 day ponding test. Table 5 - 9 presents a summary of the chloride ion penetrability categories, chloride ion penetration depths, coulombs passed, and SR.

Table 5 - 9 Summary Table of Penetrability Category, Penetration Depth, Coulombs Passed and Surface Resistivity

Penetrability Category	Penetration Depth (mm)	Coulombs Passed (Coulombs)	Surface Resistivty (kΩ-cm)
High	> 1.3	> 4,000	< 12
Moderate	0.8 – 1.3	2,000 - 4,000	12 - 21
Low	0.55 – 0.8	1,000 - 2,000	21 - 37
Very Low	0.35 – 0.55	100 - 1,000	37 - 254
Negligible	< 0.35	< 100	> 254

Typically, concrete with RCP results of less than 1000 coulombs is specified by the engineer or owner for concrete elements under extremely aggressive environments (Pfeifer, McDonald and Krauss 1994). From Table 5 - 9, this corresponds to a *Very Low* and *Negligible* category. Because the RCP results are based on 90 day ponding tests on specimen that were cured for 28 days, SR at 28 days will be evaluated for each mixture in this investigation.

At 28 days, only the metakaolin and silica fume mixtures were in the *Very Low* category, corresponding to a RCP value less than 1000 coulombs (Table 5 - 10). Every other mixture showed lower SR. Therefore, based on the 1000 coulomb limit, only the metakaolin and silica fume mixtures are acceptable for use in an extremely aggressive

environment. The mixtures that are below the limit are presented in bold typeface. However, this limit is somewhat flawed because of the early age at which mixtures are evaluated. The use of some mineral admixtures delays hydration beyond 28 days. Consequently, a mixture that has high SR at later ages will be rejected because of its low early SR. For example, the ultrafine fly ash mixtures are deemed unacceptable based upon the 1000 coulomb limit at 28 days. However, they showed large increases in SR after 28 days. Eventually, the ultrafine fly ash mixtures were comparable to that of the silica fume and metakaolin mixtures—which were both acceptable at 28 days. Therefore, a more refined approach that incorporates the reactivity of the mixture is need for evaluation of chloride ion penetrability.

Table 5 - 10 Surface Resistivity (kΩ-cm)

Mix	3 day	7 day	28 day	91 day	364 day
CRTL1	**8**	**9**	**13**	**16**	**17**
CRTL2	**7**	**8**	**13**	**30**	69
SLAG1	**6**	**10**	**25**	43	80
SLAG2	**6**	**11**	**29**	55	92
SLAG3	**6**	**11**	**28**	42	72
META1	**8**	**29**	57	75	136
META2	**8**	**34**	61	94	177
META3	**9**	**31**	82	105	186
UFA1	**5**	**7**	**25**	75	169
UFA2	**6**	**8**	**29**	86	*200
UFA3	**6**	**7**	**32**	96	*200
SF1	**7**	**14**	78	140	*200
SF2	**6**	**15**	93	175	*200

Rapid Migration Test (NTBuild 492)

Like surface resistivity tests, rapid migration tests (RMT) are electrical tests that rely on estimating the concrete permeability based upon the electrical conductivity properties of a concrete. The RMT applies a potential to a concrete to force chloride ion to migrate through the concrete. After the test is complete, penetration depths are

measured. Because the penetrability of the concrete is based on the interconnectivity of voids, the use of mineral admixtures will reduced the depth of chloride ion penetration by creating a denser, less permeable paste structure through pozzolanic reactions.

Figure 5 - 28 shows the average Non-Steady-State Migration Coefficient of slag mixtures plotted against the control mixtures. From this plot it is clear that at 28 days, all slag mixtures showed lower migration coefficients than the control mixtures. At this age, the slag within the concrete had started to hydrate. The reactive silica contained within the slag particles is beginning to convert CH to C-S-H. This new CSH product is now much more dense and homogenous compared to that of the control mixtures. Thus, the migration coefficients are decreased.

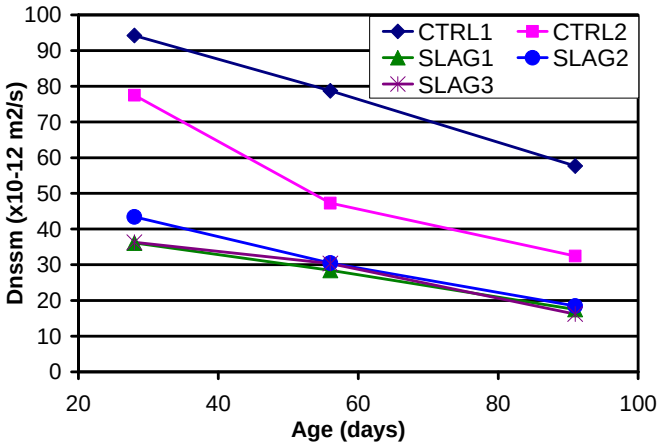

Figure 5 - 28 Average Migration Coefficient of Slag Mixtures

At 56 days, CTRL2 shows a 49% decrease in migration coefficient, while CTRL1 only showed a 16% decrease (Table 5 - 11). The slag mixtures showed less of a decrease in migration coefficients when compared to CTRL2, however, each slag mixtures had a lower migration coefficients at this age. At 91 days, both control mixtures showed a decrease in migration coefficient of about 30%. Each slag mixture showed a larger decrease (39% to 49%) in migration coefficient than the control mixtures. The migration

coefficient in CTRL2 was about half that of CTRL1, while each slag mixture was ¼ of CTRL1.

Table 5 - 11 Decrease in Migration Coefficient (%)

Mix	Age (days)	
	28-56	56-91
CTRL1	16	27
CTRL2	39	31
SLAG1	21	39
SLAG2	30	39
SLAG3	16	47
META1	25	49
META2	2	46
META3	32	32
UFA1	34	74
UFA2	49	37
UFA3	39	63
SF1	13	69
SF2	52	42

Figure 5 - 29 shows the average Non-Steady-State Migration Coefficient of metakaolin mixtures plotted against the control mixtures. At all ages, each metakaolin mixture showed a lower migration coefficient when compared to the control mixtures. At 28 days, the migration coefficients in the metakaolin mixtures were roughly 25% of that of CTRL1. At ages of 56 and 91 days, the metakaolin mixtures showed a continual decrease in migration coefficients, ranging from 2% to 32% and 32% to 49%, respectively. The migration coefficient for the metakaolin mixtures were again approximately 25% of CTRL1 at 56 days, and 17% at 91 days.

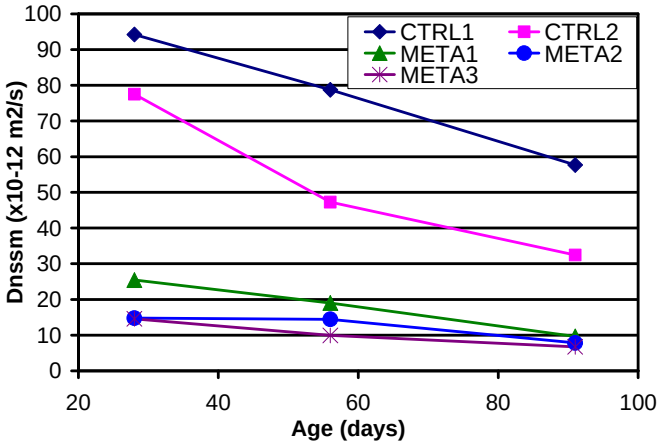

Figure 5 - 29 Average Migration Coefficient of Metakaolin Mixtures

Figure 5 - 30 shows the average Non-Steady-State Migration Coefficient of ultrafine fly ash mixtures plotted against the control mixtures. At all ages, each ultrafine fly ash mixtures showed a lower migration coefficient when compared to the control mixtures. At 28 days, the migration coefficients in the ultrafine fly ash mixtures were roughly ½ of that of CTRL1. At ages of 56 and 91 days, the ultrafine fly ash mixtures showed a continual decrease in migration coefficients, ranging from 34% to 49% and 37% to 74%, respectively. The migration coefficient for the ultrafine fly ash mixtures were approximately ¼ of CTRL1 at 56 days, and $^{1}/_{6}$ at 91 days.

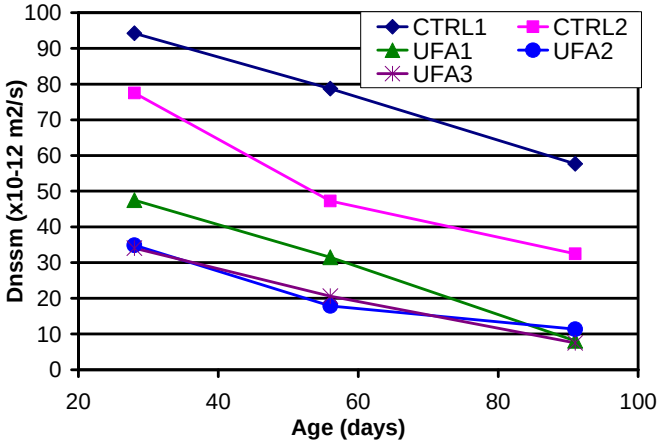

Figure 5 - 30 Average Migration Coefficient of Ultrafine Fly Ash Mixtures

Figure 5 - 31 shows the average Non-Steady-State Migration Coefficient of silica fume mixtures plotted against the control mixtures. At all ages, each mixture showed a lower migration coefficient when compared to the control mixtures. Indeed, both silica fume mixtures show the lowest migration coefficients of all mixtures at all ages. At 28 days, the migration coefficients in the silica fume mixtures were nearly a 10% of that of CTRL1. At ages of 56 and 91 days, the silica fume mixtures showed a continual decrease in migration coefficients, ranging from 13% to 52% and 42% to 69%, respectively. The migration coefficient for the metakaolin mixtures were again approximately 13% of CTRL1 at 56 days, and 10% at 91 days.

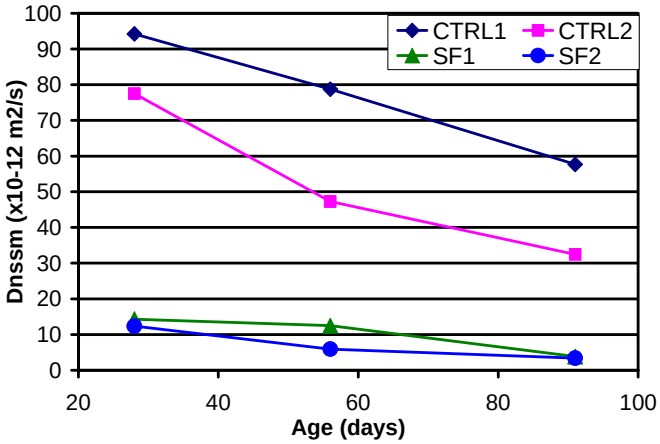

Figure 5 - 31 Average Migration Coefficient of Silica Fume Mixtures

Acceptance criteria for RMT results have not been established. However, Stanish (et al 2005) has developed a relation between the result of RMT and RCP (Table 5 - 12).

Table 5 - 12 RMT and RCP relationship

RMT value (mm/V*hr.)	RCP Value (Coulomb)
0.034	3000
0.024	2000
0.012	800

Typically, concrete mixtures that allow less than 1000 coulombs of charge to pass is specified by the engineer or owner for concrete elements in extremely aggressive

environments (Pfeifer, McDonald and Krauss 1994). Through a linear interpolation of the data in Table 5 - 12, a RMT value of 0.014 mm/V*hr. was found to correlate to an RCP value of 1000 coulombs. Based upon the maximum 1000 coulomb limit, an assessment of acceptable mixtures can now be made in Table 5 - 13. The mixtures that exceed the limit are illustrated in bold typeface. The data leading to the 1000 coulomb limit was based on 90-day ponding tests that were cured for 28 days. Therefore, 28 day RMT values will be discussed.

Table 5 - 13 RMT Values (mm/V*hr)

Mixture	28	56	91
CTRL1	**0.029**	**0.029**	**0.021**
CTRL2	**0.025**	**0.020**	0.014
SLAG1	**0.016**	0.014	0.010
SLAG2	**0.016**	**0.015**	0.009
SLAG3	**0.017**	**0.017**	0.010
META1	0.013	0.011	0.007
META2	0.008	0.009	0.006
META3	0.009	0.007	0.005
UFA1	**0.019**	0.014	0.006
UFA2	**0.015**	0.010	0.008
UFA3	**0.017**	0.012	0.005
SF1	0.009	0.007	0.006
SF2	0.008	0.005	0.004

It appears that only the metakaolin and silica fume mixtures have RMT values lower than 0.014. Based upon the 1000 coulomb limit, all other mixtures are not acceptable mixtures to be used in extremely aggressive environments. However, this limit is somewhat flawed because of the early age at which mixtures are evaluated. The use of some mineral admixtures delays hydration beyond 28 days. Consequently, a mixture that has high RMT values at later ages will be rejected because of its low early RMT. For example, the ultrafine fly ash mixtures showed a large increase in RMT values after 28 days. Eventually, the RMT values were comparable to that of the

metakaolin and silica fume mixtures—which were both acceptable at 28 days. Therefore, a more refined approach that incorporates the reactivity of the mixture is need for evaluation of chloride ion penetrability.

Water Permeability (UF Method)

The results gathered from the water permeability test are scattered and inconclusive (Table 5 - 14). The most likely cause of variation in coefficients of permeability is caused by poor bond between the concrete specimen and the epoxy barrier. Detailed test results are provide in Appendix A.

Table 5 - 14 Coefficient of Permeability

Mixtures	Kp (ft/hr)
CRTL1	8.89E-10
CTRL2	8.97E-10
SLAG1	9.81E-10
SLAG2	3.77E-10
SLAG3	4.97E-10
META1	4.45E-10
META2	7.06E-10
META3	1.06E-09

Mixtures	Kp (ft/hr)
UFA1	5.45E-10
UFA2	8.03E-10
UFA3	1.01E-09
SF1	6.28E-10
SF2	4.34E-10

CHAPTER 6
SELECTION OF MIX DESIGNS FOR PILES

The relative cost, mechanical properties, and durability of a concrete are all important factors in bridge construction. Therefore, each of these factors was analyzed to determine the mixtures with the most favorable attributes. Consequently, a method was selected to determine the most feasible and efficient mixtures. This chapter describes this method and the rationale for choosing the mixtures to be implemented in the piles for the Key Royale bridge replacement project.

Because of the approaching deadline for pile construction, final mixture designs were needed before later age testing could be completed. Consequently, ninety-one day data for the first series of specimens and 28 day data for the second series were available for use in selecting the mixture designs.

Selection Approach

To rank the mixture designs, a decision matrix was generated using the data collected from both mechanical and durability tests. In addition, relative costs were included. Each set of results were assigned weighting factors to adjust for their relative importance. These results were then normalized to the CTRL1 mix (cement only) and summed to result in a single score for that mix. For consistency, each of the normalized values was adjusted so that the more favorable results were less than 1.0. Scores were ranked to aid in selection of the best mix design for each class of mineral admixture. The following sections describe each of the three major selection criteria along with the rationale for the weighting factors.

Selection Criterion I: Cost

Although perhaps not the most important factor, material cost often plays a significant role in bridge design and construction. Because of this, cost was a major selection criterion in the decision matrix.

Water, coarse aggregate and fine aggregate quantities are relatively constant among the possible mixtures; consequently, only the relative costs of the cement and mineral admixtures were included. Market costs ($/ton) were collected for cement, fly ash, slag, metakaolin, ultrafine fly ash, and silica fume from the appropriate manufacturers (Table 6 - 1). The relative costs are the ratio of the mineral admixture to that of the cement

Table 6 - 1 Material Costs

	Cost ($/Ton)	Relative Cost
Cement	95	1.000
Fly Ash	42	0.442
Slag	90	0.947
Metakaolin	480	5.053
Ultrafine Fly Ash	1000	10.526
Silica Fume	600	6.316

Selection Criterion II: Mechanical Properties

The mechanical tests included in the decision matrix were compressive strength, flexural strength, modulus of elasticity, and shrinkage (Table 6 - 2). Because the data were highly variable, and splitting tensile strength tests were not included in the analysis. Results from Poisson's ratio were also excluded because they were inconclusive.

Table 6 - 2 Normalized Mechanical Test Results

	Compressive Strength	Flexural Strength	Modulus of Elasticity	Shrinkage
CRTL1	1.000	1.000	1.000	1.000
CTRL2	0.956	1.092	0.993	0.917
SLAG1	0.978	1.049	0.905	0.852
SLAG2	0.986	1.043	0.914	0.685
SLAG3	1.065	1.132	0.914	0.750
META1	0.983	1.086	0.951	0.676
META2	0.974	1.056	1.008	0.583
META3	0.967	1.041	1.006	0.630
UFA1	0.988	1.084	0.921	0.917
UFA2	1.000	1.081	0.871	0.574
UFA3	0.989	1.091	0.912	0.537
SF1	0.979	1.108	0.934	0.796
SF2	0.974	0.987	0.926	0.704

Time constraints for the approaching construction deadlines for the field portion of the investigation did not allow for 365 day age data. Therefore, 91 day age data for compressive strength were analyzed. Complete testing data from the linear shrinkage tests were available.

Because of the mechanical errors in the testing setup for modulus of elasticity, additional mixtures were produced to retest these specimens. At the time the mixtures were selected, only 28 day modulus of elasticity data were available to be used in the mixture determination process. Similarly, flexural strength specimens were recreated and tested. Twenty-eight day data were available for analysis.

Selection Criterion III: Durability

The durability tests included in the decision matrix were surface resistivity, rapid migration test, volume of voids, absorption, and sulfate expansion of mortar specimens (Table 6 - 3). Because of time constraints, results from the corrosion of embedded steel reinforcement and bulk diffusion tests, ASTM G109 and ASTM C1585 respectively, were not available to be used in the decision matrix. Water permeability results were also

not included because it was determined that the data were erroneous due to leaks in the bond between the concrete and epoxy.

Table 6 - 3 Normalized Durability Test Results

	Surface Resistivity	RMT	Voids	Absorption	Sulfate Expansion
CRTL1	1.000	1.000	1.000	1.000	1.000
CTRL2	0.511	0.563	0.993	0.997	0.886
SLAG1	0.360	0.303	0.977	0.982	0.963
SLAG2	0.285	0.320	0.941	0.938	0.874
SLAG3	0.369	0.281	1.046	1.054	0.977
META1	0.208	0.167	1.082	1.096	0.666
META2	0.167	0.136	1.078	1.092	0.609
META3	0.149	0.117	1.119	1.131	0.715
UFA1	0.208	0.141	1.026	1.033	0.932
UFA2	0.181	0.262	0.999	1.005	0.729
UFA3	0.163	0.130	1.029	1.038	0.786
SF1	0.111	0.143	0.980	1.000	0.540
SF2	0.089	0.092	0.960	0.978	0.591

Importance Factors

An average normalized test result was calculated for each of the three major categories, cost, mechanical properties, and durability. One consequence of this approach was that each test method result, within their own category, was weighted equally. Therefore, each category was also assigned an importance factor. Because the focus of this investigate was on the durability aspect of concrete mixtures, the durability test category was assigned an importance factor of 50%. The mechanical test category was assigned a factor of 40%, while cost was assigned a value of 10%. The final score for each mixture design was calculated using the following equation:

$$\text{Score} = 10\%*\text{Cost} + 40\%*\text{Mechanical Properties} + 50\%*\text{Durability} \quad (6\text{-}1)$$

Because each value was normalized so that the more favorable result was represented by a number less then 1.0, the mixture with the lowest score then indicated the mixture design with the most favorable attributes. Therefore, from each class of mineral admixtures, the mixture design with the lowest score was selected. Table 6 - 4 summarizes the normalized results for the selection criterion for each mixture with the final score.

Table 6 - 4 Summary of Normalized Results and Equation Values

Mixture	Cost	Mechanical Tests	Durability Tests	Equation Value
CRTL1	1.000	1.000	1.000	**1.000**
CTRL2	0.900	0.989	0.790	**0.881**
SLAG1	0.886	0.946	0.717	0.826
SLAG2	0.884	0.907	0.672	**0.787**
SLAG3	0.881	0.965	0.745	0.847
META1	1.224	0.924	0.644	0.814
META2	1.305	0.905	0.616	**0.801**
META3	1.386	0.911	0.646	0.826
UFA1	1.852	0.977	0.668	0.910
UFA2	2.043	0.881	0.635	**0.874**
UFA3	2.233	0.882	0.629	0.891
SF1	1.272	0.955	0.555	0.786
SF2	1.378	0.898	0.542	**0.768**

From these data, CTRL1 and CTRL2 were selected to be the control mixtures for the field investigation. SLAG2, META2, UFA2 and SF2 were selected because of they had the lowest final score within each class of mineral admixtures. For clarity, SLAG2 contained 30% slag, META2 contained 10% metakaolin, UFA2 contained 12% ultrafine fly ash, and SF2 contained 9% silica fume.

CHAPTER 7
CONCLUSIONS AND RECOMMENDATIONS

In order to provide sufficient laboratory test data in which the Florida Department of Transportation (FDOT) can utilize in assessing the implementation of alternative mineral admixtures in Florida Concretes, various plastic, mechanical, and durability testes were conducted. Thirteen mixtures were investigated that contained fly ash in conjunction with varying proportions of slag, metakaolin, ultrafine fly ash, and silica fume. Plastic property tests were conducted on temperature, air content, slump, bleeding, and setting times. The mechanical test procedures included compressive strength, flexural strength, splitting tensile strength, modulus of elasticity, and Poisson's ratio. Several durability related tests were performed; these tests included, surface resistivity, rapid migration test, volume of voids, absorption, water permeability, shrinkage, sulfate expansion, and corrosion of embedded steel reinforcement. Additionally, this research provided the FDOT with a recommendation of the most effective mixtures containing various pozzolans for the utilization in the piling of the Key Royale bridge replacement project. Conclusions are as follows:

- It was found that the plastic properties, volume of voids, and absorption were not significantly affected by the implementation of any of the mineral admixtures.
- In the compressive strength tests, the metakaolin mixtures performed the best at ages of less than 28 days. At 28 days, each mixture exhibited nearly equal compressive strength in which the silica fume mixtures showed the highest. At later ages, all mixtures displayed larger strength than the control mixture. However, at 365 days each mixture containing mineral admixtures were nearly equal.

- In the modulus of rupture (MOR) tests, the ultrafine fly ash mixtures showed the lowest MOR at 7 days, while the metakaolin mixture showed the highest. At 28 days, all mixtures showed nearly equal MOR as the control, excluding the ultrafine fly ash mixtures—as they were lower. At 365 days, the slag mixtures displayed the highest MOR, while the ultrafine fly ash mixtures showed the lowest. It was also found that ACI's equation overestimated the MOR for nearly all mixtures. The 7 day test showed the greatest amount of overestimation, while the 365 day tests showed the least amount of overestimation.
- The metakaolin mixture showed the best results for modulus of elasticity (MOE), as they were nearly equal to the control at all ages. The silica fume mixtures displayed the lowest MOE at 7 days, and the highest at 365 days.
- Poisson's ratio appeared to be unaffected by the use of mineral admixtures, as the average ratio was about 0.25 for all ages.
- The use of mineral admixtures improved the resistance to shrinkage; each mixtures exhibited lower linear shrinkage than the control. The 14% ultrafine fly ash mixture showed the lowest amount of shrinkage, followed by the 12% ultrafine fly ash, then 10% metakaolin.
- In the sulfate attack experiments, it was found that the expansion, when compared to the control, was less than 0.5% for mortar and 0.05% for concrete specimens. Generally, the silica fume mixtures showed the lowest amount of expansion, followed by the metakaolin mixtures. However, the 14% ultrafine fly ash mixture showed the largest decrease (54%) in expansion from the control in the concrete specimens.

- The surface resistivity was significantly affected by the use of mineral admixtures. At ages beyond 3 days, each mixture showed higher surface resistivity than the control mixture. The slag mixtures showed the lowest surface resistivity, with the exception of the control mixtures. The silica fume mixtures showed the largest surface resistivity, followed by the ultrafine fly ash, then metakaolin.
- The chloride ion penetrability was also significantly affected by mineral admixtures. At each age, all mixtures showed an improvement in migration coefficients when compared to the control. The silica fume showed the best performance, followed closely by metakaolin. The ultrafine showed the least improvement of all the mineral admixtures at 28 days; however by 91 days, the slag mixtures showed the least improvement. A relation to the 1000 coulomb limit was also made for RMT results. Again, only the metakaolin and silica fume mixtures were the only acceptable mixtures to be used in an extremely aggressive environment at 28 days. However, at 91 days, all mixtures (excluding CTRL1) becomes acceptable.
- Based on results from the decision matrix, the most efficient proportions of mineral admixtures to be used in conjunction with 18% fly ash were: 30% slag, 10% metakaolin, 12% ultrafine fly ash, and 9% silica fume.

APPENDIX A
LABORATORY MIX TESTING DATA

Table A - 1 Plastic Properties Tests

Mix	Density (lb/ft^3)	Slump (in)	Air (%)	Bleed (%)	Initial Set (min)	Final Set (min)	Mix Temp. (^oF)	Air Temp. (^oF)
CTRL1	145	5.75	2.0	0.00	300	395	81	75
CTRL2	145	6.00	1.5	0.10	330	400	84	75
SLAG1	144	6.50	1.1	0.19	340	430	81	75
SLAG2	144	6.00	1.0	0.17	355	460	81	75
SLAG3	146	6.50	0.6	0.27	300	445	80	75
META1	144	6.25	1.4	0.00	375	435	84	75
META2	144	7.25	1.5	0.00	390	470	80	75
META3	144	6.00	1.4	0.00	N/A	N/A	80	75
UFA1	146	5.75	0.6	0.55	375	465	78	75
UFA2	145	6.75	1.8	0.00	385	485	78	75
UFA3	144	8.00	1.6	0.00	400	480	78	75
SF1	143	6.25	2.3	0.00	370	445	76	75
SF2	143	6.00	2.3	0.00	385	465	76	75

Table A - 2 Compressive Strength

Mix	3—day (psi)	7—day (psi)	28—day (psi)	91—day (psi)	365—day (psi)
CTRL1	7,760	8,740	8,780	9,480	9,750
CTRL2	6,830	7,990	8,290	9,920	10,250
SLAG1	6,160	7,620	8,730	9,690	10,400
SLAG2	5,750	7,510	8,640	9,620	10,330
SLAG3	4,890	6,790	8,700	8,900	9,380
META1	7,770	8,860	8,860	9,650	10,170
META2	7,050	8,960	8,840	9,740	10,310
META3	7,300	8,960	8,960	9,810	10,590
UFA1	5,310	6,490	8,470	9,590	10,090
UFA2	5,650	6,770	8,780	9,480	10,090
UFA3	5,680	6,790	8,730	9,590	10,110
SF1	6,170	7,280	8,950	9,680	10,240
SF2	6,230	7,830	9,180	9,730	10,340

Table A - 3 Flexural Strength for Initial Series of Mixtures

Mix	3—day (psi)	7—day (psi)
CTRL1	1,021	1,139
CTRL2	993	1,043
SLAG1	976	1,086
SLAG2	977	1,092
SLAG3	984	1,006
META1	991	1,049
META2	1,132	1,079
META3	1,079	1,094
UFA1	817	1,051
UFA2	872	1,054
UFA3	922	1,045
SF1	1,009	1,028
SF2	1,051	1,154

Table A - 4 Flexural Strength for Second Series of Mixtures

Mix	3—day (psi)	7—day (psi)	365—day (psi)
CTRL1	1,021	1,139	1,121
CTRL2	993	1,043	1,165
SLAG1	976	1,086	1,145
SLAG2	977	1,092	1,238
SLAG3	984	1,006	1,242
META1	991	1,049	1,060
META2	1,132	1,079	1,122
META3	1,079	1,094	1,180
UFA1	817	1,051	1,057
UFA2	872	1,054	1,088
UFA3	922	1,045	1,132
SF1	1,009	1,028	1,139
SF2	1,051	1,154	1,208

Table A - 5 Averaged Flexural Strength

Mix	3—day (psi)	7—day (psi)	365—day (psi)
CTRL1	987	1049	1,121
CTRL2	964	1024	1,165
SLAG1	886	1033	1,145
SLAG2	922	1043	1,238
SLAG3	906	997	1,242
META1	901	954	1,060
META2	1,008	1029	1,122
META3	964	1003	1,180
UFA1	793	974	1,057
UFA2	834	977	1,088
UFA3	853	984	1,132
SF1	971	1022	1,139
SF2	994	1091	1,208

Table A - 6 Modulus of Elasticity

Mix	7—day ($psi*10^6$)	28—day ($psi*10^6$)	365—day ($psi*10^6$)
CTRL1	5.10	5.85	5.82
CTRL2	4.91	5.80	5.85
SLAG1	4.82	5.29	5.49
SLAG2	5.11	5.34	5.72
SLAG3	5.16	5.35	5.71
META1	5.18	5.86	5.88
META2	5.36	5.89	5.93
META3	5.52	5.88	5.80
UFA1	5.14	5.38	5.95
UFA2	4.87	5.09	5.68
UFA3	4.67	5.33	5.58
SF1	4.63	5.46	5.90
SF2	4.77	5.46	5.97

Table A - 7 Poisson's Ratio

Mix	7—day	28—day	365—day
CTRL1	0.258	0.278	0.273
CTRL2	0.179	0.281	0.183
SLAG1	0.260	0.261	0.204
SLAG2	0.282	0.256	0.313
SLAG3	0.253	0.263	0.297
META1	0.268	0.291	0.227
META2	0.259	0.255	0.212
META3	0.247	0.255	0.207
UFA1	0.242	0.243	0.263
UFA2	0.236	0.264	0.366
UFA3	0.243	0.252	0.219
SF1	0.227	0.259	0.276
SF2	0.247	0.259	0.219

Table A - 8 Splitting Tensile Strength

Mix	3—day (psi)	7—day (psi)	28—day (psi)	91—day (psi)	365—day (psi)
CTRL1	1,227	1,184	987	1,007	1,192
CTRL2	1,041	916	1,035	1,196	1,214
SLAG1	951	980	1,248	1,153	1,302
SLAG2	969	949	1,197	989	1,251
SLAG3	1,021	848	892	962	1,058
META1	1,235	1,189	1,085	915	999
META2	1,191	1,259	1,300	1,304	966
META3	1,306	1,064	1,425	1,300	932
UFA1	936	757	812	1,015	794
UFA2	770	1,078	1,079	1,118	953
UFA3	572	1,040	1,057	1,026	819
SF1	1,213	1,131	987	1,107	749
SF2	1,224	1,208	977	1,193	834

Table A - 9 Linear Shrinkage, Volume of Voids, Absorption, and Permability

Mix	Shrinkage (%)	Voids (%)	Absorption (%)	Kp ($ft*10^{-10}/hr$)
CTRL1	0.0360	13.9	6.31	8.89
CTRL2	0.0330	13.8	6.30	8.97
SLAG1	0.0307	13.6	6.20	9.81
SLAG2	0.0247	13.1	5.92	3.77
SLAG3	0.0270	14.5	6.66	4.97
META1	0.0243	15.0	6.92	4.45
META2	0.0210	15.0	6.89	7.06
META3	0.0227	15.5	7.14	10.63
UFA1	0.0330	14.2	6.52	5.45
UFA2	0.0207	13.9	6.34	8.03
UFA3	0.0193	14.3	6.56	1.01
SF1	0.0287	13.6	6.31	6.28
SF2	0.0253	13.3	6.18	4.34

Table A - 10 Sulfate Expansion

Mixture	Concrete Expansion (%)	Mortar Expansion (%)
CTRL1	0.0179	0.0361
CTRL2	0.0143	0.0320
SLAG1	0.0158	0.0348
SLAG2	0.0147	0.0316
SLAG3	0.0260	0.0353
META1	0.0142	0.0254
META2	0.0137	0.0245
META3	0.0123	0.0250
UFA1	0.0167	0.0337
UFA2	0.0127	0.0297
UFA3	0.0083	0.0275
SF1	0.0102	0.0195
SF2	0.0100	0.0213

Table A - 11 Surface Resistivity

Mixture	3 day	7 day	28 day	91 day	364 day
CRTL1	8	9	13	16	17
CRTL2	7	8	13	30	69
SLAG1	6	10	25	43	80
SLAG2	6	11	29	55	92
SLAG3	6	11	28	42	72
META1	8	29	57	75	136
META2	8	34	61	94	177
META3	9	31	82	105	186
UFA1	5	7	25	75	169
UFA2	6	8	29	86	*200
UFA3	6	7	32	96	*200
SF1	7	14	78	140	*200
SF2	6	15	93	175	*200

Table A - 12 Rapid Migration Test

Mixture	28	56	91
CTRL1	0.029	0.029	0.021
CTRL2	0.025	0.020	0.014
SLAG1	0.016	0.014	0.010
SLAG2	0.016	0.015	0.009
SLAG3	0.017	0.017	0.010
META1	0.013	0.011	0.007
META2	0.008	0.009	0.006
META3	0.009	0.007	0.005
UFA1	0.019	0.014	0.006
UFA2	0.015	0.010	0.008
UFA3	0.017	0.012	0.005
SF1	0.009	0.007	0.006
SF2	0.008	0.005	0.004

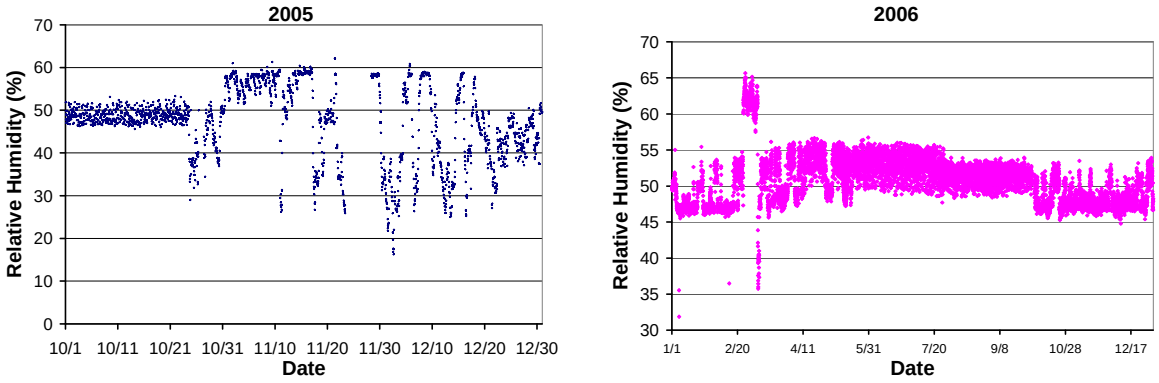

a) b)

Figure A - 1 Relative Humidity in Dry Curing Room for a) 2005 and b) 2006

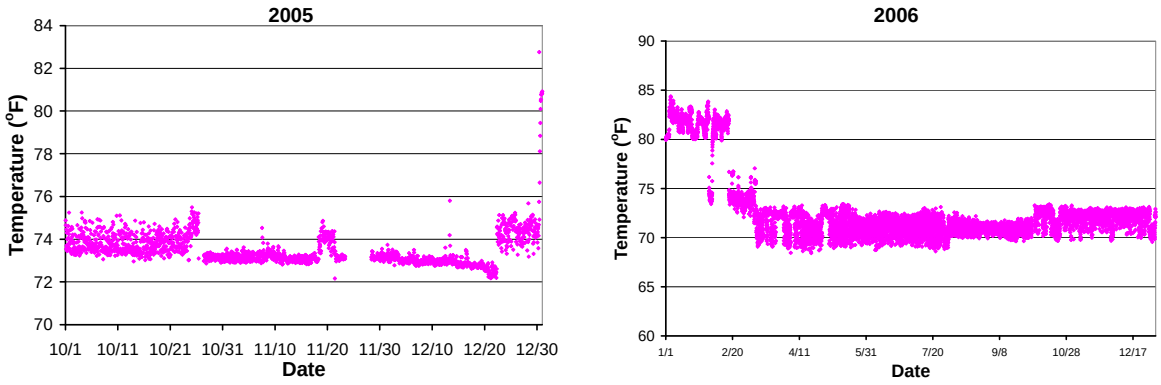

a) b)

Figure A - 2 Temperature in Dry Curing Room for a) 2005 and b) 2006

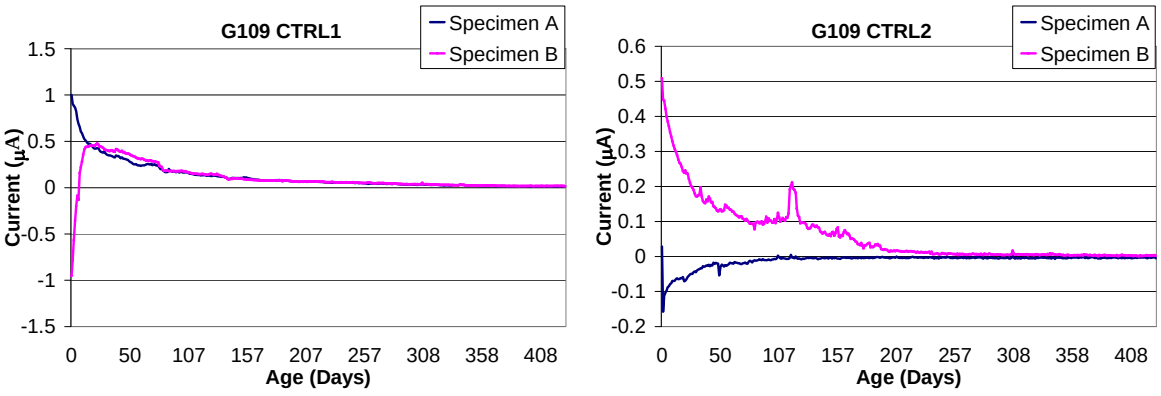

a) b)

Figure A - 3 Corrosion of Embedded Steel Reinforcement for a) CTRL1 and b) CTRL2

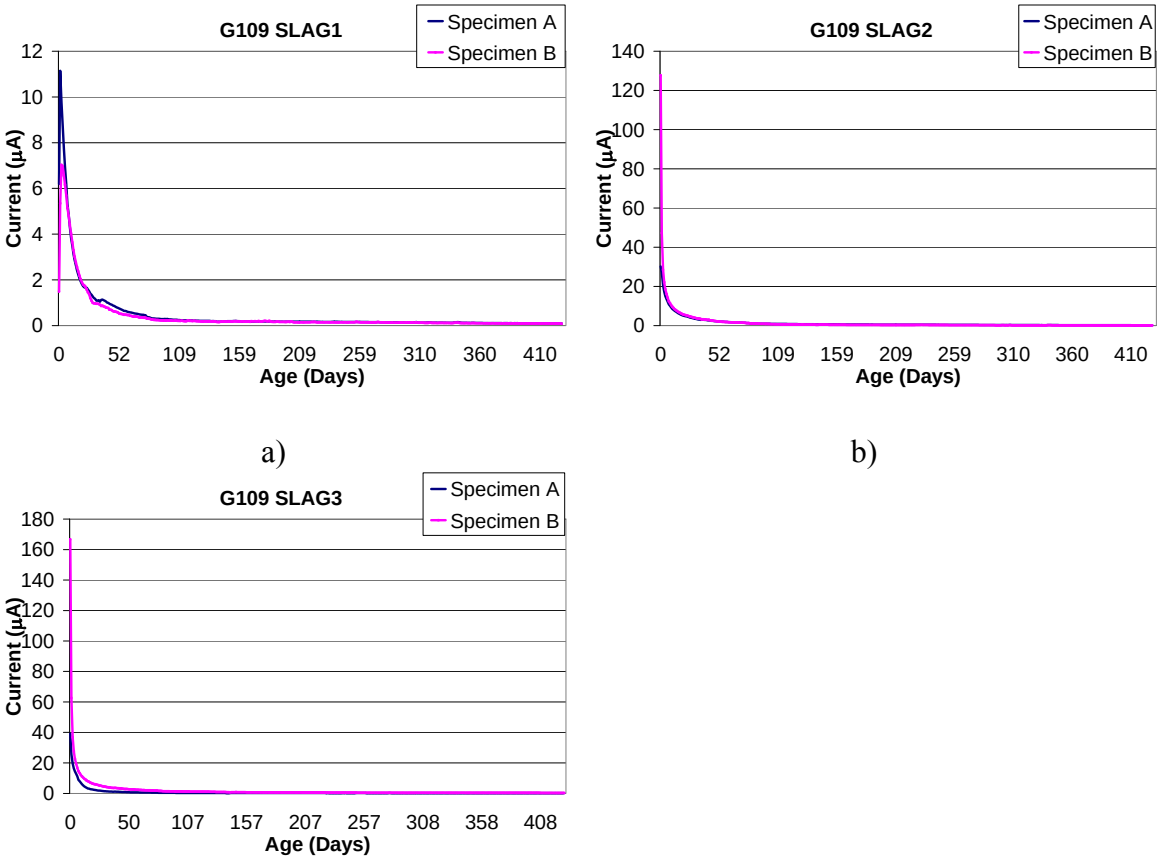

Figure A - 4 Corrosion of Embedded Steel Reinforcement for a) SLAG1, b) SLAG2, and c) SLAG3

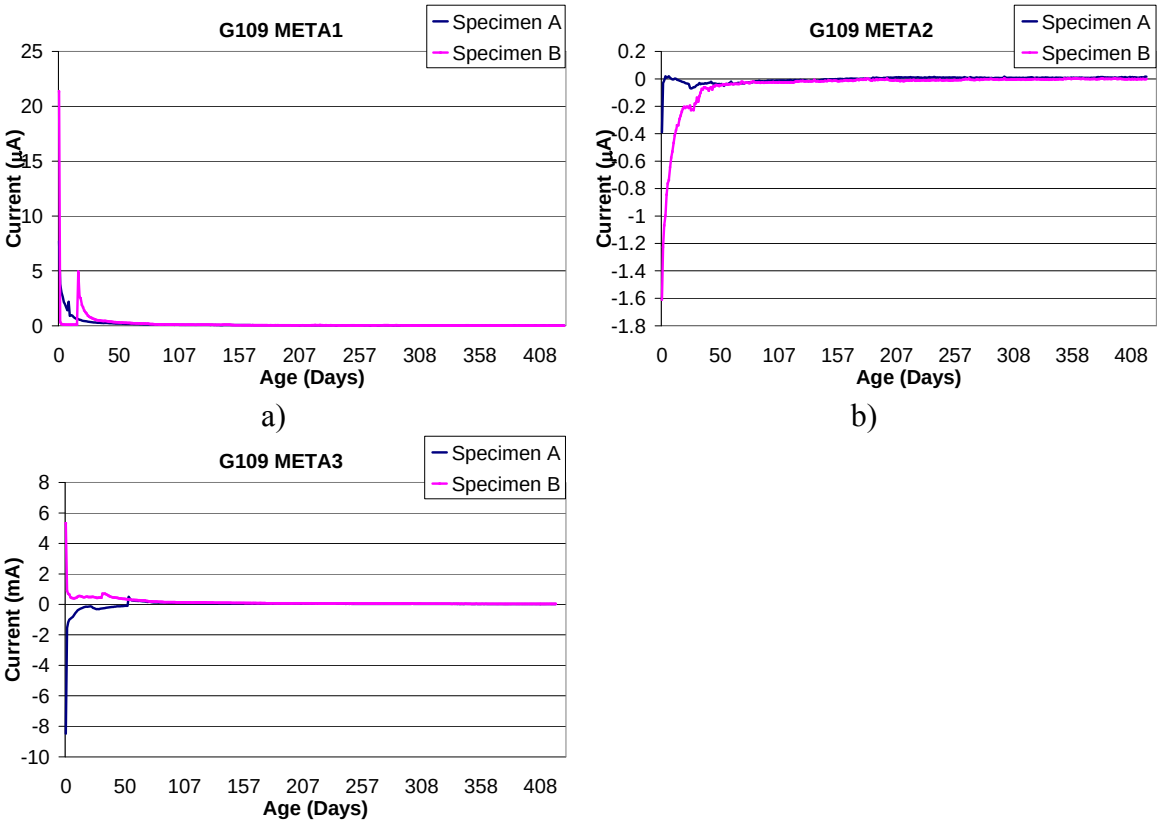

Figure A - 5 Corrosion of Embedded Steel Reinforcement for a) META1, b) META2, and c) META3

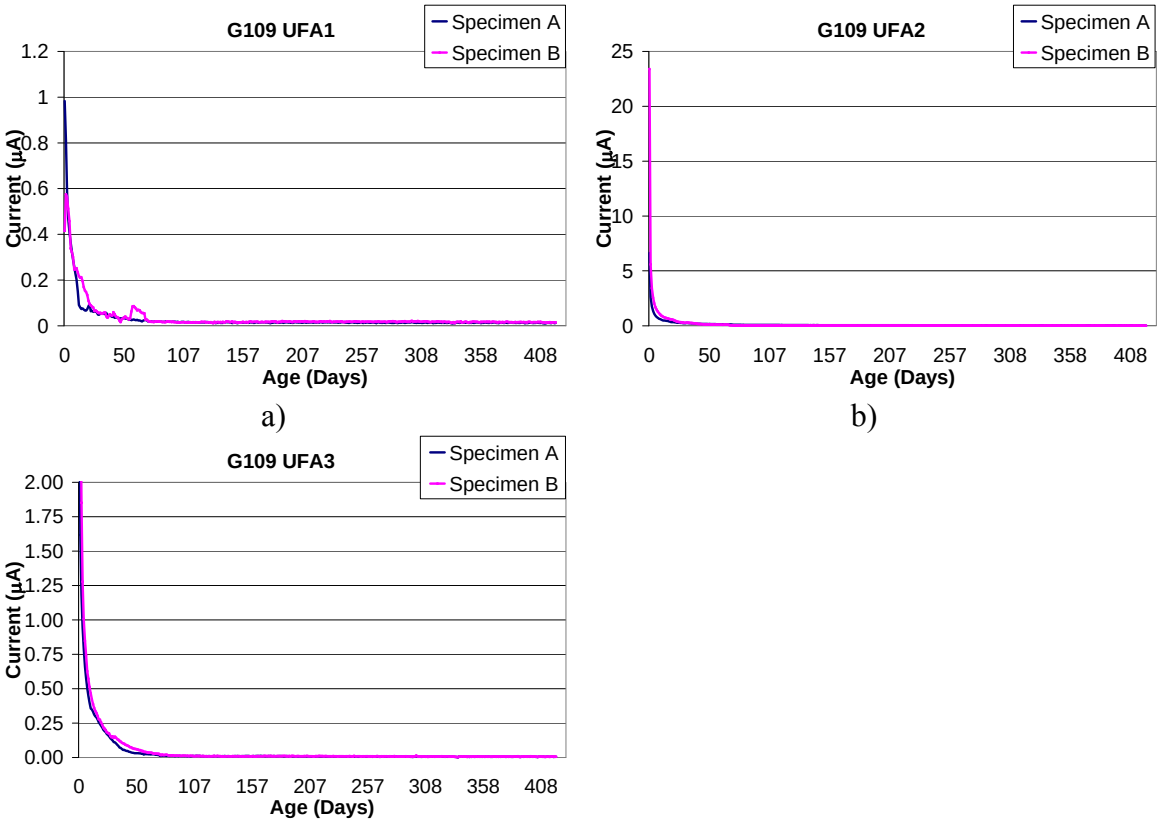

Figure A - 6 Corrosion of Embedded Steel Reinforcement for a) UFA1, b) UFA2, and c) UFA3

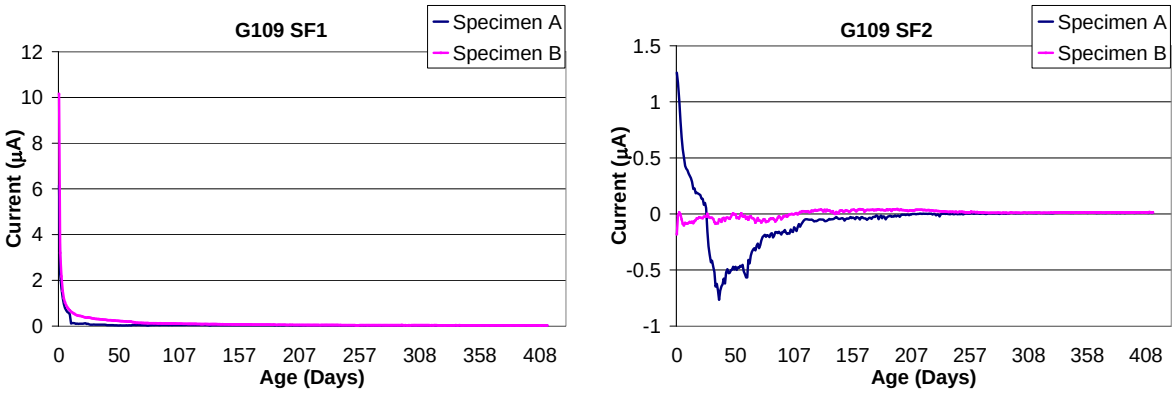

Figure A - 7 Corrosion of Embedded Steel Reinforcement for a) SF1 and b) SF2

APPENDIX B
LABORATORY MIX STATISTICAL DATA

Table B - 1 Compressive Strength

Mix	3—day	7—day	28—day	91—day	365—day
CTRL1	0.3	2.2	1.3	0.8	1.4
CTRL2	1.5	0.6	4.3	2.4	4.6
SLAG1	1.5	3.6	7.7	3.8	3.8
SLAG2	1.1	5.5	6.7	4.7	1.8
SLAG3	6.0	1.3	4.3	3.1	3.0
META1	1.3	5.2	3.1	9.5	3.1
META2	0.0	3.3	2.7	7.3	3.2
META3	3.0	2.1	2.9	4.8	4.5
UFA1	3.4	2.8	2.6	5.0	5.0
UFA2	3.9	2.4	1.1	2.2	4.9
UFA3	2.5	2.4	4.1	1.4	3.6
SF1	1.2	8.2	2.1	3.1	3.9
SF2	2.4	6.4	5.4	3.8	1.8

Table B - 2 Flexural Strength for Initial Series of Mixtures

Mix	3—day	7—day
CTRL1	3.1	2.4
CTRL2	4.7	8.9
SLAG1	4.6	5.5
SLAG2	3.2	2.4
SLAG3	3.4	9.2
META1	3.8	4.9
META2	5.0	7.2
META3	2.5	6.5
UFA1	11.2	3.5
UFA2	8.1	6.0
UFA3	1.6	6.3
SF1	3.9	4.1
SF2	6.1	4.9

Table B - 3 Flexural Strength for Second Series of Mixtures

Mix	3—day	7—day	365—day
CTRL1	1.4	4.2	7.0
CTRL2	2.1	4.8	4.6
SLAG1	1.6	6.7	3.3
SLAG2	3.0	5.5	1.7
SLAG3	0.7	6.1	2.9
META1	5.8	10.8	5.2
META2	0.6	2.1	0.7
META3	4.5	5.7	2.1
UFA1	3.4	6.0	5.0
UFA2	5.6	9.1	7.8
UFA3	1.4	4.1	5.9
SF1	1.0	4.8	6.3
SF2	1.7	7.9	7.9

Table B - 4 Splitting Tensile Strength

Mix	3—day	7—day	28—day	91—day	365—day
CTRL1	26.2	3.9	2.0	1.2	3.5
CTRL2	16.6	11.8	11.9	11.7	5.5
SLAG1	10.1	15.2	13.1	6.7	12.4
SLAG2	11.1	16.3	13.7	12.4	20.3
SLAG3	13.3	8.4	10.4	17.4	23.9
META1	13.1	7.7	14.6	27.2	18.5
META2	27.5	16.4	9.6	2.8	47.4
META3	30.0	15.9	21.1	23.8	45.7
UFA1	22.0	2.4	6.4	9.7	45.5
UFA2	20.2	16.9	25.6	18.0	34.6
UFA3	18.4	16.3	20.1	9.1	15.8
SF1	24.4	3.4	6.6	3.6	33.3
SF2	18.0	12.3	14.3	19.1	37.1

Table B - 5 Linear Shrinkage, Volume of Voids, Absorption, and Permeability

Mix	Shrinkage	Voids	Absorption
CTRL1	12.1	4.1	4.9
CTRL2	6.1	2.6	2.5
SLAG1	13.2	2.4	1.3
SLAG2	27.0	2.3	1.7
SLAG3	6.4	1.7	1.9
META1	8.6	2.4	1.8
META2	20.2	3.7	1.9
META3	3.1	4.1	2.0
UFA1	4.6	2.3	2.0
UFA2	43.4	2.6	1.4
UFA3	36.7	1.4	1.9
SF1	17.6	2.1	1.8
SF2	6.0	2.9	2.8

Table B - 6 Sulfate Expansion

Mixture	Concrete Expansion (%)	Mortar Expansion (%)
CTRL1	0.0179	0.0361
CTRL2	0.0143	0.0320
SLAG1	0.0158	0.0348
SLAG2	0.0147	0.0316
SLAG3	0.0260	0.0353
META1	0.0142	0.0254
META2	0.0137	0.0245
META3	0.0123	0.0250
UFA1	0.0167	0.0337
UFA2	0.0127	0.0297
UFA3	0.0083	0.0275
SF1	0.0102	0.0195
SF2	0.0100	0.0213

Table B - 7 Surface Resistivity

	3 day	7 day	28 day	91 day	364 day
CRTL1	2.2	2.0	7.0	3.6	0.4
CRTL2	5.1	2.6	4.1	4.9	0.9
SLAG1	4.3	5.6	8.0	5.7	9.3
SLAG2	2.2	3.3	6.1	8.7	2.8
SLAG3	4.8	3.2	7.9	8.1	6.8
META1	4.0	5.3	9.8	8.1	5.3
META2	1.4	4.7	3.5	7.1	3.6
META3	3.5	5.7	4.0	2.8	5.7
UFA1	3.4	3.0	5.8	7.2	2.8
UFA2	4.5	6.1	5.8	2.4	*0.0
UFA3	3.5	3.5	10.7	7.7	*0.0
SF1	4.6	1.6	11.9	5.3	*0.0
SF2	7.2	5.1	7.1	2.5	*0.0

Table B - 8 Rapid Migration Test

Mixture	28	56	91
CTRL1	7.8	28.4	25.1
CTRL2	8.6	7.9	27.3
SLAG1	9.2	17.8	34.1
SLAG2	30.0	3.9	30.0
SLAG3	0.5	8.2	36.4
META1	27.6	9.1	31.1
META2	26.2	42.5	46.4
META3	13.0	8.7	15.6
UFA1	38.1	11.2	11.0
UFA2	19.0	4.3	25.1
UFA3	20.1	15.3	19.8
SF1	33.6	5.2	92.9
SF2	1.3	46.4	33.4

APPENDIX C
LABORATORY MIX NORMALIZED DATA

Table C - 1 Cost

	Cost ($/Ton)	Relative Cost
Cement	95	1.000
Fly Ash	42	0.442
Slag	90	0.947
Metakaolin	480	5.053
Ultrafine Fly Ash	1000	10.526
Silica Fume	600	6.316

Table C - 2 Mechanical Tests

	Compressive Strength	Flexural Strength	Modulus of Elasticity	Shrinkage
CRTL1	1.000	1.000	1.000	1.000
CTRL2	0.956	1.092	0.993	0.917
SLAG1	0.978	1.049	0.905	0.852
SLAG2	0.986	1.043	0.914	0.685
SLAG3	1.065	1.132	0.914	0.750
META1	0.983	1.086	0.951	0.676
META2	0.974	1.056	1.008	0.583
META3	0.967	1.041	1.006	0.630
UFA1	0.988	1.084	0.921	0.917
UFA2	1.000	1.081	0.871	0.574
UFA3	0.989	1.091	0.912	0.537
SF1	0.979	1.108	0.934	0.796
SF2	0.974	0.987	0.926	0.704

Table C - 3 Durability Tests

	Surface Resistivity	RMT	Voids	Absorption	Sulfate Expansion
CRTL1	1.000	1.000	1.000	1.000	1.000
CTRL2	0.511	0.563	0.993	0.997	0.886
SLAG1	0.360	0.303	0.977	0.982	0.963
SLAG2	0.285	0.320	0.941	0.938	0.874
SLAG3	0.369	0.281	1.046	1.054	0.977
META1	0.208	0.167	1.082	1.096	0.666
META2	0.167	0.136	1.078	1.092	0.609
META3	0.149	0.117	1.119	1.131	0.715
UFA1	0.208	0.141	1.026	1.033	0.932
UFA2	0.181	0.262	0.999	1.005	0.729
UFA3	0.163	0.130	1.029	1.038	0.786
SF1	0.111	0.143	0.980	1.000	0.540
SF2	0.089	0.092	0.960	0.978	0.591

Table C - 4 Summary

Mixture	Cost	Mechanical Tests	Durability Tests	Equation Value
CRTL1	1.000	1.000	1.000	1.000
CTRL2	0.900	0.989	0.790	0.881
SLAG1	0.886	0.946	0.717	0.826
SLAG2	0.884	0.907	0.672	0.787
SLAG3	0.881	0.965	0.745	0.847
META1	1.224	0.924	0.644	0.814
META2	1.305	0.905	0.616	0.801
META3	1.386	0.911	0.646	0.826
UFA1	1.852	0.977	0.668	0.910
UFA2	2.043	0.881	0.635	0.874
UFA3	2.233	0.882	0.629	0.891
SF1	1.272	0.955	0.555	0.786
SF2	1.378	0.898	0.542	0.768

LIST OF REFERENCES

Akkaya, Y., Ouyang, C., Shah, S., "Effect of Supplementary Cementitious Materials on Shrinkage and Crack Development in Concrete," Cement & Concrete Composites, 2007, V. 29, pp. 117-123.

Badogiannis, E., Kakali, G., Dimopoulou, G., Chaniotakis, E., Tsivilis, S., "Metakaolin as a Main Cement Constituent. Exploitation of Poor Greek Kaolins," Cement and Concrete Composites, 2005, V. 27, pp. 197-203.

Bai, J., Wild, S., Ware, J. A., Saber, B. B., "The use of neutal networks to predict workability of concrete incorporating metakaolin and fly ash," Advances in Engineering Software, 2003, V. 34, pp. 663-669.

Brooks, J. J., Megat Johari, "The effects of metakaolin on creep and shrinkage of concrete," Cement & Concrete Composites, 2001, V. 23, pp. 495-502.

Brooks, J. J., Megat Johari, M. A., Mazloom, M., "The effects of admixtures on the setting time of high-strength concrete," Cement & Concrete Composites, 2000, V. 22, pp. 293-301.

Chini, A.R., Muszynski, L.C., Hicks, J., "Determination of Acceptance Permeability Characteristics for Performance-Related Specifications for Portland Cement Concrete," Florida Department of Transportation, 2003, Final Report No. BC 354-41.

FDOT 346 (2004). "Florida Department of Transportation Standard Specification for Road and Bridge Construction." Florida Department of Transportation (FDOT).

FDOT (July 2004). "Florida Department of Transportation Structures Design Guidelines." Florida Department of Transportation (FDOT).

FM 5-516 (2000). "Determining Low-Levels of Chloride in Concrete and Raw Materials." Florida Department of Transportation (FDOT).

FM5-578 (2004). "Concrete Resistivity as an Electrical Indicator of Permeability." Florida Department of Transportation (FDOT).

Frias, M., Sanchez de Rojas, M. I., Cabrara, J., "The Effect that the Pozzolanic Reaction of Metakaolin has on the Heat Evolution on Metakaolin-Cement Mortars," Cement and Concrete Research, 2000, V. 30, pp.209-216.

Gonen, T., Yazicioglu, S., "The Influence of Mineral Admixtures on the Short and Long-Term Performance of Concrete," Building and Environment, 2006.

Heikal, M., Morsy, M. S., Aiad, I., "Effect of treatment temperature on the early hydration characteristics of superplasticized silica fume blended cement pastes," Cement and Concrete Research, 2005, V. 35, pp. 680-687.

Hooton, R.D.,Thomas, M.D.A., Stanish, K., "Prediction of Chloride Penetration in Concrete." Final Report No. FHWA/RD-00/142, 2001, Federal Highway Administration.

Jones, M. R., McCarthy, A., Booth, A. P. P. G., "Characteristics of the Ultrafine Component of Fly Ash," Fuel, 2006, V. 85, pp. 2250-2259.

Khatib, J. M., and Wild, S., "Sulfate Resistance of Metakaolin Mortar," Cement and Concrete Research, 1998, V. 28, pp. 83-92.

Kim, H., Lee, S., Moon, H., "Strength Properties and Durability Aspects of High Strength Concrete Using Korean Metakaolin," Construction and Building Materials, 2007, V. 21, pp. 1229-1237.

Langan, B. W., Weng, K., Ward, M.A., "The Effect of Silica Fume and Fly Ash on Heat of Hydration of Portland Cement," Cement and Concrete Research, 2002, V. 32, pp. 1045-1051.

Larsen, T. J., Armaghani, J. M., "Quality Concrete with Fly Ash," Florida Department of Transportation, 1987, Tallahassee, Fl.,

McCarthy, M. J., Dhir, R. K., "Development of High Volume Fly Ash Cements For Use in Concrete Construction, Fuel, 2005, V. 84, pp. 1423-1432.

Mirza, J., Mirza M. S., Roy, V., Saleh, K., "Basic rheological and mechanical properties of high-volume fly ash grouts," Construction and Building Materials, 2002, V. 16, pp. 353-363.

Mindess, S., Young, J. F., and Darwin, D. (2003). *Concrete*, Second Edition, Pearson Education, Inc., Upper Saddle River, New Jersey

Mouli, M., Khelafi, H., "Performance Characteristics of Lightweight Aggregate Concrete Containing Natural Pozzolans," Building and Environment, 2006, V 84, pp.1423-1432.

Nassif, H. H., Najm, H., Suksawang, N., "Effect of pozzolanic materials and curing methods on the elastic modulus of HPC," Cement and Concrete Composites, 2005, V. 27, pp. 661-670.

NT BUILD 492 (1999). "Concrete, mortar and cement-based repair materials: Chloride Migration Coefficient from Non-Steady-Stade Migration Experiments." Nordtest method.

Parande, A. K., Babu, B. R., Karthik, M. A., Kumar, D., Palaniswamy, N., "Study on Strength and Corrosion Performance for Steel Embedded in Metakaolin Blended Concrete and Mortar," Construction and Building Materials, 2006.

Personal Communication with Charles Ishee, January 29, 2005.

Pfeifer, D.W., McDonald, D.B., Krauss, P.D., "The rapid chloride permeability test and its correlation to the 90-day chloride ponding test." PCI Journal, 1994, 41(4), pp. 82–95.

Qian, X., Li, Z., "The Relationship Between Stress and Strain for High-performance Concrete with Metakaolin," Cement and Concrete Research, 2001, V. 31, pp. 1607-1611.

Saraswathy, V., Song, H,. "Electrochemical Studies on the Corrosion Performance of Steel Embedded in Activated Fly Ash Blended Concrete," Electrochimica Acta, 2006, V. 51, pp. 4601-4611.

Skalny, J., Marchand, J.,and Odler, I. (2002). *Sulfate Attack on Concrete*, Spon Press, New York, New York.

Sioulas, B., Sanjayan, J. G., "Hydration Temperatures in Large High-strength Cconcrete Columns Incorporating Slag," Cement and Concrete Research, 2000, V. 30, pp. 1791-1799.

Soongswang, P., Tia, M., Bloomquist, D., Meletiou, C., and Sessions, L., "Efficient Test Setup for Determining the Water-Permeability of Concrete," Transportation Research Record, 1988, V. 1204, pp. 77-82.

Stanish, K., Hooton, R.D., Thomas, M.D.A., "The Rapid Migration Test for HPC," HPC Bridge Views, Jan.-Feb. 2005, V. 37, pp. 3.

Streicher, P.E., Alexander, M.G., "A Chloride Conduction Test for Concrete." Cement and Concrete Research,1995, V. 25, pp. 1284-1294.

Tang, L., Nilsson, L., "Rapid Determination of the Chloride Diffusivity in Concrete by Applying an Electrical Field." ACI Materials Journal, 1992, V. 89, pp. 49-53.

Tang, L. (1996). "Chloride Transport In Concrete – Measurement and Prediction," PhD Dissertation, Chalmers University of Technology, 1996.

Tia, M., Bloomquist, D., Yang. M. C. K., Soongwang, P., Meletiou, C. A., Amornsrivilai, P., Dobson, E., Richardson, D., "Field and Laboratory Study of Modulus of Rupture and Permeability of Structural Concrete in Florida," Florida Department of Transportation Technical Report, 1990.

Tia, M., Bloomquist, D., Meletiou, C. A., Amornsrivilai, Shih, C., Richardson, D., Dobson, E., "Extension of Field and Laboratory Study of Modulus of Rupture and Permeability of Structural Concrete in Florida," Florida Department of Transportation Technical Report, 1991.

Wainwright, P. J., Rey, N., "The Influence of Ground Granulated Blastfurnace Slag (GGBFS) Additions and Time Delay on the Bleeding of Concrete," Cement & Concrete Composites, 2000, V. 22, pp. 253-257.

Whiting, D., Mohamad, N., "Electrical Resistivity of Concrete-A Literature Review." Portland Cement Association, 2003, R&D Serial No. 2457.

Zongjin, L., Ding, Z., "Property Improvement of Portland Cement by Incorporating with Metakaolin and Slag," Cement and Concrete Research, 2003, V. 33, pp. 579-584.

BIOGRAPHICAL SKETCH

Edward K. Roske was born May 17, 1982 in Vero Beach, Florida, to Joyce and Ed Roske. He graduated from Sebastian River High School in June of 2000. He received his Associate of Arts degree in May of 2002 from Indian River Community College, and transferred to the University of Florida to pursue a Bachelor of Science in civil engineering in the summer of 2002. While attending the University of Florida full time, Edward worked part time for the Department of Civil Engineering, for three year as a research assistant Dr. Reynaldo Roque and Dr. Andrew Boyd. He received his Bachelor of Science in civil engineering in May of 2005, graduating with honors.

Edward continued his education by entering graduate school to pursue a Master of Engineering in the Materials Group of the Civil and Coastal Engineering Department in May 2005. After graduating form the University of Florida with a Master of Engineering, Edward plans on working with URS Corporation as a bridge design engineer.